AIRCRAFT MOTION DYNAMICS AND LATERAL TRAJECTORY TRACKING
ALGORITHM DESIGN FOR THE ENHANCEMENT OF FLIGHT SAFETY

A THESIS SUBMITTED TO
THE GRADUATE SCHOOL OF NATURAL AND APPLIED SCIENCES
OF
MIDDLE EAST TECHNICAL UNIVERSITY

BY

CAHİDE YELİZ GÜNHAN

IN PARTIAL FULFILLMENT OF THE REQUIREMENTS
FOR
THE DEGREE OF MASTER OF SCIENCE
IN
ELECTRICAL AND ELECTRONICS ENGINEERING

JUNE 2018

Approval of the thesis:

AIRCRAFT MOTION DYNAMICS AND LATERAL TRAJECTORY TRACKING ALGORITHM DESIGN FOR THE ENHANCEMENT OF FLIGHT SAFETY

submitted by CAHİDE YELİZ GÜNHAN in partial fulfillment of the requirements for the degree of **Master of Science in Electrical and Electronics Engineering Department, Middle East Technical University** by,

Prof. Dr. Halil Kalıpçılar   _____
Dean**,** Graduate School of **Natural and Applied Sciences**

Prof. Dr. Tolga Çiloğlu   _____
Head of Department, **Electrical and Electronics Engineering**

Prof. Dr. Kerim Demirbaş   _____
Supervisor, **Electrical and Electronics Engineering Dept., METU**

Examining Committee Members:

Prof. Dr. Kemal Leblebicioğlu   _____
Electrical and Electronics Engineering Dept., METU

Prof. Dr. Kerim Demirbaş   _____
Electrical and Electronics Engineering Dept., METU

Assoc. Prof. Dr. Emre Tuna   _____
Electrical and Electronics Engineering Dept., METU

Assoc. Prof. Dr. Mustafa Doğan   _____
Control and Automation Engineering Dept., Istanbul Technical University

Assoc. Prof. Dr. Nursel Akçam   _____
Electrical and Electronics Engineering Dept., Gazi University

Date: 11/06/2018

I hereby declare that all information in this document has been obtained and presented in accordance with academic rules and ethical conduct. I also declare that, as required by these rules and conduct, I have fully cited and referenced all material and results that are not original to this work.

Name, Last name: Cahide Yeliz Günhan

Signature:

ABSTRACT

AIRCRAFT MOTION DYNAMICS AND LATERAL TRAJECTORY TRACKING ALGORITHM DESIGN FOR THE ENHANCEMENT OF FLIGHT SAFETY

Günhan, Cahide Yeliz
M.S., Department of Electrical and Electronics Engineering
Supervisor: Prof. Dr. Kerim Demirbaş

June 2018, 109 Pages

This thesis aspires to cover the fundamentals of an aircraft control for Flight Management System (FMS). FMS, trajectory tracking and performance requirements of a flight are the focal points of the thesis. In view of this, the thesis consists of the outlined components to achieve its goal; (i) generating paths - which denotes the creation of reference paths for trajectory by complying with the avionic performance standardizations, (ii) controlling the aircraft – which propagates the control commands by using flight motion dynamics and simulate real aircraft's motion for the FMS algorithm, (iii) lateral trajectory tracking – which aims to find and follow the different kind of paths in lateral axis such as straight line path, curved path and paths in a narrow area with a high performance, (iv) performance evaluation – focuses on the avionic standardizations that are from RNP-RNAV while controlling the aircraft, generating the path and tracking the trajectory to evaluate and increase the performance for flight safety.

Keywords: Flight Management System (FMS), Trajectory tracking, Required Navigation Performance (RNP), Area Navigation (RNAV)

ÖZ

UÇUŞ GÜVENLİĞİNİ ARTTIRMAK AMAÇLI, HAVA ARACI HAREKET DİNAMİKLERİ VE YANAL ROTA TAKİBİ ALGORİTMA TASARIMI

Günhan, Cahide Yeliz
Yüksek Lisans, Elektrik ve Elektronik Mühendisliği Bölümü
Tez Yöneticisi: Prof. Dr. Kerim Demirbaş

Haziran 2018, 109 Sayfa

Bu tez kapsamında uçağın temel fonksiyonlarının, Uçuş Yönetim Sistemi içinde kontrol edilmesi amaçlanmaktadır. Uçak Yönetim Sistemi, yörünge takibi ve uçuşun performans kriterleri bu tezin temel odağındadır. Tezin amacına ulaşabilmesi için gerekli modüller şu şekilde özetlenebilir; (i) yol üretimi – yörünge için aviyonik performans standartlarına uygun referans yollar yaratmayı amaçlamaktadır, (ii) uçağı kontrol etme – uçuş hareket dinamiklerini kullanarak kontrol komutlarını üretmeyi ve Uçuş Yönetim Sistemi algoritması için, gerçek uçak hareketlerinin simülasyon çalışmasını gerçekleştirmeyi hedeflemektedir, (iii) yanal rota takibi – düz çizgi, dönüşlü yol ve dar alanlarda yer alan yollar gibi değişik türde bir çok rotayı yüksek performansla yanal eksende bulmayı ve takip etmeyi amaçlamaktadır, (vi) performans değerlendirme – uçak kontrolünü sağlarken, yol üretirken ve rota takibi esnasında uçuş güvenliğini değerlendirmek ve arttırmak için RNP ve RNAV standartlarının gerekleri olan aviyonik standartlarına odaklanmaktadır.

Anahtar Kelimeler: Uçuş Yönetim Sistemi, Rota Takibi, Gerekli Seyrüsefer Performansı (RNP), Saha Seyrüseferi (RNAV)

To my family…

ACKNOWLEDGMENTS

I would like to express my gratitude and thanks to my supervisor Prof. Dr. Kerim DEMİRBAŞ who guided me throughout this work with his valuable comments, support, understanding and patience.

I would also like to express my special thanks to Sevim GÜNHAN, Yeşim GÜNHAN and Ergün GÜNHAN for their love, endless support and patience.

I am indebted to my friends who have always enlightened me with their caring, understanding, wisdom and love through my entire life.

TABLE OF CONTENTS

LIST OF TABLES

TABLES

LIST OF FIGURES

FIGURES

LIST OF ABBREVIATIONS

ADC	:	Air Data Computer
ADF	:	Automatic Direction Finding
AIAA	:	International Air Transportation Association
ANP	:	Actual Navigation Performance
AoA	:	Angle of Attack
ASE	:	Altimetry System Error
ATC	:	Air Traffic Control
BADA	:	Base of Aircraft Data
CF	:	Course to a Fix
CG	:	Center of Gravity
DCM	:	Direction Cosine Matrix
DF	:	Direct to Fix
DME	:	Distance Measurement Unit
FAA	:	Federal Aviation Administration
FMS	:	Flight Management System
GBAS	:	Ground-Based Augmentation System
GNSS	:	Global Navigation Satellite Systems
ICAO	:	International Civil Aviation Organization
IF	:	Initial Fix
ILS	:	Instrument Landing System
INS	:	Inertial Navigation System
MLS	:	Microwave Landing System
NDB	:	Non-directional Beacon
NED	:	North-East-Down
NM	:	Nautical Mile
PBN	:	Performance Based Navigation
PDE	:	Path Definition Error

PEE	:	Position Estimation Error
PF	:	Pattern Fix
PSE	:	Path Steering Error
RNP	:	Required Navigation Performance
RNAV	:	Area Navigation
SID	:	Standard Instrument Departure
STAR	:	Standard Terminal Arrival Route
TACAN	:	Tactical Air Navigation System
TOD	:	Top of Descent
TR	:	Track to Fix
TSE	:	Total System Error
VA	:	Heading to an Altitude
VI	:	Heading to an Intercept
VM	:	Heading to a Manual Termination
VOR	:	VHF Omni-directional Radio Range
WCA	:	Warning, Caution, Advisory
WP	:	Waypoint
6-DOF	:	Six Degrees of Freedom

LIST OF SYMBOLS

ψ : Yaw Euler Angle

θ **:** Pitch Euler Angle

ϕ **:** Roll Euler Angle

γ : Flight Path Angle

α : Angle of Attack

W_B : Angular Velocity

V : Aircraft Velocity Vector

I : Moment of Inertia

R_θ : Pitch Transformation Matrix

R_ψ : Yaw Transformation Matrix

R_ϕ : Roll Transformation Matrix

CHAPTER 1

INTRODUCTION

Air transportation is increasing rapidly and more important day by day for travelling and transporting purposes. Therefore, aviation has been in the limelight and also has become a highly significant field to work in all around the world [2]. Besides technologic improvements in aerodynamics of aircraft, engines and avionic equipment in addition to several aviation organizations work on creating a standardization in this field. Aviation is such a unique area that whenever and wherever an incident or accident happens, it changes the rules and conventional know-how all over the world because an error in aviation is likely to be deadly and catastrophic. Accidents and incidents can be caused by several route-causes such as pilotage error, misleading of aircraft by Air Traffic Control (ATC), mechanical failures and avionic equipment errors and so forth [4]. While these reasons can cause problems independently, the problems might arise from multiple reasons through simultaneous occurrences or by following each other. To prevent all these problems from happening, flight safety has become the most crucial point of interest. Although the massive surge in flight traffic means the higher the probability of accidental occurrences, surprisingly the number of air crash and incidents has decreased in the last years thanks to numerous improvement in the field and because of the lessons learned from past experiences [2,4].

While pilots used to fly visually and with some basic analog displays in the past, now advanced avionic instruments, high-level algorithms, redundancy systems based on

back-up equipment for flight critical systems and alerting system (warning, caution, advisory (WCA)) have taken the place of the past. Moreover, in a flight, not only the avionic equipment's but also pilots have key duties mainly such as navigating, communicating, aviating, monitoring and controlling. To maintain all these duties, there are several systems and rules which are ground-aids (ATC, ground-based navigation sources), avionic equipment's on board, satellite-based systems and flight rules which pilots must follow [5]. At the same time, smart avionic equipment, advanced algorithms and automation (autopilot and fly-by-wire system) have been developed to increase flight safety and to minimize pilot judgement errors, in other words human factor, and workload on pilots during the flight such as calculations [2,5].

This thesis focuses on four main subjects to evaluate and develop. The objectives of the subjects are categorized as generating paths, controlling and modelling the aircraft, lateral trajectory tracking with the path algorithm and performance evaluation.

The thesis consists of seven chapters and the outline of the thesis are given as follows.

Chapter 1 presents an introduction by giving general information about the thesis worldwide and explain the summary of chapters in the thesis study.

In Chapter 2, fundamentals of aircraft flight mechanism are aimed to explain general aircraft concept to supply base information for the rest of the thesis. For this purpose, forces of flight, how an aircraft flies, Newton laws and Bernoulli's Principle, airfoil structure, movement axes of aircraft and control surfaces are given as core knowledge.

In Chapter 3, aircraft coordinate systems are the point of the aim of this section. Inertial (north-east-down) frame, body frame, stability axis, wind axis, velocity axes and earth frame are explained in this chapter to be able to understand aircraft coordinate systems and to use them in coordinate transformations. In transformation phase, one of the most important axes transformations which is the Euler transformation is explained by deriving yaw, pitch and roll transformation matrices. At the same time, rotation rates

with respect to the change in aircraft orientation and aerodynamic forces on the body frame are the topics of aircraft coordinate systems which are given here.

In Chapter 4, flight motion dynamic is explained, and the formulation of flight motion dynamic is derived to determine aircraft's motion. Force and momentum acting on body, moment of inertia and the angular velocity, symmetry on the axes of aircraft are used for the derivation of the formulas. The chapter has a crucial significance of the thesis because the equations are prerequisites for creating the lateral trajectory tracking algorithm to represent aircraft's motion and one of the main aims of the thesis which is the controlling of the aircraft. Also, the section uses all the previous chapters to derive motion such as the information about forces acting on the aircraft, axis movement and aircraft coordinate systems.

In Chapter 5, Flight Management System (FMS) is introduced. FMS is a complicated system which needs several inputs from outside and the other avionic systems. Furthermore, flight planning, trajectory prediction, lateral guidance and performance computation are the functional blocks of FMS which make it complicated and at the same time very important for this thesis to achieve generating paths and performance evaluation goals. RNAV-RNP standardization and types, navigation error terms and phases of a flight are given here to explain general concept which the algorithm uses for performance evaluation and flight safety. For the path generating aim, difference between conventional routes, RNAV and RNP, ARINC-424 Path-Terminator leg types and notation, transitions between legs are also served.

In Chapter 6, aircraft modeling, path algorithm design and the results of the studies are carried out. Base of Aircraft Data (BADA) is presented in the section to model the real aircraft's reactions in aircraft motion. The real aircraft data and the coefficients are described to make the algorithm's results more realistic. Path algorithm is designed in this chapter. The formulation of the path algorithm and the variation due to parameter change are the focus of the algorithm. The results of the studies show the results and simulations of the algorithm. The results include all the components of the

thesis which are path generation, controlling the motion, modelling the aircraft, lateral trajectory tracking and performance computation.

In Chapter 7, the summary of the studies is given as conclusions. The main idea of the thesis and the judgement of the results which are obtained are aimed to be explained and finalized.

CHAPTER 2

FUNDAMENTALS OF AIRCRAFT FLIGHT MECHANISM

This chapter provides general information about aircraft flight mechanism. In the beginning, the main forces of the aircraft and especially the lift force and airfoil structure of wings are the first aim of this section to be able to explain how an aircraft flies with physical facts.

The second aim is to explain control surfaces of the aircraft. How control surfaces make the aircraft move freely in three axes is going to be explained by using the main forces and the physical facts.

All the information targets to build a baseline for the thesis to understand and develop the rest.

2.1   Forces of Flight

There are four main forces which act on aircraft in air. These are called thrust, drag, lift, and weight that keep the aircraft in balance. Understanding how these forces work is very crucial for flight to work out how an aircraft flies and how to control them by using flight control surfaces. Four of the main forces are explained in detail below.
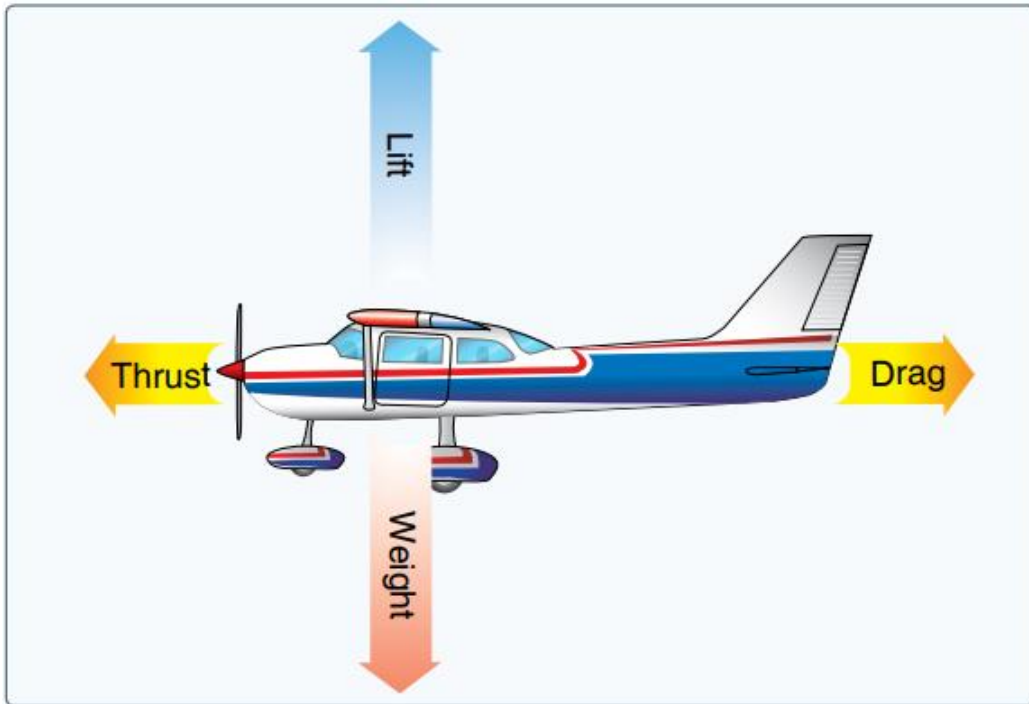
Figure 1 Forces acting on an aircraft

Thrust is a mechanical force produced by the aircraft engine to make the aircraft go forward by pushing air back. This force is also known as opposite force of drag. According to Newton's 3rd law, forces always occur in pairs which are opposite each other. Whether those forces are in balance or not determines the motion of aircraft from Newton's second law of motion which is defined as a net force equal to the change in momentum with a change in time. Momentum is defined to be the mass m of an object times its velocity V [2]. The Newton's laws of motion are given in Table 1.

Table 1 Basic Rules for Motion [3]

Newton's First Law	:	Every object persists in its state of rest or uniform motion in a straight line unless it is compelled to change that state by forces impressed on it
Newton's Second Law	:	Force is equal to the change in momentum per change in time. For a constant mass, force equals mass times acceleration
Newton's Third Law	:	For every action, there is an equal and opposite re-action
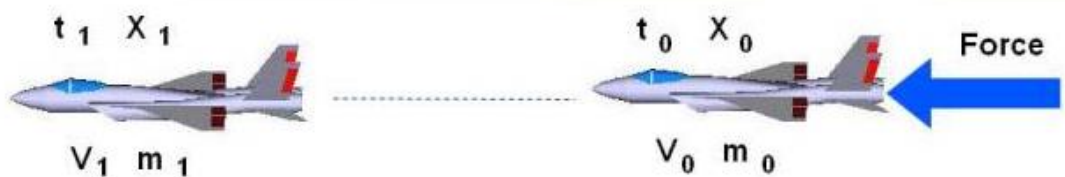
Figure 2 The second law of motion

The formula of the second law in shown in Figure 2 is expressed in Equation (2.5) where; the t is time, V is velocity, m is mass and a is acceleration.

$$\text{Force} = \text{Change of Momentum with Change of Time} \tag{2.1}$$

$$\text{Difference form:} \quad \vec{F}_{net} = \frac{m_1 \vec{V_1} - m_0 \vec{V_0}}{t_1 - t_0} \tag{2.2}$$

$$\text{With constant mass:} \quad \vec{F}_{net} = m \left(\frac{\vec{V_1} - \vec{V_0}}{t_1 - t_0} \right) \tag{2.3}$$

$$\vec{a} = \Delta V / \Delta t \tag{2.4}$$

$$\vec{F}_{net} = m\vec{a} \tag{2.5}$$

In Equation (2.3) and (2.5), velocity, acceleration, momentum and force are vector quantities. Furthermore, if an object accelerates, it means there must be a net force acting on it. A net force ($\vec{F}_{net}$) can be explained as the sum of all the forces acting on an object.

$$\vec{F}_{net} = \vec{F_1} + \vec{F_2} + \ldots + \vec{F_N} \qquad (2.6)$$

Equation (2.6) shows the sum of N forces acting on an object. In this context, thrust and drag are the forces which generate the net force for acceleration as shown in Figure 3. Drag opposes thrust and acts rearward parallel to the relative wind. In other words, this rearward, retarding force is caused by the wing, rotor, fuselage, and other protruding objects [2].
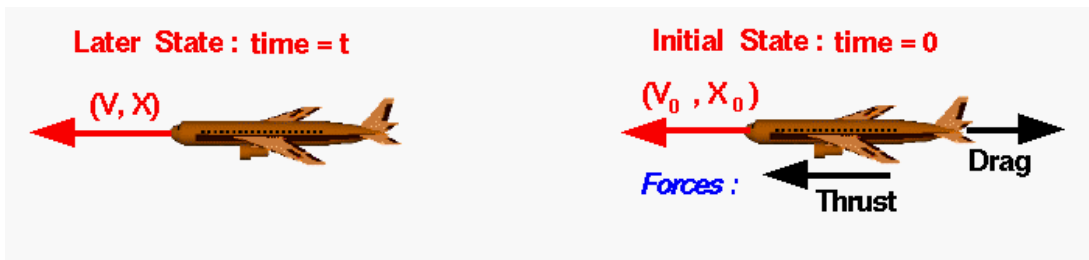
Figure 3 Newton's 2nd law on aircraft

$$\vec{F}_{net} = Thrust - Drag \quad \text{for aircraft} \qquad (2.7)$$

$$Acceleration = \begin{cases} No\ Acceleration, & Thrust = Drag \\ Positive\ Acceleration, & Thrust > Drag \\ Negative\ Acceleration, & Thrust < Drag \end{cases} \qquad (2.8)$$

Equation (2.8) shows the acceleration change depending on magnitudes of thrust and drag forces. In detail, when thrust and drag are equal, it means the aircraft is in balance

and has constant speed, in other words there is no acceleration. If thrust is greater than drag or vice versa, it is termed that the forces are unbalanced, and the aircraft has acceleration to the direction of the greater force. As a conclusion, aircrafts only get positive acceleration to move forward when thrust overcomes drag, otherwise aircrafts are pushed backward.

Lift is the force which makes aircraft differ from other vehicles by holding them in the air. The force is generated mostly by wings with Bernoulli's Principle. This principle is based on a theory which is called "Longer Path" theory, or "Equal Transit Time" theory. The wings of aircraft have a special curved shape whose name is "airfoil" to create different path distance between the upper side and the bottom side of the wing in Figure 4.
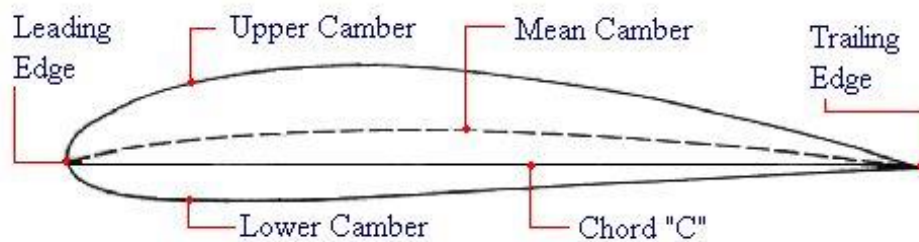
Figure 4 Airfoil

The forward part and rounded part of an airfoil is called the leading edge while the aft, narrow and tapered part is called the trailing edge. Chord is defined as an imaginary and straight line between the leading and trailing edges.

While the bottom side of airfoil looks flatter and shorter, the upper side of the airfoil has curved and long surface. When an aircraft moves through the air, air also moves over its surface. According to Equal Transit Time of Bernoulli's Principle, while moving, air separates two sides of airfoil at leading edge and the separated air must meet at the end of the airfoil which is trailing edge at the same time. To meet trailing edge at the same time, the air molecules which flow over the top must be faster than

the air molecules going underneath. This speed difference creates pressure difference which can be explained by Bernoulli's Equation which is given below [5].

$$Total\ Pressure\left(P_T\right) = Dynamic\ Pressure\left(P_D\right) + Static\ Pressure\ (P_S) \qquad (2.9)$$

$$P_D = \frac{\rho V^2}{2} \qquad (2.10)$$

$$P_S = P + \rho gh \qquad (2.11)$$

P = pressure
V = velocity
ρ = density
g = gravity
h = elevation

The Bernoulli equation is given below.

$$Energy\ per\ unit\ volume\ before =\ Energy\ per\ unit\ volume\ after \qquad (2.12)$$

$$\left(P_T\right)_1 = \left(P_T\right)_2 = Constant \qquad (2.13)$$

The Bernoulli Equation can be considered as statement of the conservation of energy principle which is appropriate for flowing fluids. There are two components of total air pressure which are dynamic and static pressure. Dynamic pressure refers to kinetic energy of the air, so velocity of the top must be higher to reach the trailing edge on time. Thus, dynamic pressure at the upper side is higher than the dynamic pressure at the bottom side in Figure 5. On the contrary, static pressure on the top is lower than static pressure underneath of airfoil to keep total pressures at both sides constant because of energy conservation. Thus, pressure difference can be mentioned between two sides as high-pressure area at the bottom, low-pressure area at the top. Fluids

always tend to move from high pressure zone to low pressure zone that creates a force on the airfoil from the bottom to the top which is known as lift force.
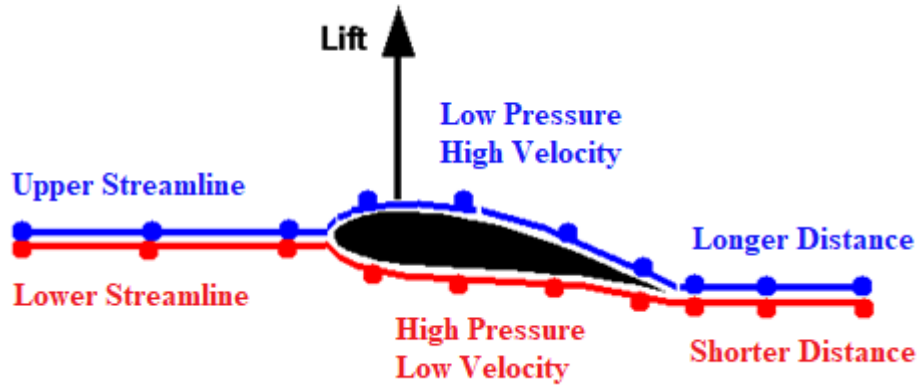
Figure 5 Bernoulli principle on airfoil

As thrust and drag are opposite forces, lift also has an opposite force which is known as weight. It is the total load of the aircraft itself, the crew, the fuel, and the cargo or baggage. The force also can be described as the force of gravity because it acts vertically downward through the aircraft's center of gravity (CG) [2]. For level flight which means flying at constant altitude, lift and weight must be in balance. As a result of the four forces, to be able to mention flying straight and level at a constant speed, lift must be in balance with weight, in the same way thrust must be equal to drag. On the contrary, when this balance disappear, aircraft starts rising or descending with vertical forces unbalance status as well as the speed of the aircraft goes up or down with horizontal forces change.

2.2   Control Surfaces

There are three imaginary axes through which aircraft can move around these lines in air. When aircraft rotates around an axis, it can be imagined as a wheel that rotates

11

around an axle. The lines are named as lateral axis, longitudinal axis and vertical axis as shown in Figure 6. Lateral axis is the line from one wing tip to the other wing tip and the movement around this axis is called pitch. Longitudinal axis lies from the nose of the aircraft to the tail and this movement is called roll. Vertical axis runs vertically through the center of the aircraft so that an aircraft can move around this line which is known as yaw.
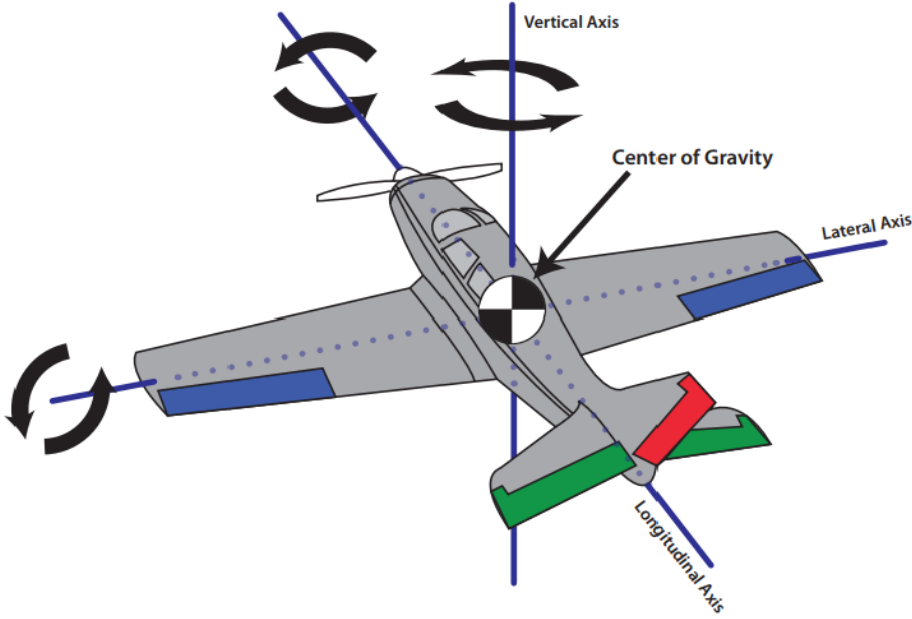
Figure 6 The axes of flight [6]

To be able to achieve these movement, a plane has three major surfaces on the structure of it which are called aileron, elevator and rudder. The detailed information of the surfaces is needed to understand how these mechanic surfaces work. Especially, which factors affect lift force is the main subject to enlighten air-lift relation on surfaces. Basically, Angle of attack (AoA) which is going to be explained later, airfoil shape, flow condition, airspeed and density make a difference on lift force. Using control

surfaces is mostly related to changing the shape of airfoil which increases or decreases lift force on the surfaces whose shape has been changed. As explained before in this thesis, airfoil has a special camber shape to create pressure difference between the upper and bottom sides of the wings. Also, according to the Bernoulli principle the air which comes across to the leading edge of the wing must meet at the trailing edge at the same time. Moreover, profile drag increases when it hits more surfaces. Based on these facts, if the camber side of the airfoil surfaces increases, air has longer path to arrive at the trailing edge. The faster the movement of the air, the more pressure difference it gets so lift effect increases because of this gap and vice versa for decreasing the surface area. Control surfaces' functions can be explained by using the information of imaginary axes and the effects which change the lift force as a base. The surfaces are illustrated on the aircraft in Figure 7.
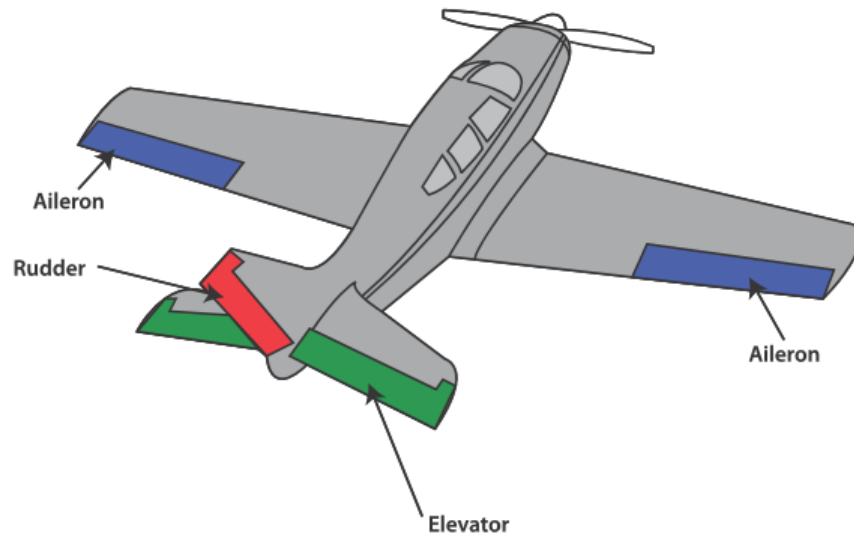
Figure 7 Control surfaces [6]

Aileron is located on the left and right main wings and let the aircraft make roll movement by working inversely meaning when one aileron goes up, the other one goes

down to create lift difference between the right and left wings. In detail, when aileron is going down, it increases airfoil surface and in the same way increases the lift force as shown in Figure 8. Thus, there is an opposite relation with ailerons movement and the lift on the wings.
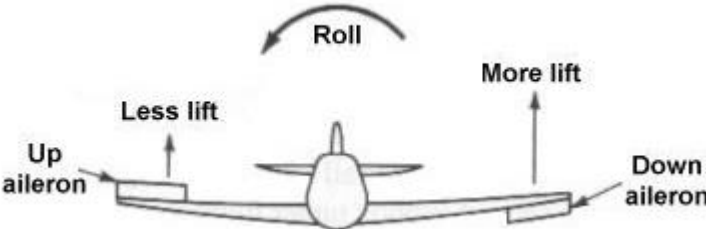
Figure 8 Ailerons position and roll

When aileron goes down, the wing goes up and similarly, when aileron is raised, the wing is lowered. Profile drag force on the raised aileron gets higher while lift is lower. The profile drag effect is presented in Figure 9.
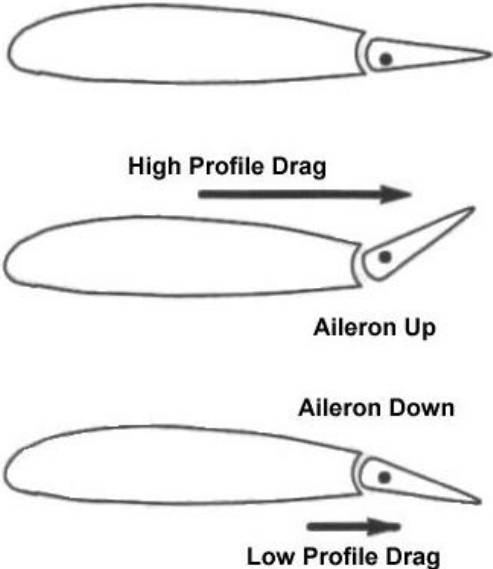
Figure 9 Profile drag

In addition to the main wings, there are two other small wings located on the tail part of the aircraft. These wings serve two main purposes on an aircraft which are to stabilize the airplane when the center of gravity and center of lift are not in line with one another and to allow the plane have pitch movement as shown in Figure 10.

Figure 10 Balancing duty of elevator

Elevators work together and at the same direction unlike ailerons but theoretically the operating logic is the same such that when the elevators go down, lift force increases and the tail goes up while nose goes down which is referred to as pitch-up. On the contrary, elevators on the up position have less lift force and more profile drag so it makes the nose move up and move the tail down termed as pitch-down. The movements which are created by elevators are given in Figure 11.
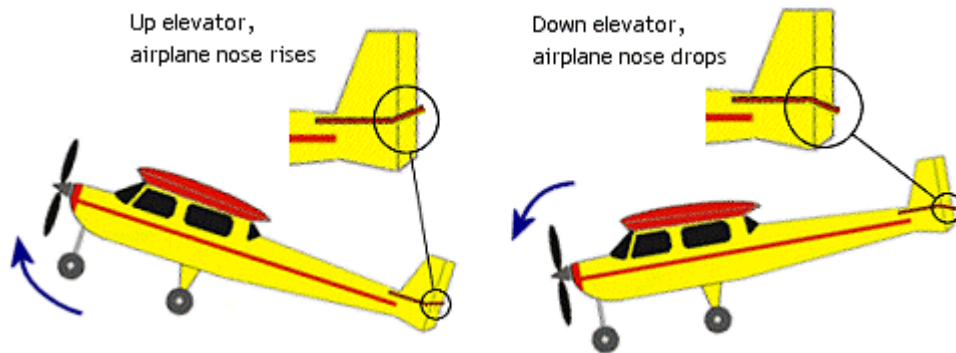
Figure 11 Elevators position and pitch

The last axis movement of aircrafts is yaw that is provided by rudder which is located on the vertical axis of the tail giving it the name vertical stabilizer. Rudder provides the capability to pilots to control the position of the nose of the aircraft on the vertical axis. If the rudder is applied to the left, the plane's nose goes left, and with the same logic, when the rudder turns to the right, the plane's nose moves right on the vertical axis as shown in Figure 12.
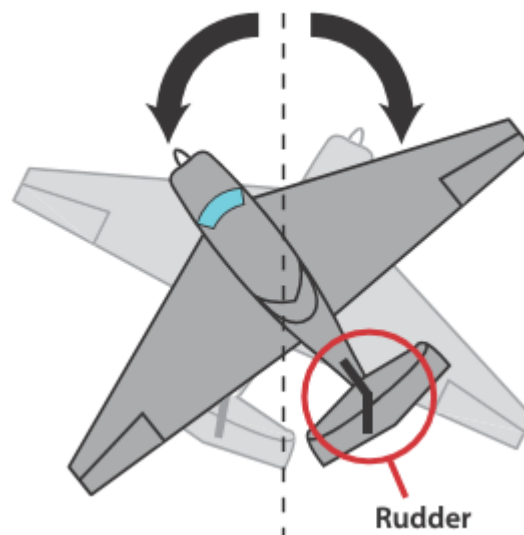
Figure 12 Rudder and yaw

Aileron, elevator and rudder can be classified as primary flight controls of aircraft. Furthermore, there are some mechanical systems that help to improve the control of the flight which are categorized as secondary flight controls. Flaps, spoilers, slats can be counted in this category. The primary and the secondary flight control systems of the aircraft are essential to keep an aircraft floating [2]. The summary information of parts of a plane is shown in Figure 13.
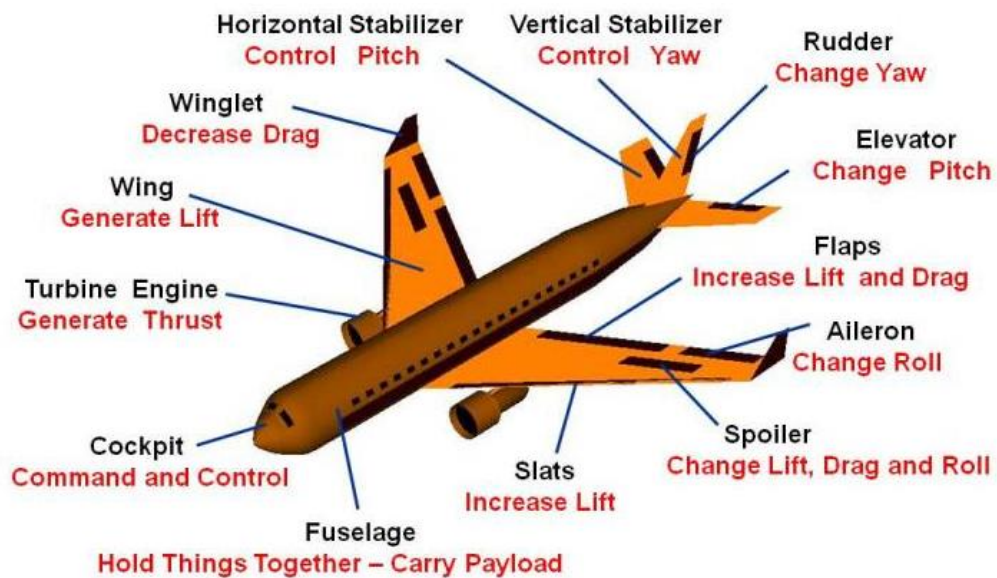
Figure 13 An overview of an airplane's parts and functions

CHAPTER 3

AIRCRAFT COORDINATE SYSTEMS

In this chapter, the coordinate systems which are used in aviation are presented. Firstly, the Aircraft reference coordinate systems are explained one by one. After that, the transformations between reference systems are explained and the transformation matrices are derived in the chapter.

3.1   Six Degrees of Freedom

Figure 14 Six degree of freedom

Figure 14 represents forces ($\vec{F}$), linear velocity ($\vec{V}$), and angular velocity ($\vec{W}$) on an airframe rigid body. They can be shown in vector form as below;

$$\vec{F} = \begin{bmatrix} x \\ y \\ z \end{bmatrix} , \quad \vec{V} = \begin{bmatrix} u \\ v \\ w \end{bmatrix} , \quad \vec{W} = \begin{bmatrix} p \\ q \\ r \end{bmatrix} \tag{3.1}$$

The aircraft is modelled with six degrees of freedom (6-DOF) which define the specific number of axes that a rigid body is abl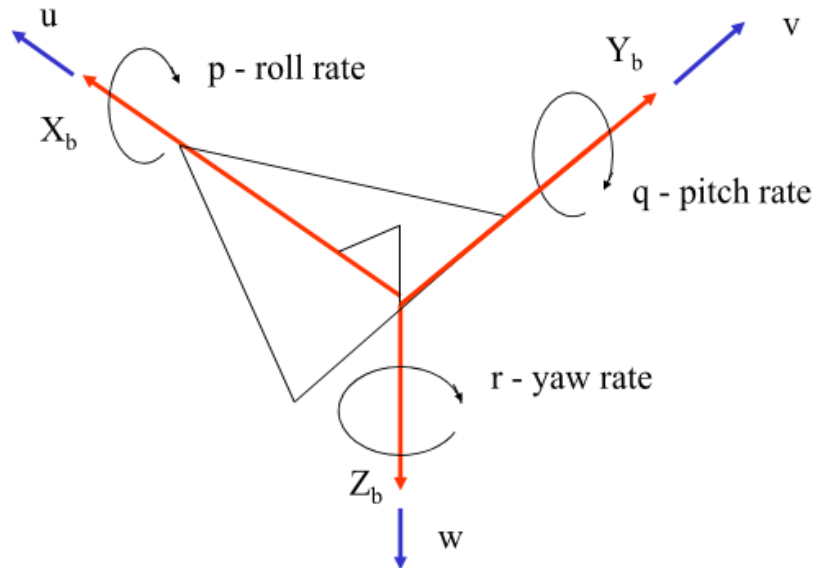e to freely move in three-dimensional space. These free movement on axes can be categorized as translational and rotational. Translational velocity of the aircraft is created by linear velocity vector $\vec{V} = \{u, v, w\}$ while rotational is from the angular velocity $\vec{W} = \{p, q, r\}$.

3.2   Aircraft Reference Coordinate Systems

To create a new mathematic model and algorithm for an aircraft, firstly the coordinate system where the model is going to be built on must be determined and how it is supposed to be used must be understood. Describing the motion of aircraft is a very complex phenomenon so suitable coordinate systems are supposed to be chosen to make this complexity as easy as possible to understand and turn into a mathematic model [7,9]. In this section, right-handed coordinate systems which are going to be used to characterize the forces and moments applied to aircraft motion will be presented.

3.2.1   Inertial (North-East-Down) Frame

The North-East-Down Frame (NED) axes are defined with the origin at the aircraft center of gravity, x-axis positive north, y-axis positive east, and z-axis positive down as in Figure 15 . For the purposes of this discussion, "down" represents the direction

20

from the aircraft center of gravity downward along the direction of the local gravity vector. Thus, the local gravity vector always points to the center of the earth. The Earth is considered spherical with uniform mass distribution [10]. Furthermore, the North-East plane of the NED frame is defined as horizontal plane.
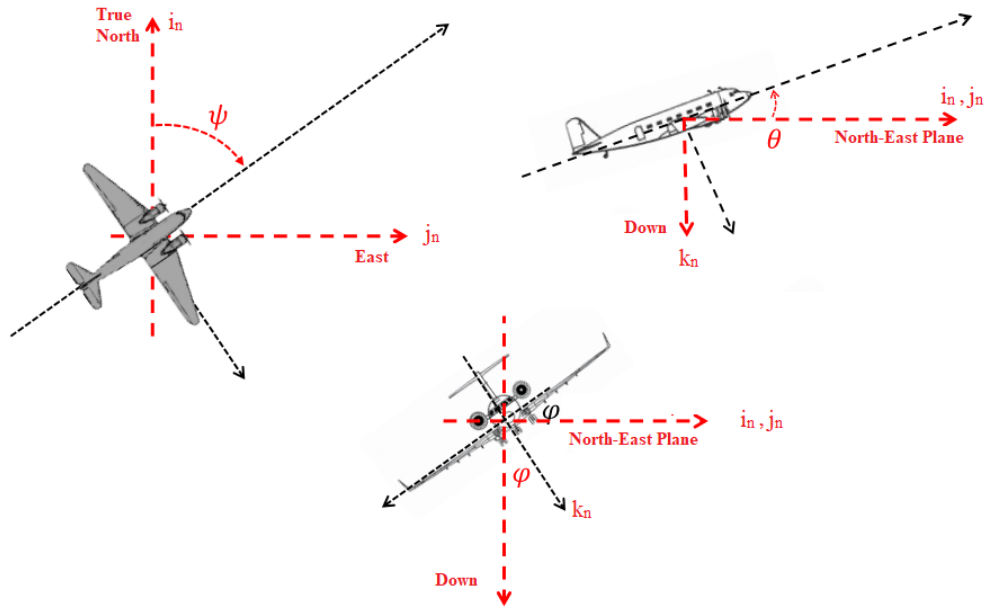
Figure 15 Inertial (North-East-Down) frame

3.2.2 Body Frame

The body frame is a coordinate system which is described on the fuselage of the aircraft. The mass origin is located at the center of gravity (CG) of the aircraft. The x-axis lies through nose direction of the body while the y-axis points the starboard wing. From the right-hand rule, z-axis points out downwards of the aircraft. In body frame, vectors are generally described with a subscript b as follows.

$$\vec{V}_b = \begin{bmatrix} u \\ v \\ w \end{bmatrix} \tag{3.2}$$

Figure 16 shows the body frame on the aircraft.
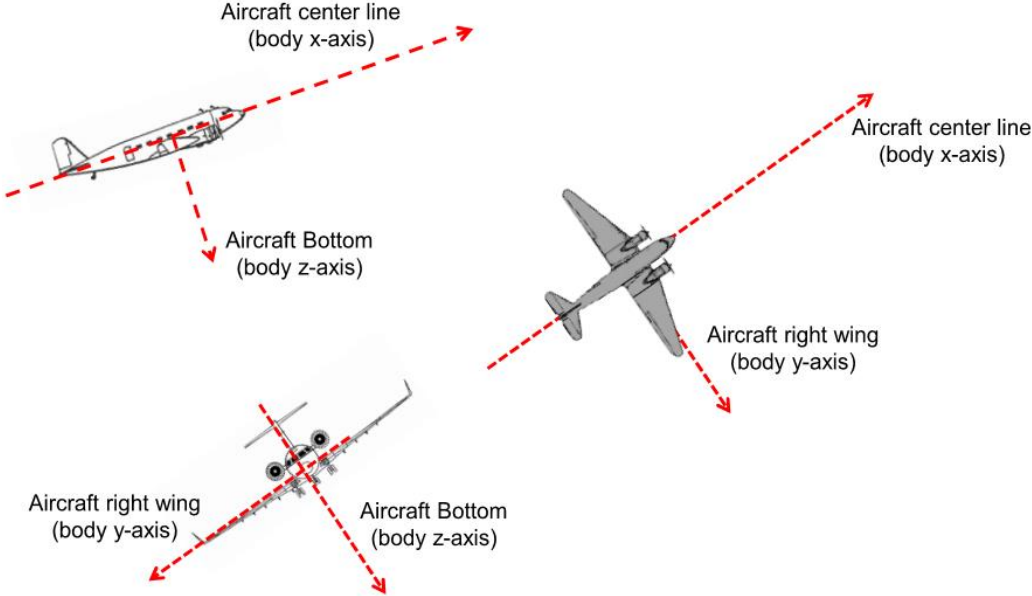
Figure 16 Body frame

3.2.3 Stability and Wind Axes

Stability and wind axes can be explained with a relationship between the velocity of the aircraft and the body axes. These axes have the same origin with body axes. However, they are not body fixed because their orientations change with the changes of the aircraft velocity vector. Stability, wind and body axes are illustrated in Figure 17.
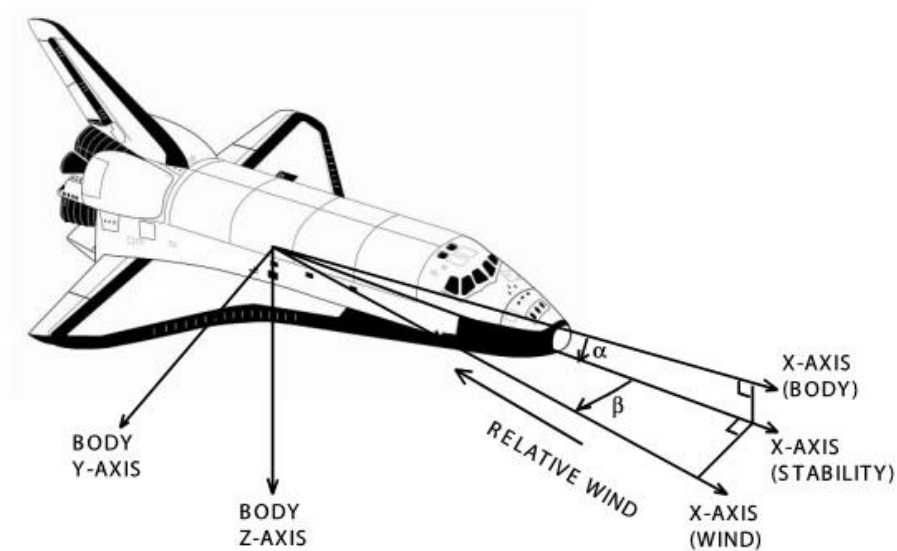
Figure 17 Wind and stability axes of aircraft

Figure 17 illustrated the wind and stability axes of the aircraft. As explained in Section 1, forces are generated while the aircraft moves through the air. To generate lift force, the wings must have a positive angle which is known as angle of attack (AoA) and is denoted by α. On the contrary of the other axes, the angle of attack is defined as a left-handed rotation about the body y-axis. Angle of attack is the angle between the body x-axis and the projection vector of the aircraft velocity vector.

The wind axes are formed by rotating about the stability z-axis to align the stability x-axis with the aircraft velocity vector. Side-slip is the angle between the aircraft velocity vector and the projection vector of the aircraft velocity vector. This angle is donated by β.
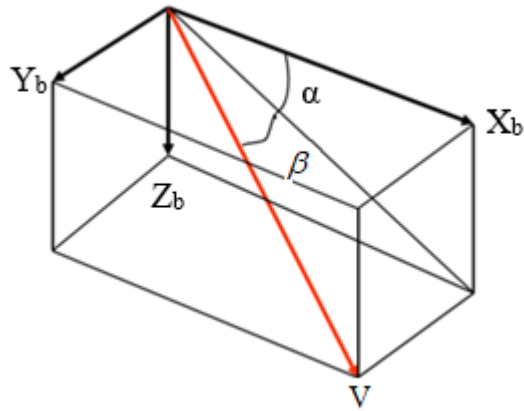
Figure 18 Angle of attack, side-slip and projection vector

The transformation between the stability and wind axes and between the stability axes and body axes are derived as follow;

$$u = V \cos \beta \cos \alpha \qquad (3.3)$$

$$v = V \sin \beta \qquad (3.4)$$

$$w = V \cos \beta \sin \alpha \qquad (3.5)$$

$$\begin{bmatrix} \mathbf{X} \\ \mathbf{Y} \\ \mathbf{Z} \end{bmatrix}_{STAB} = \begin{bmatrix} \cos \alpha & 0 & \sin \alpha \\ 0 & 1 & 0 \\ -\sin \alpha & 0 & \cos \alpha \end{bmatrix} \begin{bmatrix} \mathbf{X} \\ \mathbf{Y} \\ \mathbf{Z} \end{bmatrix}_{BODY} \qquad (3.6)$$

$$\begin{bmatrix} \mathbf{X} \\ \mathbf{Y} \\ \mathbf{Z} \end{bmatrix}_{WIND} = \begin{bmatrix} \cos \beta & \sin\beta & 0 \\ -\sin\beta & \cos \beta & 0 \\ 0 & 0 & 1 \end{bmatrix} \begin{bmatrix} \mathbf{X} \\ \mathbf{Y} \\ \mathbf{Z} \end{bmatrix}_{STAB} \qquad (3.7)$$

The stability and wind axes are used for derivation of flight motion dynamic equations such as lift, drag forces and pitching, rolling, yawing moments. These coordinate

systems are suitable for these calculations because the forces are normal to the airflow across the airframe.

3.2.4   Velocity Axes

Velocity axes depends on the velocity vector of an aircraft. The x-axis lies through velocity vector and the others are perpendicular to the x-axis. The axes and angles are shown in Figure 19.
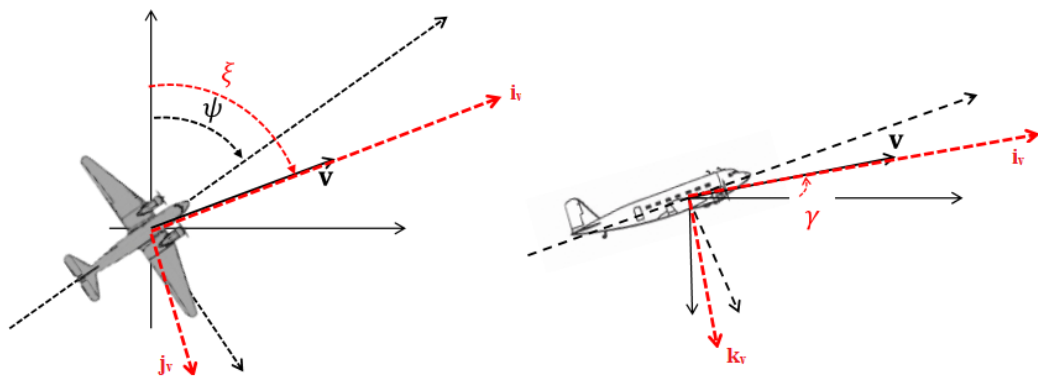
Figure 19 Velocity axes

ψ is the lateral heading angle from NED frame which shows the angle between true-north and x-axis of body frame. Similarly, 'ξ' is the angle between true-north and x-axis of velocity frame. 'γ' is called flight path angle which is the angle between x-axis of velocity frame and north-east plane. As it is explained in Stability and Wind Frames heading, the angle between x-axis of velocity frame and x-axis of body frame is known as angle of attack so there is a relationship between pitch angle (θ), flight path angle (γ) and angle of attack (α) when no side slip as shown below.

$$\theta = \gamma + \alpha \tag{3.8}$$
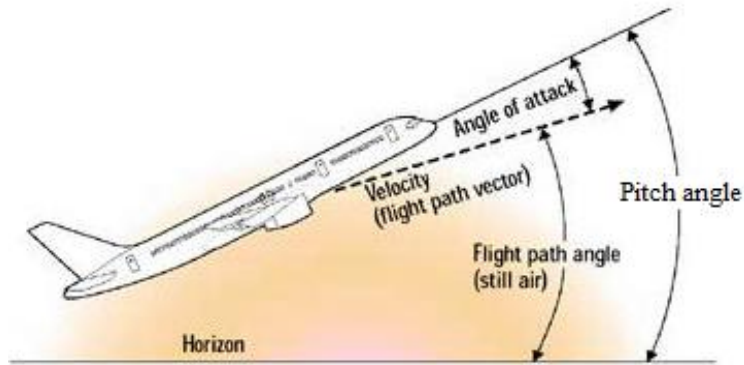
Figure 20 Relationship between pitch angle, flight path angle and angle of attack

During a level flight, flight path angle is equal to zero so $\theta = \alpha$ can be assumed.

3.2.5 Earth Frame

The Earth frame is described with an origin which is through the center of the Earth and Earth fixed axes. X axis points toward the mean meridian of Greenwich in equatorial plane, Z axis lies along with the spin axis of the Earth and through the north pole. X axis points toward the sphere of the earth at 0° latitude and 0° longitude which is known as meridian of Greenwich. Y axis is the orthogonal axis of x and z axes with respect to right hand rule.

Earth frame continuously rotates with an angular velocity of w.

$$w_{ie}^e = \begin{bmatrix} 0 & 0 & \Omega \end{bmatrix} \tag{3.9}$$

Ω is the angular speed of the earth and it is shown in equation (3.10).

$$\Omega = (7.2921150 \pm 0.0000001) \times 10^{-5} \text{ rad/sec} \tag{3.10}$$

3.3　Coordinate Transformation

To obtain flight motion dynamic equations, Cartesian coordinate systems are needed to be converted from one system to another. This is often the very problem in aviation where several coordinate systems are presented. There are several methods to explain the transformation between coordinate systems but mathematically, the problem can be resolved as simply by using matrix techniques. In this thesis, Direction Cosine Matrix (DCM) method is going to be used to carry out all transformations. Basically, there is an essential information needed in calculations which is aerodynamic angles between Cartesian coordinate systems. The vectors of one coordinate system must be chosen as 'base vectors' which means the quantities of the vectors do not change during the transformation. In other words, base vectors can be called reference-axes system while the other system which is under translation is pronounced as transformed-axes system. In this section, translation matrices between coordinate systems will be derived and presented.

$$\vec{V}_n = \begin{bmatrix} v_n \\ v_e \\ v_d \end{bmatrix}$$

Velocity Angles
(flight path angle, track)

Inertial Frame
(NED)

Euler Angles
(roll, pitch, yaw)

$\vec{V}$ Velocity Axes

Body Frame $\vec{V}_b = \begin{bmatrix} u \\ v \\ w \end{bmatrix}$

Bank Angle

Wind Axes

Airflow Angles
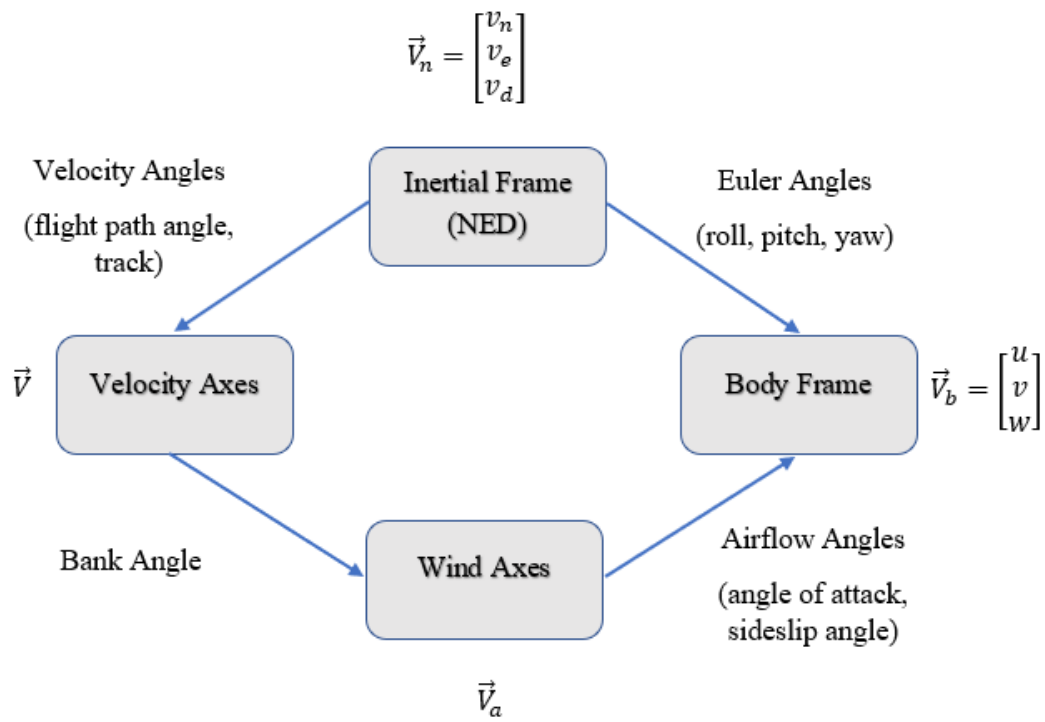(angle of attack, sideslip angle)

$\vec{V}_a$

Figure 21 Transformation between frames

3.3.1 Euler Transformation
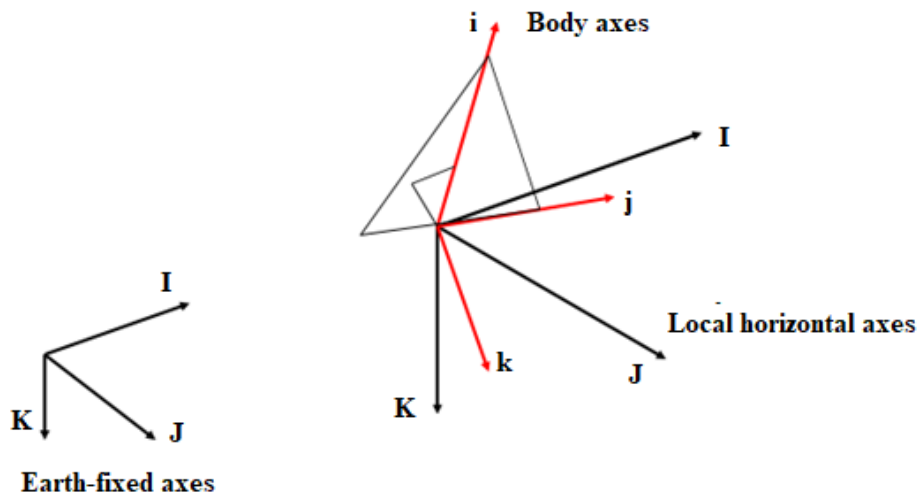
Figure 22 Earth fixed axes vs. body axes

28

Figure 22 represents basis vectors of earth fixed axes and body axes. To align the basis vectors of earth fixed axes I, J, K must be expressed in terms of the basis vectors of the body axes i, j, k. Euler angles are used for this alignment of body axes to earth frame or vice versa. There are three Euler angles which are called Yaw Euler angle (ψ), Pitch Euler angle (θ), and Roll Euler angle (ϕ). Step by step operation is needed to be derived transformation matrix between basis.

3.3.1.1 Transformation Matrix of Yaw Euler Angle

To provide Yaw Euler angle transformation, the z-axis of the earth frame and the z-axis of the first coordinate system must be aligned at first. After that, coefficients of the x-axis and y-axis of the earth frame can be transformed to first coordinate system with respect to ψ angle.
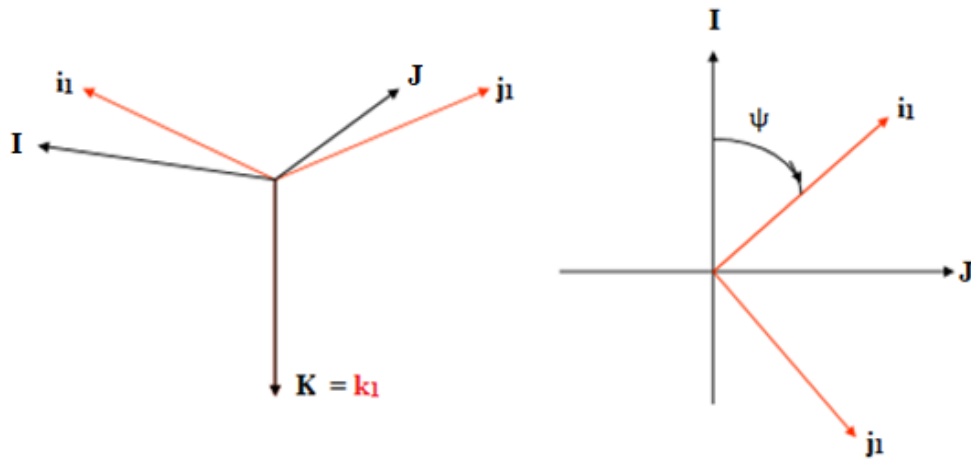
Figure 23 Transformation with Yaw Euler Angle

Figure 23 shows the axes of first coordinate system with i_1, j_1, k_1 and earth fixed frame with I, J, K. The vector of earth fixed frame is pronounced as base vector here. The coefficients of the yaw transformation matrix ($\begin{bmatrix} R_\psi \end{bmatrix}$) are shown in equation (3.11) and (3.12).

$$\begin{bmatrix} i_1 \\ j_1 \\ k_1 \end{bmatrix} = \begin{bmatrix} R_\psi \end{bmatrix} \begin{bmatrix} I \\ J \\ K \end{bmatrix} \tag{3.11}$$

$$\begin{bmatrix} i_1 \\ j_1 \\ k_1 \end{bmatrix} = \begin{bmatrix} cos\psi & sin\psi & 0 \\ -sin\psi & cos\psi & 0 \\ 0 & 0 & 1 \end{bmatrix} \begin{bmatrix} I \\ J \\ K \end{bmatrix} \tag{3.12}$$

3.3.1.2 Transformation Matrix of Pitch Euler Angle

In this step, i_1, j_1, k_1 are the components of new base vector. Second coordinate system i_2, j_2, k_2 can be obtained by using Pitch Euler angle transformation with θ angle and the new base vector. Components of second coordinate system are shown in Figure 24.
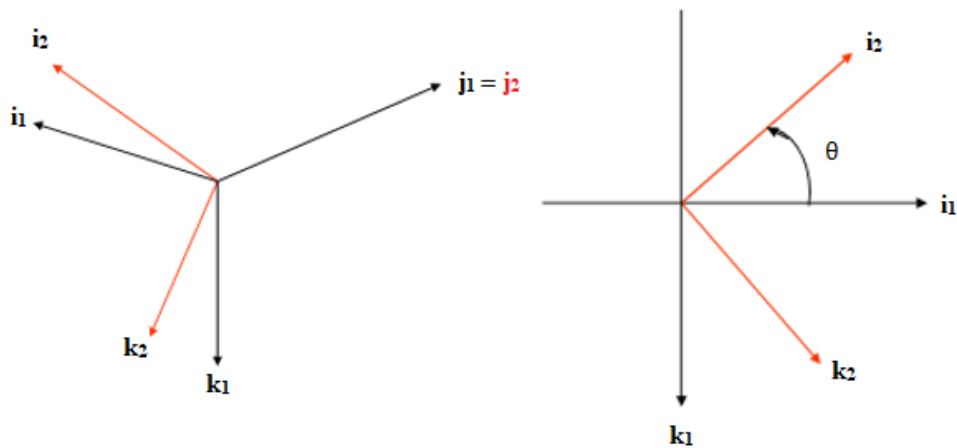
Figure 24 Transformation with Pitch Euler Angle

The coefficients of the pitch transformation matrix ($[R_\theta]$) are shown in equation (3.13).

$$\begin{bmatrix} i_2 \\ j_2 \\ k_2 \end{bmatrix} = [R_\theta] \begin{bmatrix} i_1 \\ j_1 \\ k_1 \end{bmatrix} \tag{3.13}$$

$$\begin{bmatrix} i_2 \\ j_2 \\ k_2 \end{bmatrix} = \begin{bmatrix} cos\theta & 0 & -sin\theta \\ 0 & 1 & 0 \\ sin\theta & 0 & cos\theta \end{bmatrix} \begin{bmatrix} i_1 \\ j_1 \\ k_1 \end{bmatrix} \tag{3.14}$$

3.3.1.3 Transformation Matrix of Roll Euler Angle

The second coordinate system is the new base vector for the roll transformation step. The base vector can be transformed into the body frame with respect to ϕ angle as shown in Figure 25.
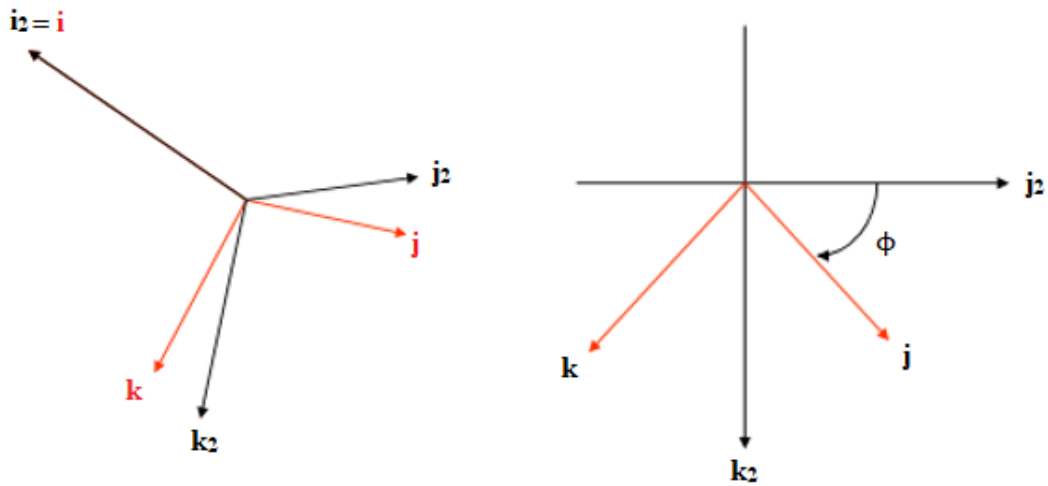
Figure 25 Transformation with Roll Euler Angle

The coefficients of the roll transformation matrix ($\begin{bmatrix} R_\phi \end{bmatrix}$) are shown in equation (3.15) and (3.16).

$$\begin{bmatrix} i \\ j \\ k \end{bmatrix} = \begin{bmatrix} R_\phi \end{bmatrix} \begin{bmatrix} i_2 \\ j_2 \\ k_2 \end{bmatrix} \tag{3.15}$$

$$\begin{bmatrix} i \\ j \\ k \end{bmatrix} = \begin{bmatrix} 1 & 0 & 0 \\ 0 & \cos\phi & \sin\phi \\ 0 & -\sin\phi & \cos\phi \end{bmatrix} \begin{bmatrix} i_2 \\ j_2 \\ k_2 \end{bmatrix} \tag{3.16}$$

32

Final step:

The transformation matrix between the body frame and earth frame can be determined by using matrix multiplication of transformation matrices of the roll Euler angle, pitch Euler angle and yaw Euler angle. The order of transformation matrices has a critical importance. The transformation from earth frame to body frame is shown in equation (3.17).

$$\begin{bmatrix} i \\ j \\ k \end{bmatrix} = \begin{bmatrix} R_\phi \end{bmatrix}\begin{bmatrix} R_\theta \end{bmatrix}\begin{bmatrix} R_\psi \end{bmatrix}\begin{bmatrix} I \\ J \\ K \end{bmatrix} \tag{3.17}$$

To be able to obtain inverse matrix, there is a highly important information here is that transformation matrix is orthogonal which means the inverse of the matrix is equal to the transpose of the matrix as shown in equation (3.18).

$$[R]^{-1} = [R]^T \tag{3.18}$$

By applying equation (3.18) to equation (3.17), equation (3.19) can be obtained.

$$\begin{bmatrix} I \\ J \\ K \end{bmatrix} = \left(\begin{bmatrix} R_\phi \end{bmatrix}\begin{bmatrix} R_\theta \end{bmatrix}\begin{bmatrix} R_\psi \end{bmatrix}\right)^{-1}\begin{bmatrix} i \\ j \\ k \end{bmatrix} = \begin{bmatrix} R_\psi \end{bmatrix}^T \begin{bmatrix} R_\theta \end{bmatrix}^T \begin{bmatrix} R_\phi \end{bmatrix}^T \begin{bmatrix} i \\ j \\ k \end{bmatrix} \tag{3.19}$$

Equation (3.20) illustrates the final transformation matrix from body frame to earth frame.

$$\begin{bmatrix} I \\ J \\ K \end{bmatrix} = \begin{bmatrix} cos\psi & -sin\psi & 0 \\ sin\psi & cos\psi & 0 \\ 0 & 0 & 1 \end{bmatrix}\begin{bmatrix} cos\theta & 0 & sin\theta \\ 0 & 1 & 0 \\ -sin\theta & 0 & cos\theta \end{bmatrix}\begin{bmatrix} 1 & 0 & 0 \\ 0 & cos\phi & -sin\phi \\ 0 & sin\phi & cos\phi \end{bmatrix}\begin{bmatrix} i \\ j \\ k \end{bmatrix} \tag{3.20}$$

3.4 Rotation Rates and Change in Aircraft Orientation

The angular velocity $\vec{W}$ is described as follow.

$$\vec{W} = p\boldsymbol{i} + q\boldsymbol{j} + r\boldsymbol{k} \qquad (3.21)$$

In equation (3.21), "p, q, r" are called rotation rates and referred to roll rate, pitch rate and yaw rate, respectively. There is a relationship between Euler angles (ψ, θ, ϕ) and rotational rates. Angular velocity vector can be written in terms of the rate of change in orientation as follows.

$$\vec{W} = \psi' \boldsymbol{K} + \theta' \boldsymbol{j}_1 + \phi' \boldsymbol{i}_2 \qquad (3.22)$$

In equation (3.22), remember the transformation between axes in Euler transformation chapter. Thus Equation (3.23), (3.24) and (3.25) can be obtained from the transformation.

$$\boldsymbol{K} = -\sin\theta\,\boldsymbol{i} + \cos\theta\sin\phi\,\boldsymbol{j} + \cos\theta\cos\phi\,\boldsymbol{k} \qquad (3.23)$$

$$\boldsymbol{j}_1 = \boldsymbol{j}_2 = \cos\phi\,\boldsymbol{j} - \sin\phi\,\boldsymbol{k} \qquad (3.24)$$

$$\boldsymbol{i}_2 = \boldsymbol{i} \qquad (3.25)$$

In the light of such information, if equations (3.23), (3.24) and (3.25) are written in terms of "i, j, k", the following matrix which shows the relation between rotational rates and change in orientation can be obtained.

$$\begin{bmatrix} p \\ q \\ r \end{bmatrix} = \begin{bmatrix} -\sin\theta & 0 & 1 \\ \cos\theta\sin\phi & \cos\phi & 0 \\ \cos\theta\cos\phi & -\sin\phi & 0 \end{bmatrix} \begin{bmatrix} \psi' \\ \theta' \\ \phi' \end{bmatrix} \qquad (3.26)$$

The inverse relation can be written by using inverse matrix. The inversion yields;

$$\phi^{'} = p + \left(q\,sin\phi + rcos\phi\right)\tan\theta \qquad (3.27)$$

$$\theta^{'} = q\,cos\phi - rsin\phi \qquad (3.28)$$

$$\psi^{'} = \left(q\,sin\phi + rcos\phi\right)\sec\theta \qquad (3.29)$$

3.5 Aerodynamic Forces on the Body Frame

Aerodynamic forces can be expressed in terms of angle of attack and side-slip which are mentioned in CHAPTER 2. Drag force, also called air resistance, is the opposite aero-force to aircraft velocity vector (V) whereas lift force is perpendicular to aircraft velocity vector. The force which is in the direction of the roll, and perpendicular to the flight path is called side force. The side force is a concept which is mostly used in connection with the turning of an aircraft. The derivation of these forces in terms of α and β is shown below.
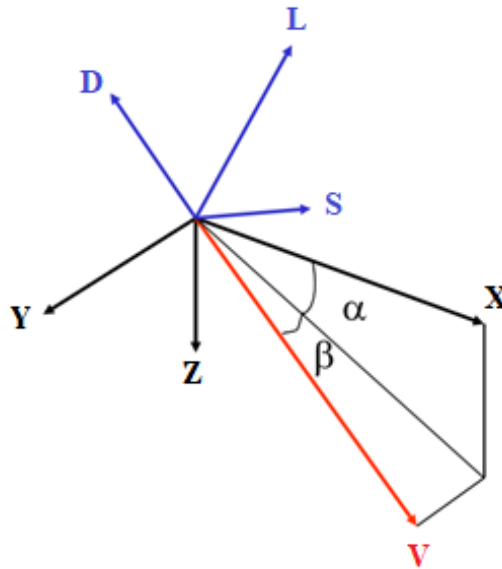

Figure 26 Forces on body frame

$$\begin{bmatrix} D \\ S \\ L \end{bmatrix} = \begin{bmatrix} \cos\beta & \sin\beta & 0 \\ -\sin\beta & \cos\beta & 0 \\ 0 & 0 & 1 \end{bmatrix} \begin{bmatrix} \cos(-\alpha) & 0 & -\sin(-\alpha) \\ 0 & 1 & 0 \\ \sin(-\alpha) & 0 & \cos(-\alpha) \end{bmatrix} \begin{bmatrix} X \\ Y \\ Z \end{bmatrix} \qquad (3.30)$$

$$D = -\left(X\cos\alpha + Z\sin\alpha \right)\cos\beta - Y\sin\beta \qquad (3.31)$$

$$S = \left(X\cos\alpha + Z\sin\alpha \right)\sin\beta - Y\cos\beta \qquad (3.32)$$

$$L = X\sin\alpha - Z\cos\alpha \qquad (3.33)$$

The inverse relation is also possible. Equations (3.31), (3.32) and (3.33) express the equations of axes in terms of angle of attack, side-slip, lift, drag and side-force.

$$X = L\sin\alpha + \left(S\sin\beta - D\cos\beta \right)\cos\alpha \qquad (3.34)$$

$$Y = -\left(S\cos\beta + D\sin\beta \right) \qquad (3.35)$$

$$Z = -L\cos\alpha + \left(S\sin\beta - D\cos\beta \right)\sin\alpha \qquad (3.36)$$

CHAPTER 4

FLIGHT MOTION DYNAMIC

4.1   Flight Motion Dynamic Derivation

The rigid body equations of motion are derived from Newton's 2nd law which is explained in CHAPTER 2. The time rates of change of linear and angular momentum are described in an inertial frame. To simplify the derivation of aircraft motion, Earth-fixed reference frame can be used as inertial frame. The expression of Newton's 2nd law is shown in equation (4.1) and equation (4.2).

$$\sum Force\ acting\ on\ body = \frac{d}{d_t}(\text{mV}) \tag{4.1}$$

$$\sum Moment\ acting\ on\ body = \frac{d}{d_t}(\text{H}) \tag{4.2}$$

The force and momentum acting on body can be written as vectoral form in three axes' components which are shown in below.

$$\vec{F} = \begin{bmatrix} f_x \\ f_y \\ f_z \end{bmatrix} \implies f_x = m\frac{d}{d_t}(\text{u}) \quad f_y = m\frac{d}{d_t}(\text{v}) \quad f_z = m\frac{d}{d_t}(\text{w}) \tag{4.3}$$

$$\vec{M} = \begin{bmatrix} L \\ M \\ N \end{bmatrix} \implies L = \frac{d}{d_t}(H_x) \qquad M = \frac{d}{d_t}(H_y) \qquad N = \frac{d}{d_t}(H_z) \tag{4.4}$$

In equation (4.3), f_x, f_y and f_z are obtained from derivation of the velocity components (u, v and w) on the x, y and z axes, respectively. There are three different kind of forces which are composed of contributions to the total aircraft force. These forces are the aerodynamic force (F_{aero}), propulsive force or thrust force (T) and gravitational forces (W) acting on the aircraft.

$$F = F_{aero} + T + W \tag{4.5}$$

$$F_{aero} = \{X_{aero}, Y_{aero}, Z_{aero}\} \tag{4.6}$$

$$T = \{T_X, T_Y, T_Z\} \tag{4.7}$$

$$W = Mg\{-\sin\theta, cos\theta sin\phi, cos\theta cos\phi\} \tag{4.8}$$

The moment equations in Equation (4.4) can be defined in a similar way as force components. L, M and N are the components of moment which is also the derivation of H_x, H_y and H_z on the x, y and z axes, respectively. Moreover, H_x, H_y and H_z are the components of angular momentum (H) which is expressed as the product of the moment of inertia (I) and the angular velocity (W_B).

$$H = I W_B \tag{4.9}$$

Equation (4.10) shows the transformation between the derivative of an arbitrary vector A referred to a rotating body frame having an angular velocity W and the derivative

of an arbitrary vector A on inertial frame. I and B refer to inertial and body frame, respectively.

$$\left[\frac{d}{d_t}(\text{A})\right]_I = \left[\frac{d}{d_t}(\text{A})\right]_B + W \, x \, A \tag{4.10}$$

Equation (4.10) can be applied to equation (4.11) as following.

$$\sum F = \left[\frac{d}{d_t}(\text{mV})\right]_I = m\left(\left[\frac{d}{d_t}(\text{V})\right]_B + W_B \, x \, \text{V}\right) \tag{4.11}$$

$$\sum F = m\left(\frac{d}{d_t}\begin{bmatrix} u \\ v \\ w \end{bmatrix} + \begin{bmatrix} p \\ q \\ r \end{bmatrix} x \begin{bmatrix} u \\ v \\ w \end{bmatrix}\right) \tag{4.12}$$

$$\sum F = m\left(\begin{bmatrix} \dot{u} \\ \dot{v} \\ \dot{w} \end{bmatrix} + \begin{bmatrix} qw - rv \\ -pw + ru \\ pv - qu \end{bmatrix}\right) \tag{4.13}$$

The scalar equations of force acting on aircraft are given in Equation (4.14), (4.15), (4.16).

$$\sum F_x = (\dot{u} + qw - rv)m \tag{4.14}$$

$$\sum F_y = (\dot{v} - pw + ru)m \tag{4.15}$$

$$\sum F_z = (\dot{w} + pv - qu)m \tag{4.16}$$

In the same way, Equation (4.10) can be used for moment acting on aircraft.

$$\sum M = \left[\frac{d}{d_t}(H)\right]_I = \left[\frac{d}{d_t}(H)\right]_B + W_B \times H \qquad (4.17)$$

In equation (4.17), the product of the moment of inertia (I) and the angular velocity (W_B) should be calculated to obtain angular momentum. From this product, the moment of inertia is determined as follows.

$$I = \begin{bmatrix} \int y^2 + z^2 dm & \int -xy dm & \int -zx dm \\ \int -yx dm & \int x^2 + z^2 dm & \int -yz dm \\ \int -xz dm & \int -zy dm & \int x^2 + y^2 dm \end{bmatrix} \qquad (4.18)$$

The terms I_{xx}, I_{yy} and I_{zz} are the principal moments of inertia of the body about the x, y and z axes, respectively.

$$I_{xx} = \int y^2 + z^2 dm \qquad (4.19)$$

$$I_{yy} = \int x^2 + z^2 dm \qquad (4.20)$$

$$I_{zz} = \int x^2 + z^2 dm \qquad (4.21)$$

The terms I_{xy}, I_{yz} and I_{zx} are the mixed indices which are pronounced as crossed moments of inertia.

$$I_{xy} = \int xy\, dm \qquad (4.22)$$

$$I_{yz} = \int yz\, dm \qquad (4.23)$$

$$I_{zx} = \int zx\, dm \qquad (4.24)$$

By using the terms of the principal moments of inertia and the crossed moments of inertia, the matrix in Equation (4.25) can be written as:

$$I = \begin{bmatrix} I_{xx} & -I_{xy} & -I_{xz} \\ -I_{xy} & I_{yy} & -I_{yz} \\ -I_{xz} & -I_{yz} & I_{zz} \end{bmatrix}$$

(4.25)

The crossed moments of inertia can be simplified based on the symmetry of the aircraft. For I_{xy} crossed moment, the contribution from the left side cancels the contribution from the right on each section along the X axis. Because of this symmetry, cross moment on X-Y plane equals to zero.
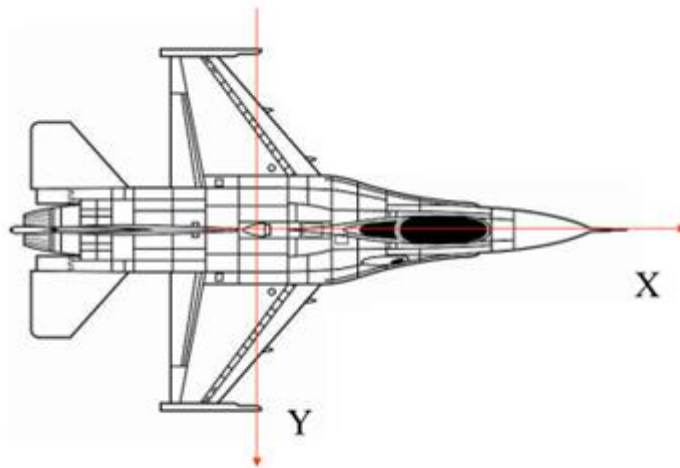
$$I_{xy} = 0$$

(4.26)

Figure 27 Symmetry on X-Y plane

In the same way, due to the symmetry of each section along the Z axis, contribution from each side cancels each other so the cross moment on Y-Z plane equals to zero.
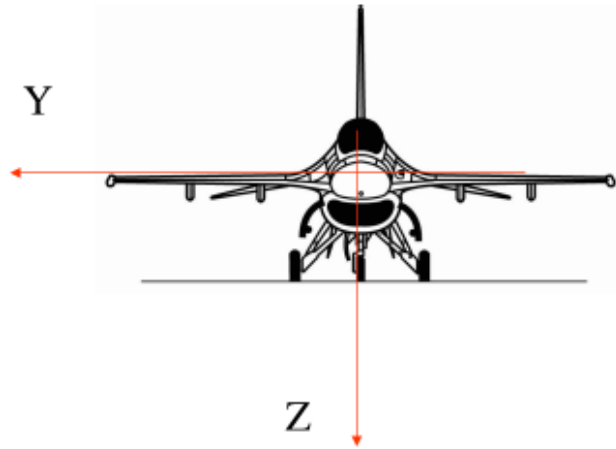
$$I_{yz} = 0$$

(4.27)

41

Figure 28 Symmetry on Y-Z plane

As it is shown in Figure 29, there is no symmetry along the Z axis or X axis so cross moment contribution on X-Z plane can't be canceled.
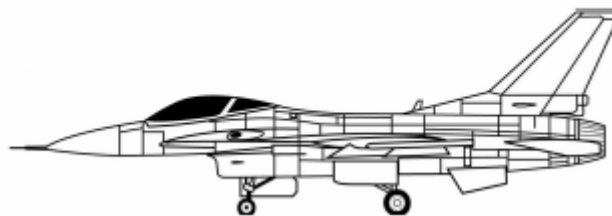

Figure 29 Symmetry on X-Z plane

After modifying inertia matrix with the symmetry on the axes, the new matrix is obtained as shown below.

$$I = \begin{bmatrix} I_{xx} & 0 & -I_{xz} \\ 0 & I_{yy} & 0 \\ -I_{xz} & 0 & I_{zz} \end{bmatrix} \qquad (4.28)$$

In view of such information, the moment equations of aircraft can be written as in Equation (4.29), (4.30), (4.31).

$$\sum M_x = L = I_{xx}p^{'} + \left(I_{zz} - I_{yy}\right)qr - I_{xz}(r^{'} + pq) \tag{4.29}$$

$$\sum M_y = M = I_{yy}q^{'} + \left(I_{xx} - I_{zz}\right)pr - I_{xz}(r^2 - p^2) \tag{4.30}$$

$$\sum M_z = N = I_{zz}r^{'} + \left(I_{yy} - I_{xx}\right)pq - I_{xz}(p^{'} - qr) \tag{4.31}$$

4.2   Motion Equations

Flight motion formulas are derived from all the information about forces acting on the aircraft, axis movement and aircraft coordinate systems. Mainly two motions can be mentioned while deriving the equations which are vertical motion and lateral motion. Vertical motion is calculated based on the angles which are pitch angle, flight path angle and angle of attack. The figure and equation of vertical motion are given in below.
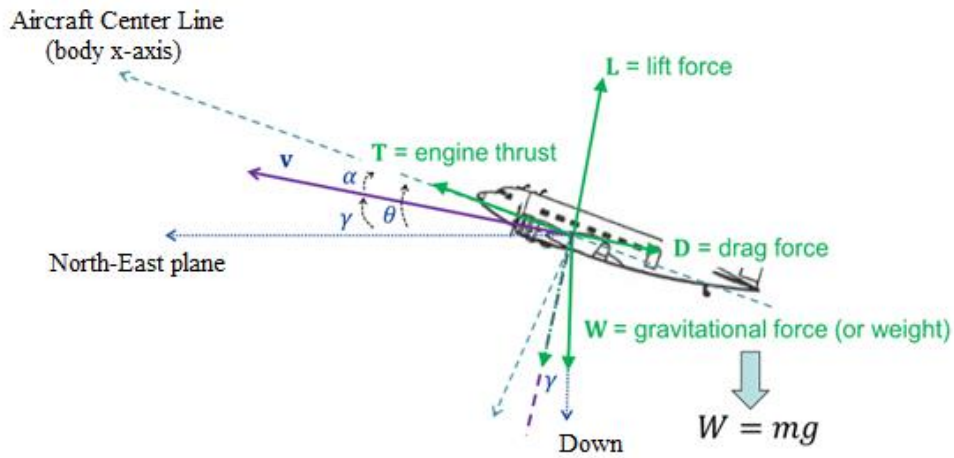
Figure 30 Vertical motion

$$T = T\cos\alpha i_w - T\sin\alpha k_w \qquad (4.32)$$

$$D = -Di_w \qquad (4.33)$$

$$L = -Lk_w \qquad (4.34)$$

$$W = -W\sin\gamma i_w + W\cos\gamma k_w \qquad (4.35)$$

Equation (4.32), (4.33), (4.34) and (4.35) describe the forces with the vectoral components of the axis. From the force theorem the equations below are obtained.

$$F = m\frac{d}{d_t}(V) = m\dot{V} = T\cos\alpha - D - W\sin\gamma \qquad (4.36)$$

$$m\dot{\gamma}V = T\sin\alpha + L - W\cos\gamma \qquad (4.37)$$

44

The component of velocity vector on the vertical axis provides the opportunity to change the height of the aircraft as shown in equation (4.38).

$$\dot{h} = V \sin \gamma \qquad (4.38)$$

In the similar way, the lateral component of the velocity vector gives the change in the distance.

$$\dot{r} = V \cos \gamma \qquad (4.39)$$

Fuel consumption changes by thrust force, velocity vector and fuel burning rate which is shown in equation (4.40).

$$\dot{W} = -\dot{m}_{fuel} = -\eta(V)T \qquad (4.40)$$

The lateral motion is based on centripetal force and bank angle as shown in Figure 31 and equations (4.41), (4.42).
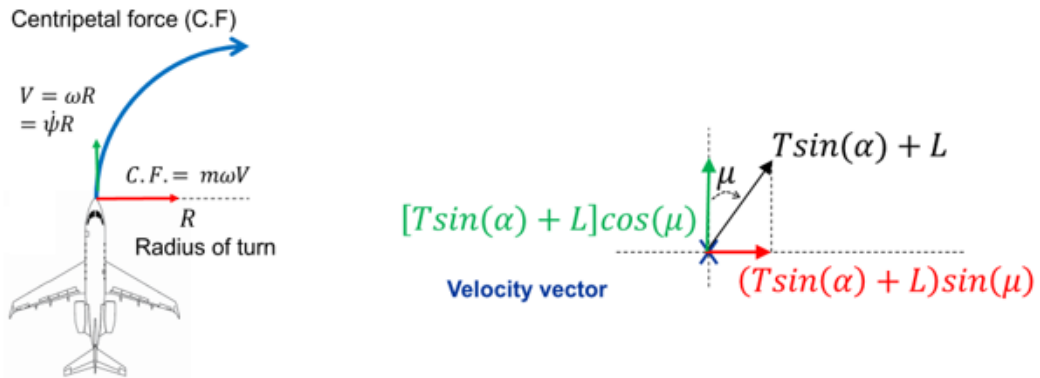

Figure 31 Lateral motion

The change in lateral heading angle is calculated by bank angle, total vertical forces and the change in distance. Bank angle also affects flight path angle in equation (4.42).

$$m\dot{\psi}V \cos \gamma = (T \sin \alpha + L) \sin \mu \qquad (4.41)$$

$$m\dot{\gamma}V = (T\sin\alpha + L)\cos\mu - W\cos\gamma \tag{4.42}$$

From all the equations above, the vector which includes changes of velocity, lateral heading angle, flight path angle, height, distance and weight is obtained to calculate motion dynamics of the aircraft in this thesis.

$$f(V,\psi,\gamma,h,r,W) = \begin{bmatrix} \dot{V} \\ \dot{\psi} \\ \dot{\gamma} \\ \dot{h} \\ \dot{r} \\ \dot{W} \end{bmatrix} = \begin{bmatrix} \left(\dfrac{g}{W}\right)(T\cos\alpha - D - W\sin\gamma) \\ \left(\dfrac{g}{WV\cos\gamma}\right)(T\sin\alpha + L)\sin\mu \\ \left(\dfrac{g}{WV}\right)\{(T\sin\alpha + L)\cos\mu - W\cos\gamma\} \\ V\sin\gamma \\ W\cos\gamma \\ -\eta(V)T \end{bmatrix} \tag{4.43}$$

The changes are used to determine current values of the aircraft by adding the changes (ΔV, $\Delta\psi$, $\Delta\gamma$, Δh, Δr, ΔW) in the previous values.

CHAPTER 5

FLIGHT MANAGEMENT SYSTEM

Flight Management System (FMS) aims to supply critical information about flight planning, trajectory prediction, lateral and vertical guidance and performance computation to the aircraft from the beginning of the flight to the end.

FMS has replaced the old conventional methods with its functionality in fuel efficiency, high-level safety, minimum pilot workload and low operating costs.

The systems need several information from the avionic system's equipment to compute FMS data like Air Data Computer (ADC), engine and fuel system, surveillance system, data entries, navigation information from the receivers etcetera. Figure 32 illustrates all the inputs flight management system gathers from several interfaces.
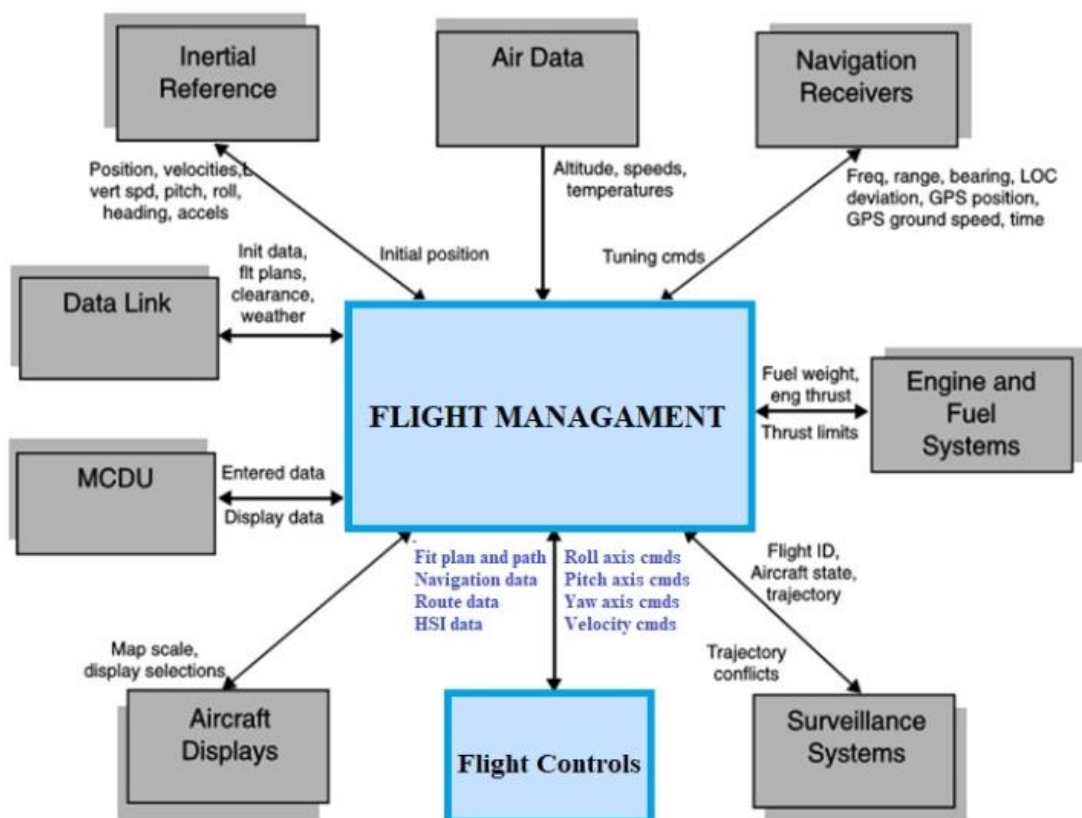
Figure 32 Inputs of FMS

In this thesis, flight control block is in the focal point to develop the FMS algorithm by using the other inputs. The algorithm has five essential functions which are navigation, flight plan, trajectory prediction, performance, guidance. The functional blocks of the system are given in Figure 33.
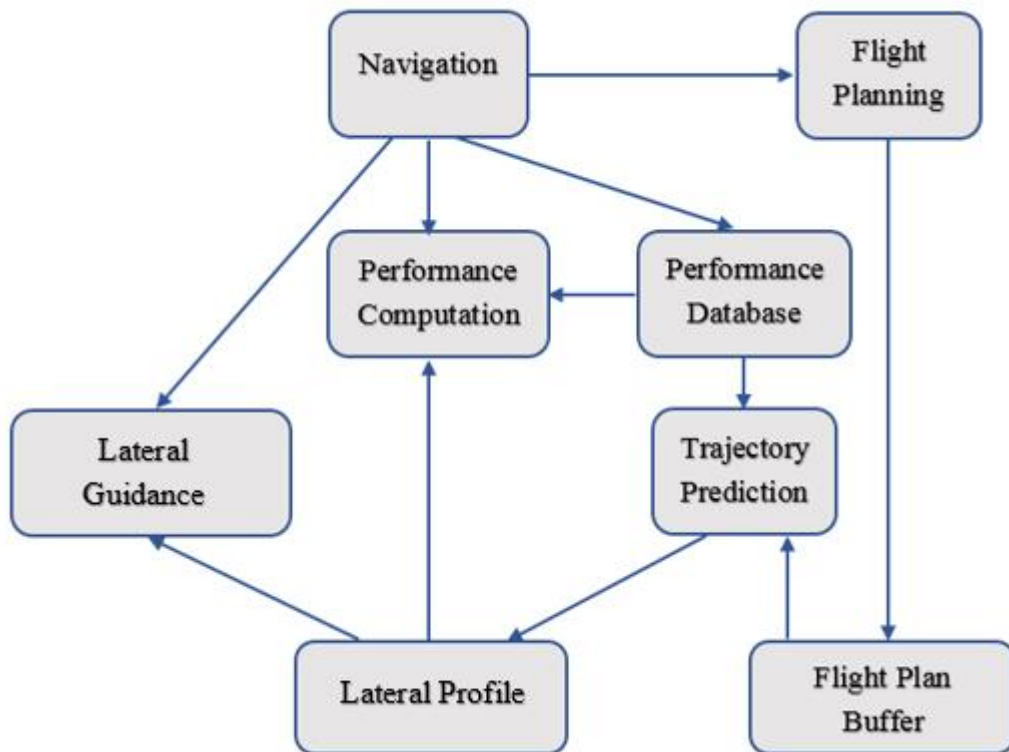
Figure 33 Functional block diagram

5.1 RNAV-RNP

RNAV is the abbreviation of area navigation. According to the International Civil Aviation Organization (ICAO), RNAV is defined as "A method of navigation which permits aircraft operation on any desired flight path within the coverage of the station-referenced navigation aids or within the limits of the capability of self-contained aids, or a combination of these." [18,19].

There are three different types of RNAV which are 2-dimension, 3-dimension and 4-dimension RNAV. While 2-dimension RNAV can give information for horizontal plane, 3-dimension RNAV can provide an opportunity for vertical guidance too. Moreover, 4-dimension RNAV supplies additional time function information to the

aircraft. Two main guidance concepts can be mentioned here that are LNAV and VNAV. These are the specific names of RNAV according to their guidance plane. LNAV is lateral navigation which provides lateral guidance to the aircraft while VNAV supplies vertical navigation.

There are some ground-based and satellite-based navigation sources which provide navigation information to RNAV. To find aircraft's position, VOR (VHF Omni-directional Radio Range), DME (Distance Measurement Unit), ILS (Instrument Landing System), ADF (Automatic Direction Finding) are used as ground-based navigation sources. Global Navigation Satellite Systems (GNSS), mostly known as GPS, is extremely useful to obtain an accurate VNAV information in three-dimensional position and in the same way supply highly accurate LNAV information in two-dimensional position. There is also a specific avionic equipment on aircraft which provide position information without the need for outside information which is called INS (Inertial Navigation System). This equipment generates its own position information with its sensors by using the first position information. INS can maintain guidance for a while without external sources but because of cumulative error, an external position information can be needed for correction.

Table 2 Navigation Sources

| Location	Avionics	Provides
Onboard	Air Data (ADC)	Pressure altitude, density altitude, OAT, TAS, EAS, AOA, etc.
	Inertial (INS)	Attitude, true heading, magnetic heading, position, velocity, groundspeed, track etc.
Space-based	Global Positioning System(GPS)	Position, velocity, groundspeed, track etc.
Terrestrial	Non-directional Beacon (NDB)	Bearing angle with respect to magnetic heading
	Distance Measuring Equipment (DME)	Slant range
	Tactical Air Navigation System (TACAN)	Slant range
	VHF Omnidirectional Range (VOR)	Bearing angle with respect to magnetic heading
Landings	Instrument Landing System (ILS)	Localizer and glideslope deviations
	Ground-Based Augmentation System (GBAS)	Localizer and glideslope deviations (ILS) corrections, integrity indicators
	Microwave Landing System (MLS)	Azimuth, elevation
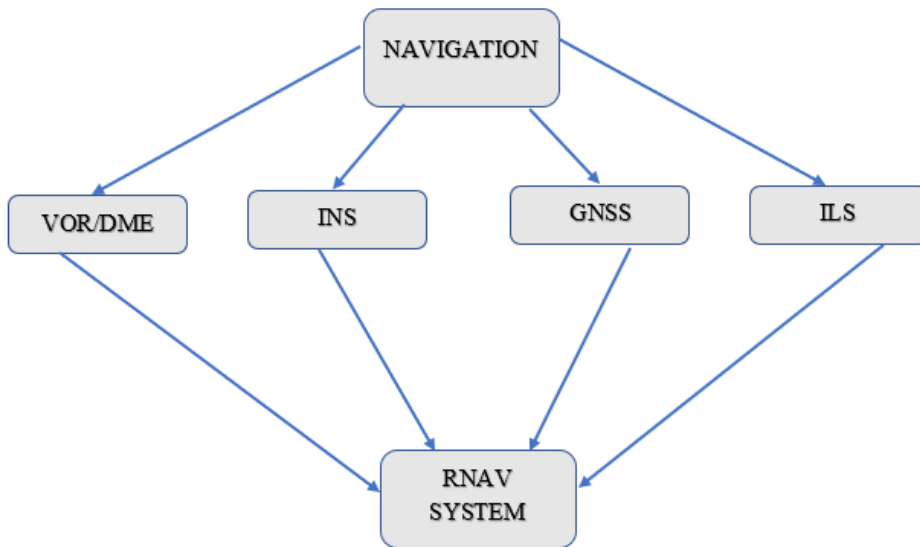
Figure 34 Inputs of RNAV

While mentioning RNAV, there is a very important concept which all legal aviation organizations work on that is Performance Based Navigation (PBN). Before explaining PBN, Required Navigation Performance (RNP) notion is supposed to be known. RNP lets aircrafts to be aviated in a specific path between two defined-waypoint with onboard alerting in space. PBN is a concept which is based on performance requirement on defined-route while aircraft operating. The main aim of PBN is to create a global standardization of RNAV and RNP specifications by identifying limitations for world-wide navigation specifications. Also, this standardization can provide some opportunities such as flying shorter distance with more efficient flight paths, increasing capacity of runways and in the air, reducing delays and fuel consumption.
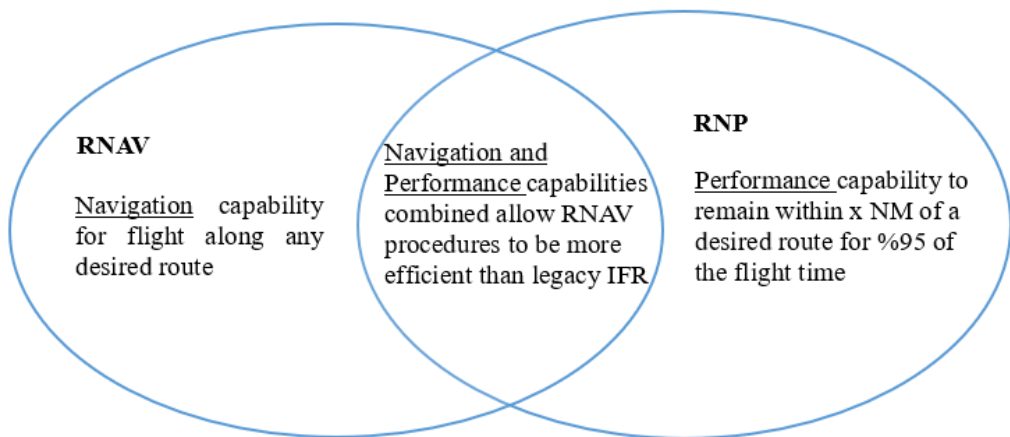
Figure 35 RNAV and RNP

Figure 35 shows the benefits of RNAV and RNP while working together. This concept has undeniable positive effects on navigation and performance. In Figure 36, three route design methods are illustrated to understand the difference between conventional route, RNAV and RNP.
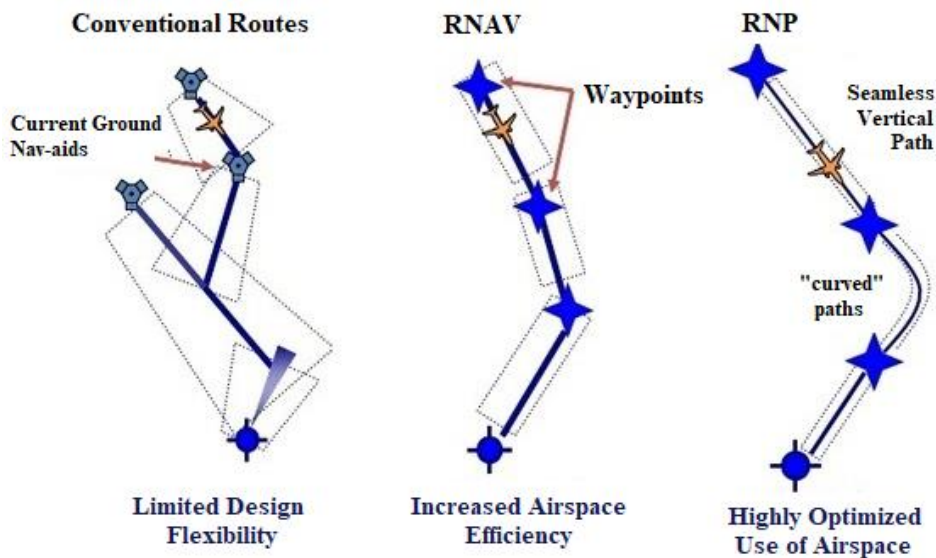

Figure 36 Conventional Routes, RNAV and RNP

5.2   Flight Plan

Flight plan means the roadmap which starts from the departure of the aircraft to arriving the destination. Waypoints, grounded navigation stations' information, routes, airport information, departure and arrival procedures are the basis of this plan.

Waypoint defines a specified geographical location with a longitudinal and latitudinal coordinate in space. To be able to fly from one waypoint to another waypoint, an area navigation route or a flight plan must be defined. In a flight, the complete flight plan is made of series of flight segments which is called phases of flight. The phases of flight can be categorized as take-off, climbing, cruise or en-route, descent and landing. Of course, some other steps can be counted as preparation of flight such as flight planning, taxing. The summary of flight phases is illustrated in Figure 37.
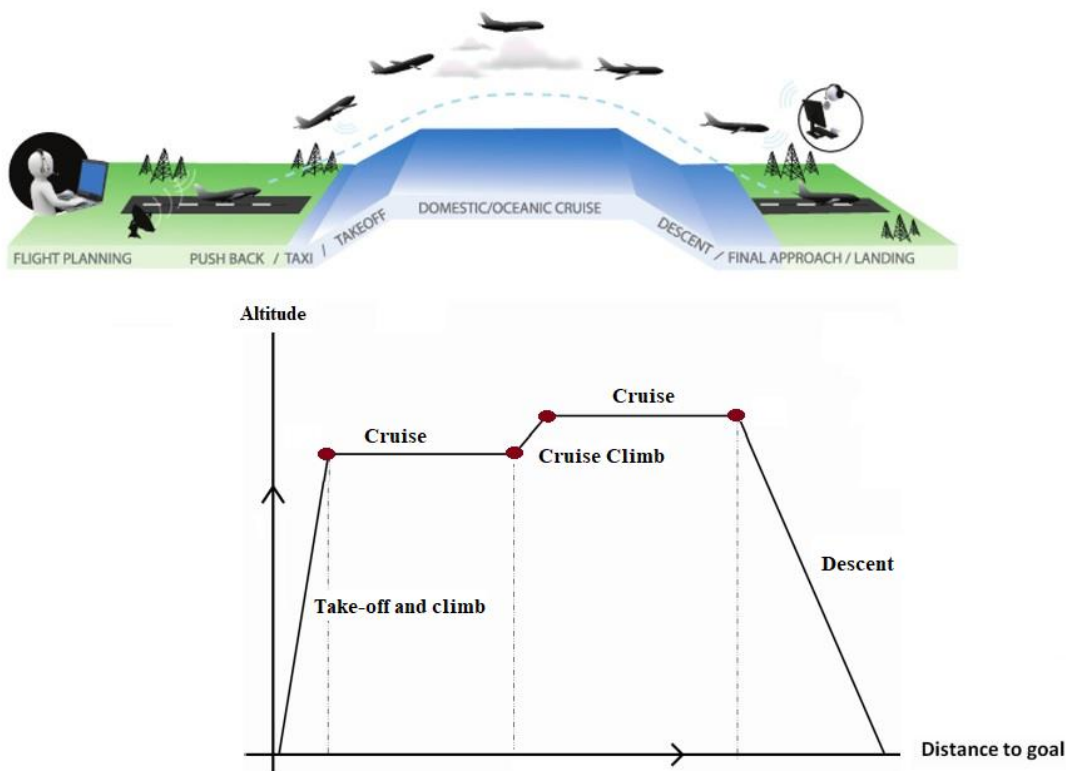

Figure 37 Phases of a flight

In every phase of flight, there are some specific procedures which pilots must carry out. Especially for take-off, descent, approach and landing phases, some standards and rules can be mentioned such as SID and STAR procedures. After take-off, a Departure procedure (SID or Standard Instrument Departure) is followed by pilots. The procedure is proceeded from take-off phase to the en-route phase and defines a pathway from runway to a waypoint on air to let the aircraft join the airway system in a controlled way.

STAR (Standard Terminal Arrival Route) is an arrival procedure which an aircraft follows before landing. This is proceeded from the en-route phase to an initial approach fix before landing so this helps the aircraft to leave the airway system in a controlled manner. An example of STAR is shown in Figure 38.
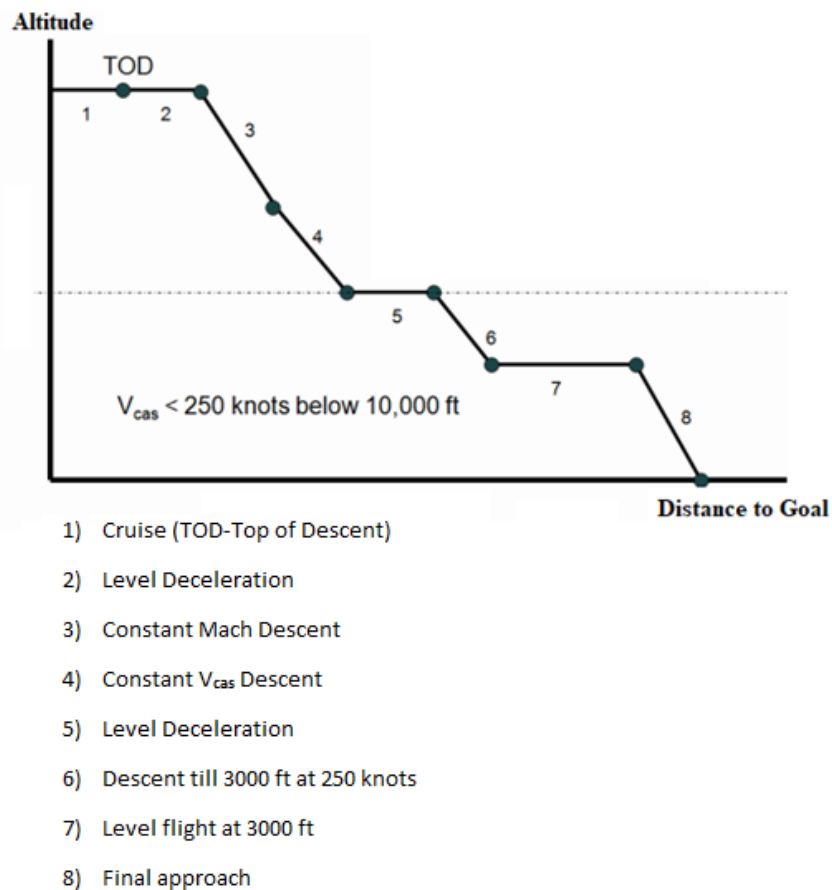

Figure 38 Standard terminal arrival route

SIDs and STARs are the procedures that aim to provide safe and efficient flights and keep the air traffic under control by using specific routings, levels, speed restrictions and check points. Basically, they provide opportunity to prevent potentially conflicting traffic.

Typically, flight plan consists of a set of points via waypoints and transitions with respect to some defined standards. ARINC-424 standard defines Path-Terminator Leg Types in use.

5.2.1 ARINC-424 Path-Terminator Leg Types

ARINC-424 standard defines a terminology for paths and terminators of an RNAV that are used from takeoff to en-route to landing. The Path and Terminator terminology aim to allow coding of Terminal Area Procedures, SIDs, STARs and Approach Procedures. Aircrafts with RNAV system use a sub-set of the ARINC 424 path terminators. Totally, there are 23 path terminators with its detailed information given in Table 4 are defined in the standard. 11 out of 23 have the majority for aircrafts to be able to fly RNAV SID, STAR and Approaches which are illustrated in Table 3 and Table 5.

Table 3 Leg and Terminator Notation

Leg Types	
Representation	**Definition**
Heading (V)	aircraft heading
Course (C)	fixed magnetic course
Track (T)	computed great circle path (slowly changing course)
Arc (A or R)	an arc defined by a center (fix) and a radius
Terminator Types	
Representation	**Definition**
Fix (F)	terminates at geographic location
Altitude (A)	terminates at a specific altitude
Intercept next leg (I)	terminates where leg intercepts the next leg
Intercept radial (R)	terminates where leg intercepts a specific VOR radial
Intercept distance (D or C)	terminates where leg intercepts a specific DME distance or distance from a fix
Manual (M)	leg terminates with crew action

Table 4 Path-Terminator Leg Types

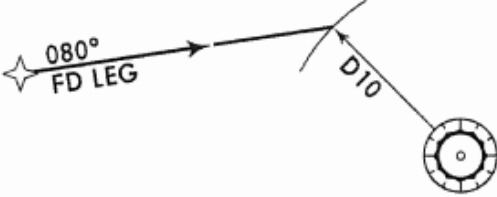| Leg Type	Figure	Explanation
IF		• The Initial Fix Leg defines a database fix as a point in space. • It is only required to define the beginning of a route or procedure.
TF		• Tract to a Fix defines a great circle track over ground between two known databases fixes • Preferred type for straight legs
RF		• Constant radius Arc Leg defines a constant radius turn between two databases fixes, lines tangent to the arc and a center fix
CF		• Course to a Fix Leg defines a specified course to a specific database fix • TF legs preferred over CF to avoid magnetic variation issues
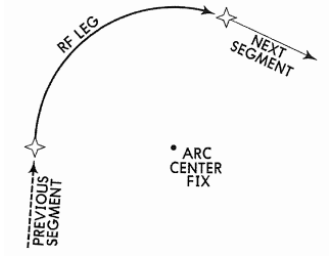
Table 4 Continued

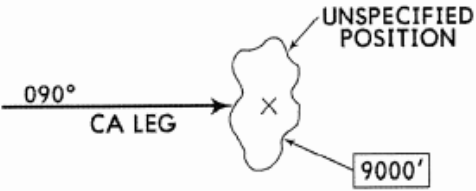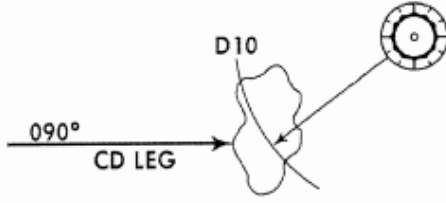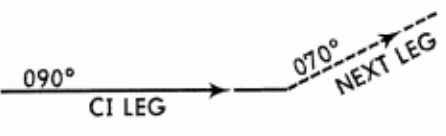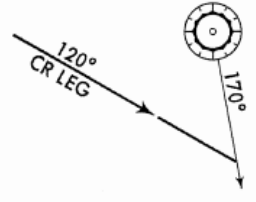| Leg Type	Figure	Explanation
DF		• Direct to a Fix Leg defines an unspecified track starting from an undefined position to a specified fix
FA		• Fix to an Altitude Leg defines a specified track over ground from a database fix to a specified altitude at an unspecified position
FC		• Track from a Fix to a Distance leg defines a specified track over ground from a database fix for a specific distance
FD		• Track from a Fix to a DME Distance Leg defines a specific track from a database fix to a specific DME Distance from a DME Navaid
FM		• From a Fix to a Manual Termination Leg defines a specified track over ground from a database fix until Manual termination of the leg
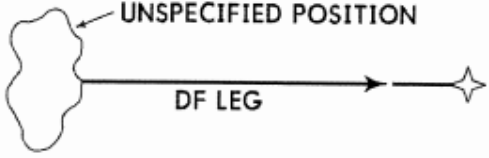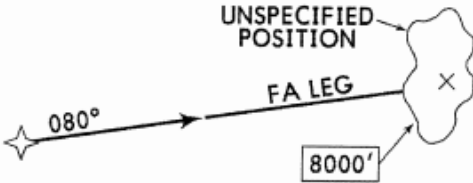
Table 4 Continued

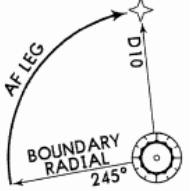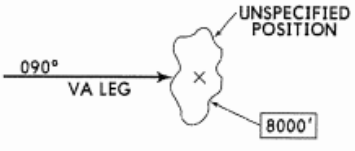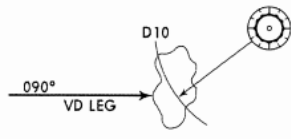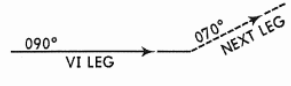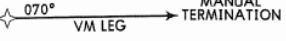| Leg Type	Figure	Explanation
CA		• Course to an Altitude Leg defines a specified course to a specified altitude at an unspecified position
CD		• Course to a DME Leg defines a specific course to a specific DME Distance which is from a specific database DME Navaid
CI		• Course to an Intercept Leg defines a specified course to intercept a subsequent leg
CR		• Course to a Radial termination Leg defines a course to a specified Radial from a specific database VOR Navaid
AF		• Arc to a Fix defines a track over ground at specified constant distance from a database DME Navaid

Table 4 Continued

Leg Type	Figure	Explanation
VA		• Heading to an Altitude termination Leg defines a specified heading to a specific Altitude termination at an unspecified position
VD		• Heading to a DME Distance termination Leg defines a specified heading terminating at a specified DME Distance from a specific database DME Navaid
VI		• Heading to an Intercept Leg defines a specified heading to intercept the subsequent leg at an unspecified position
VM		• Heading to a Manual termination Leg defines a specified heading until a Manual termination
VR		• Heading to a Radial termination Leg defines a specified radial from a specific database VOR Navaid
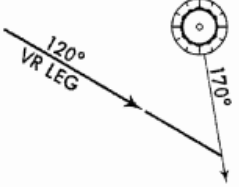
Table 4 Continued

Leg Type	Figure	Explanation
PI		• Procedure Turn leg defines a course reversal starting at a specific fix, includes Outbound Leg followed by 180 degree turn to intercept the next leg
HA		• HA leg defines racetrack pattern or course reversals at a specified database fix terminating at an altitude
HF		• HF leg defines racetrack pattern or course reversals at a specified database fix terminating at the fix after a single pattern
HM		• HM leg defines racetrack pattern or course reversals at a specified database fix with a manual termination
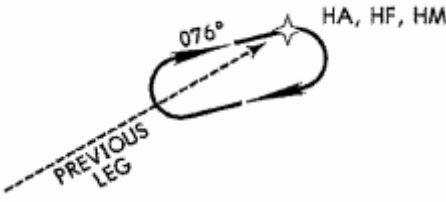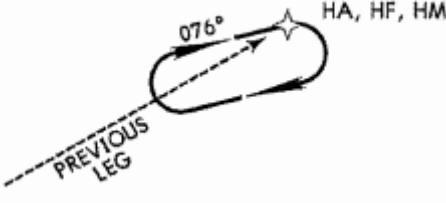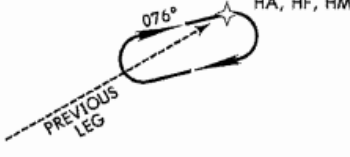
5.2.2 Path Terminator Coding Rules

In the standard, there are some specific path terminators to initiate and finalize the leg. Table 5 shows the initial and final legs of an RNAV procedure for SID, STAR, approach and missed approach.

Table 5 Initial and Final Path Terminators

RNAV Procedure	Initial Leg	Final Leg
SID	CA, CF, VA, VI	CF, DF, FM, RF, TF, VM
STAR	IF	CF, DF, FM, HM, RF, TF, VM
Approach	IF	CF, TF, RF
Missed Approach	CA, CF, DF, FA, HM, RF, VI, VM	CF, DF, FM, HM, RF, TF, VM

5.2.3 Transitions Between Legs

The route which aircraft flies on is called "leg" and it is also the way to go from one waypoint to another one. While navigating, flight management system (FMS) should draw the legs for pilot and autopilot to let them fly on a particular path.

To provide automatic transition between waypoints, two methods are in use. These are fly-by transition and fly-over transition. Fly-by transition means to pass near to a waypoint but not on it. Because of the aerodynamic limits, most of the aircrafts cannot do sharp turns so the aircraft can make a smoother transition by flying on an arc line. The transition is calculated with the formulas below.
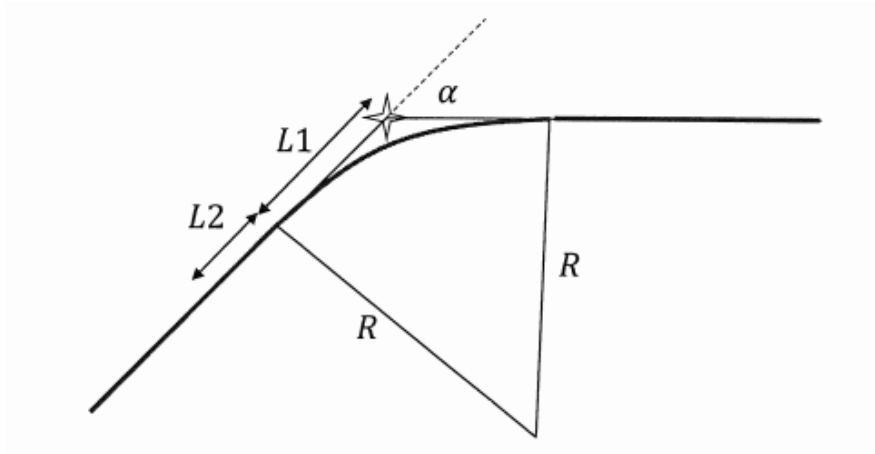
Figure 39 Fly by waypoint transition

$$R = \frac{V^2}{g \tan \varphi_{nominal}} \quad (5.1)$$

$$L = L_1 + L_2 \quad (5.2)$$

$$L_1 = R \tan 0.5\alpha \quad (5.3)$$

$$L_2 = cV \quad (5.4)$$

The formulas above are for the calculation of fly-by transition arc where α is the track/course change, L is the turn indication distance, L_2 is the roll in distance, c is the bank establishment time and V is the speed in m/s.

Fly-over waypoint as the name implies means to fly over the waypoint. In the similar way, to be able to follow the trajectory within its limitations, a suitable path is needed. Figure 40 and equation (5.5), (5.6), (5.7), (5.8), (5.9) and (5.10) illustrate the method to create the transition where α is the track/course change, L is the turn indication distance, r_1 is the roll-in radius and r_2 is the roll-out radius.
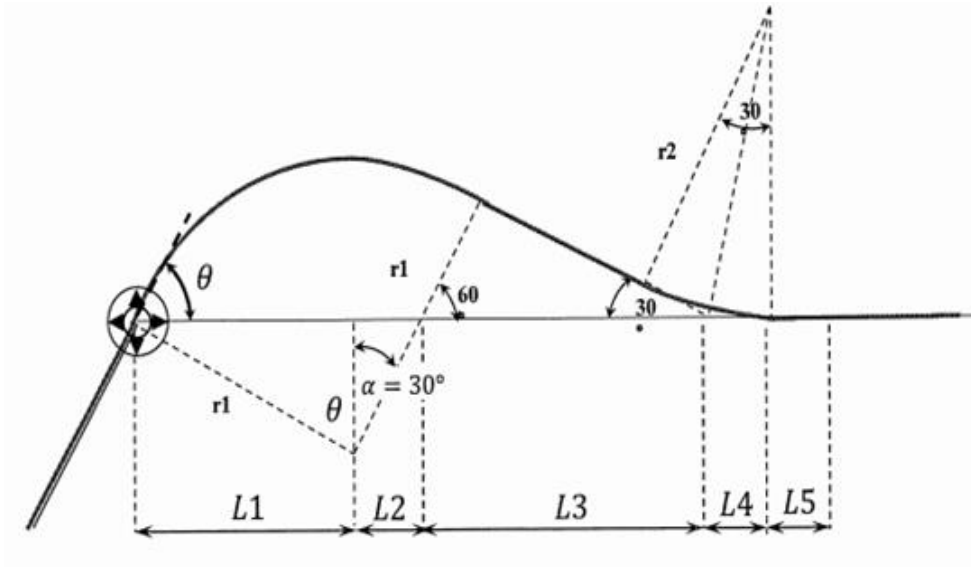
Figure 40 Fly over waypoint transitions

$$L = L_1 + L_2 + L_3 + L_4 + L_5 \tag{5.5}$$

$$L_1 = r_1 \sin \theta \tag{5.6}$$

$$L_2 = r_1 \cos \theta \tan \alpha \tag{5.7}$$

$$L_3 = r_1 \left[\frac{1}{\sin \alpha} + \frac{2 \cos \theta}{\sin(90° - \alpha)} \right] \tag{5.8}$$

$$L_4 = r_2 \tan \left(\frac{\alpha}{2} \right) \tag{5.9}$$

$$L_5 = cV \tag{5.10}$$

These calculations provide the suitable path where aircraft flies on easily. At the same time, RNP- RNAV standardizations define a performance range which aircrafts must stay in while fly-by, fly-over transition. In a flight, whereas pilot can use one of the methods for the leg transitions, choosing just one method is not obligatory because the combination of transitions is possible to use in flight plan. The combinations might be

two flight-by waypoints, fly-by then fly over transition, two fly-over waypoints and fly over then fly-by transition which are shown in below.

a) Two flight-by waypoint

Figure 41 Combinations of transitions (a), (b), (c) and (d)

b) Fly-by then fly-over transition
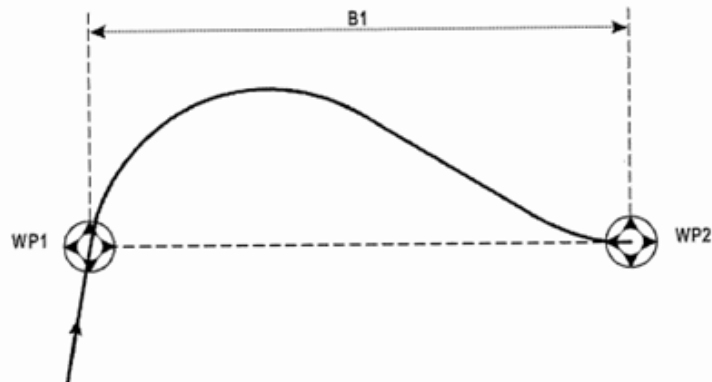
c) Two fly-over waypoint
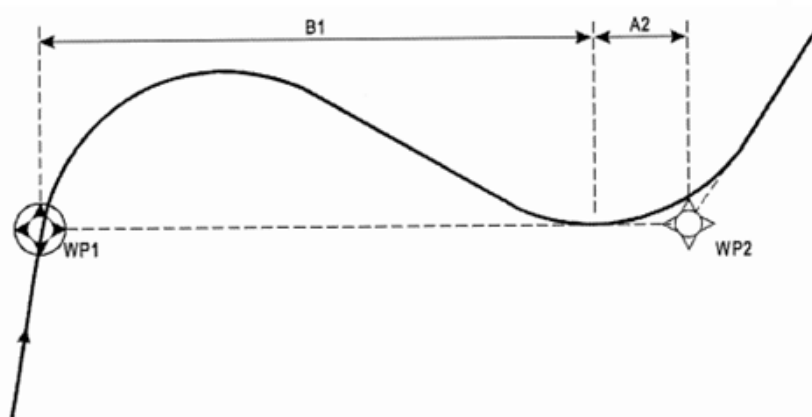
d) Fly-over then fly-by transition

Figure 41 Continued

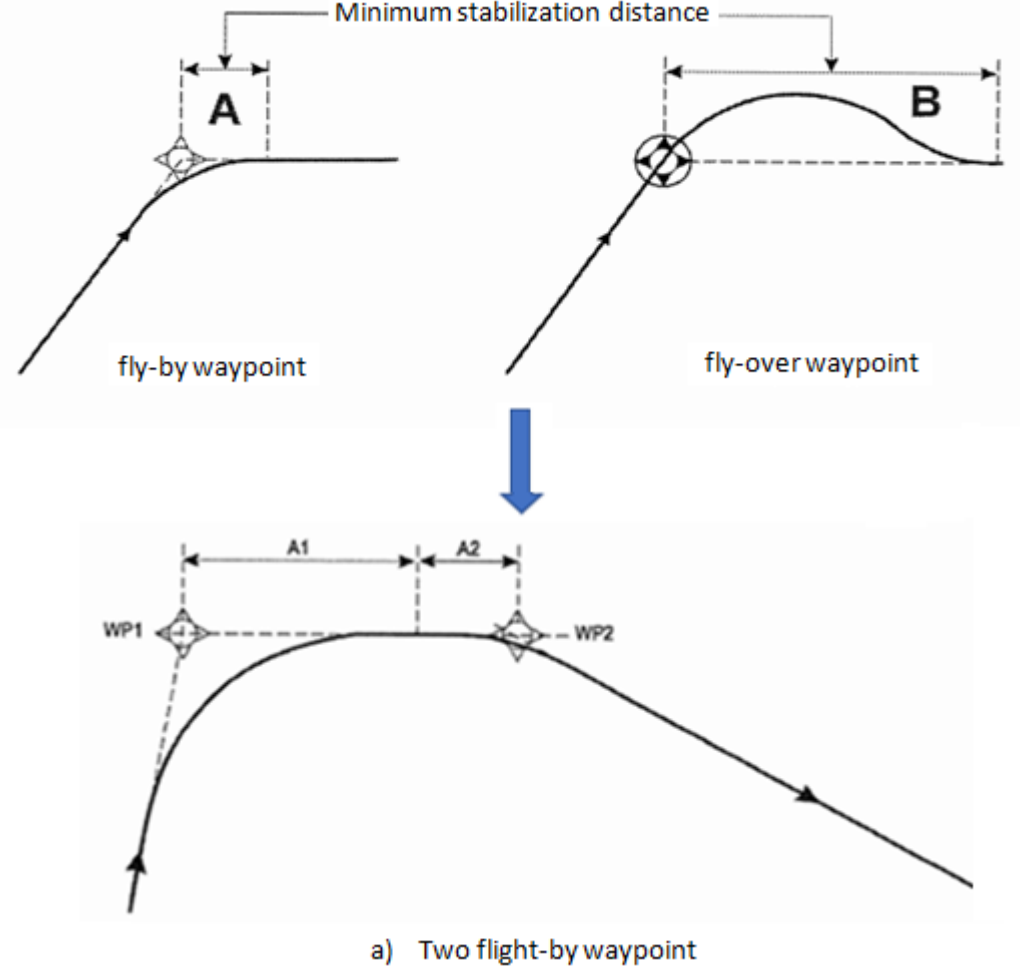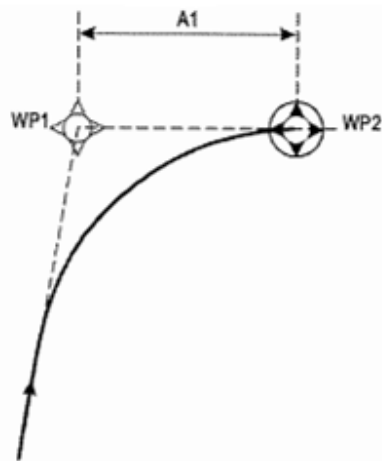## 5.3   Navigation Error Terms

Navigation error terms come into existence the combination of flight technical error and display error. In other words, the errors can occur while defining the path or estimating the position. In RNP standardization, all these errors are counted in performance requirements and they should stay in a defined range. In the first place, the error types should be understood to take into consideration in the error calculation.

Path definition error (PDE) is an error type which define the difference between the defined path and the desired path. The error between the estimated position which is the position expected with respect to indicated instruction and the true position system indicates the position estimation error (PEE). Path steering error (PSE) can be explained as the difference between estimated position and defined path. The sum of PDE, PEE and PSE is defined as total system error (TSE) at the same time it can be calculated from the difference between true position of the aircraft and desired path as shown in Figure 42 [21].
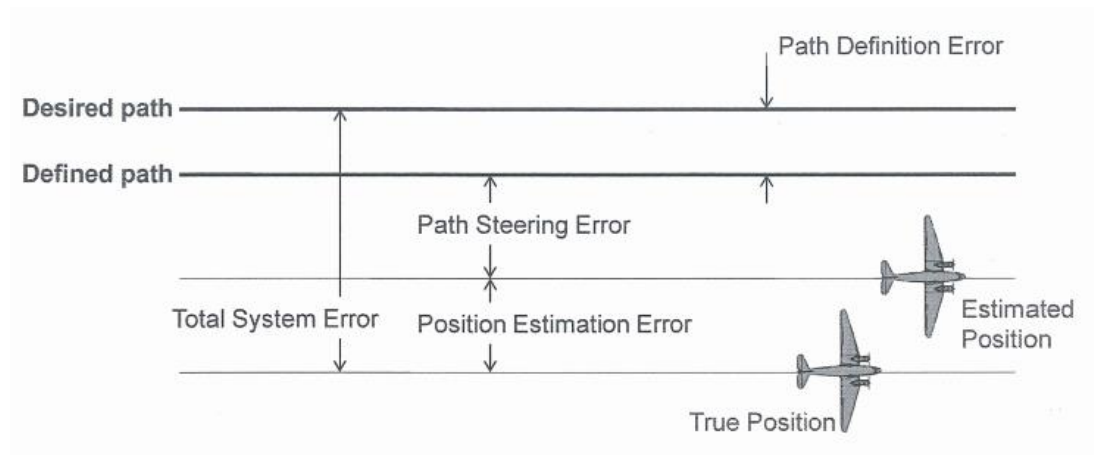
Figure 42 Lateral navigation error terms

Cross-track containment is referenced to desired path, based on position estimation error, path definition error and path steering error, detected and undetected faults.
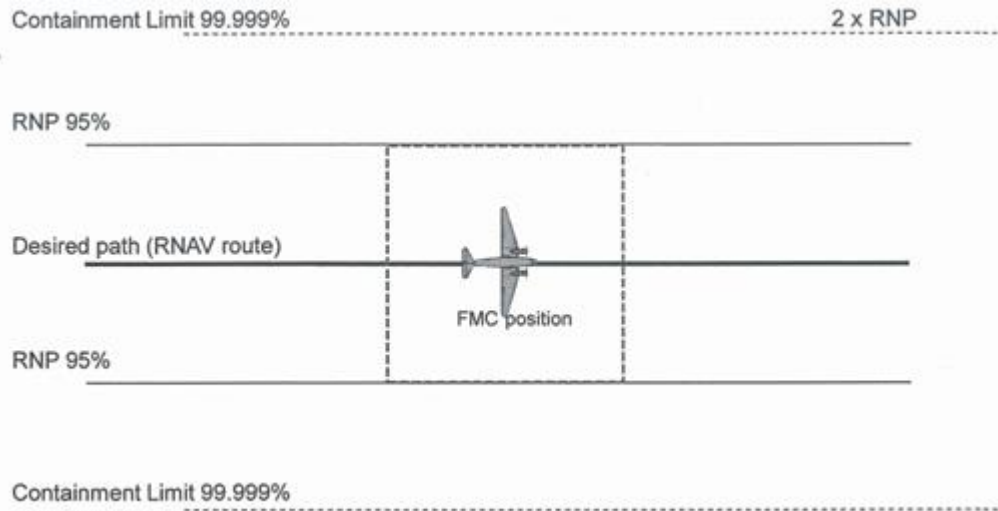
Figure 43 Navigation cross track containment

There is another notion here which is actual navigation performance. It is aimed to determine if the current performance requirement is satisfied.
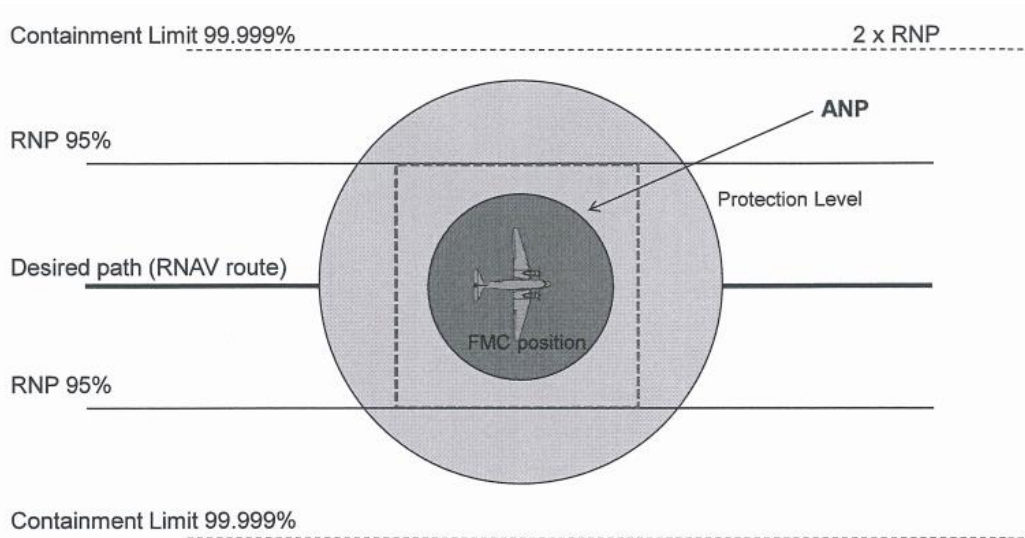
Figure 44 Actual Navigation Performance (ANP)

5.4   RNP-RNAV Types

Depending on phases of flight, RNP- RNAV accuracy show a change. The more the phase is critical, the higher accuracy is required to use. Table 6 indicates the relationship between flight phases and RNP-RNAV types.

Table 6 RNP-RNAV Types

Flight Phase	RNP-RNAV Type
Oceanic	RNP - 4.0 RNAV
Enroute	RNP - 2.0 RNAV
Terminal	RNP - 1.0 RNAV
Approach	RNP - 0.3 RNAV

For terminal phase, RNP- 1.0 RNAV is supposed to perform which means that lateral and longitudinal position accuracy must stay in the boundary of 1 NM for 95% of the flight time.

CHAPTER 6

AIRCRAFT MODELING AND PATH ALGORITHM

Modelling an aircraft is so complicated that it contains several parameters which have effects on the aircraft. To be able to build a structure for modelling, all these parameters must be thoroughly understood. Especially, they have massive effects on flight motion dynamic equations. In this thesis, to create the model of an aircraft, Base of Aircraft Data (BADA) inputs are going to be used. The inputs have several data which describes particularly the limitations of the aircraft like the maximum and minimum limits. Moreover, the data has all coefficients which are required to calculate the motion dynamic equations and presents a detailed description of aircraft type, mass, flight envelope, aerodynamic, engine thrust and fuel flow. BADA supplies different coefficients according to flight phases which are take-off, initial climb, cruise, approach and landing. Also, all this information is necessary to provide a more realistic approach while designing flight management algorithm in the thesis. Table 7 illustrates all the main blocks and the detailed information of BADA file for the aircraft modelling.

Table 7 BADA Input Blocks [22]

Model Category	Symbols	Units	Description
Aircraft Type	n_{eng}	dimensionless	Number of engines
	engine type	string	either Jet, Turboprop or piston
	wake category	string	either J, H, M or L
Mass	m_{ref}	tonnes	Reference mass
	m_{min}	tonnes	Minimum mass
	m_{max}	tonnes	Maximum mass
	m_{pyld}	tonnes	Maximum payload mass
Flight Envelope	V_{mo}	knots(CAS)	Maximum operating speed
	M_{mo}	dimensionless	Maximum operating Mach number
	h_{mo}	feet	Maximum operating altitude
	h_{max}	feet	Max.altitude at MTOW and ISA
	G_w	feet/kg	Weight gradient on max. altitude
	G_t	feet/K	Temperature gradient on max. altitude
Aerodynamic	S	m^2	Reference wing surface area
	$C_{D0,CR}$	dimensionless	Parasitic drag coefficient (cruise)
	$C_{D2,CR}$	dimensionless	Induced drag coefficient (cruise)
	$C_{D0,AP}$	dimensionless	Parasitic drag coefficient (approach)
	$C_{D2,AP}$	dimensionless	Induced drag coefficient (approach)
	$C_{D0,LD}$	dimensionless	Parasitic drag coefficient (landing)
	$C_{D2,LD}$	dimensionless	Induced drag coefficient (landing)
	$C_{D0,ALDG}$	dimensionless	Parasitic drag coeff. (landing gear)
	$(V_{stall})_l$	knots (CAS)	Stall speed [TO, IC, CR, AP, LD]
	$C_{L,BO(M=0)}$	dimensionless	Buffet onset lift coef. (jet only)

Table 7 Continued

Model Category	Symbols	Units	Description
Engine Thrust	$C_{Tc,1}$	Newton (jet/piston) Knot-Newton (turboprop)	1st max. climb thrust coefficient
	$C_{Tc,2}$	Feet	2nd max. climb thrust coefficient
	$C_{Tc,3}$	1/feet^2 (jet)	3rd max. climb thrust coefficient
	$C_{Tc,4}$	K	1st max. thrust temperature coefficient
	$C_{Tc,5}$	1/K	2nd max. thrust temperature coef.
	$C_{Tdes,low}$	dimensionless	Low altitude descent thrust coef.
	$C_{Tdes,high}$	dimensionless	High altitude descent thrust coef.
	$H_{p,des}$	feet	Transition altitude for calculation of descent thrust
	$C_{Tdes,app}$	dimensionless	Approach thrust coefficient
	$C_{Tdes,ld}$	dimensionless	Landing thrust coefficient
	$V_{des,ref}$	knots	Reference descent speed (CAS)
	$M_{des,ref}$	dimensionless	Reference descent Mach number
Fuel flow	C_{f1}	kg/(min-kN) (jet) kg/(min-kN.knot) (torboprop) kg/min (piston)	1st thrust specific fuel consumption coefficient
	C_{f2}	knots	2nd thrust specific fuel consumption coefficient
	C_{f3}	kg/min	1st descent fuel flow coefficient
	C_{f4}	feet	2nd descent fuel flow coefficient
	C_{fcr}	dimensionless	Cruise fuel flow correction coefficient

6.1   The Effects of the Aircraft Parameters Change

As mentioned before, lots of parameters are dependent on the chance of other parameters. To design a realistic algorithm, the parameters' relationship shouldn't be ignored. For example, height affects several parameters because of the nature of the air. The air density decreases when the height increases, and this creates knock-on effect on the other parameters. In the algorithm, the changes are taken in consideration and some parameters change depending on height such as temperature, speed of sound, pressure and density.
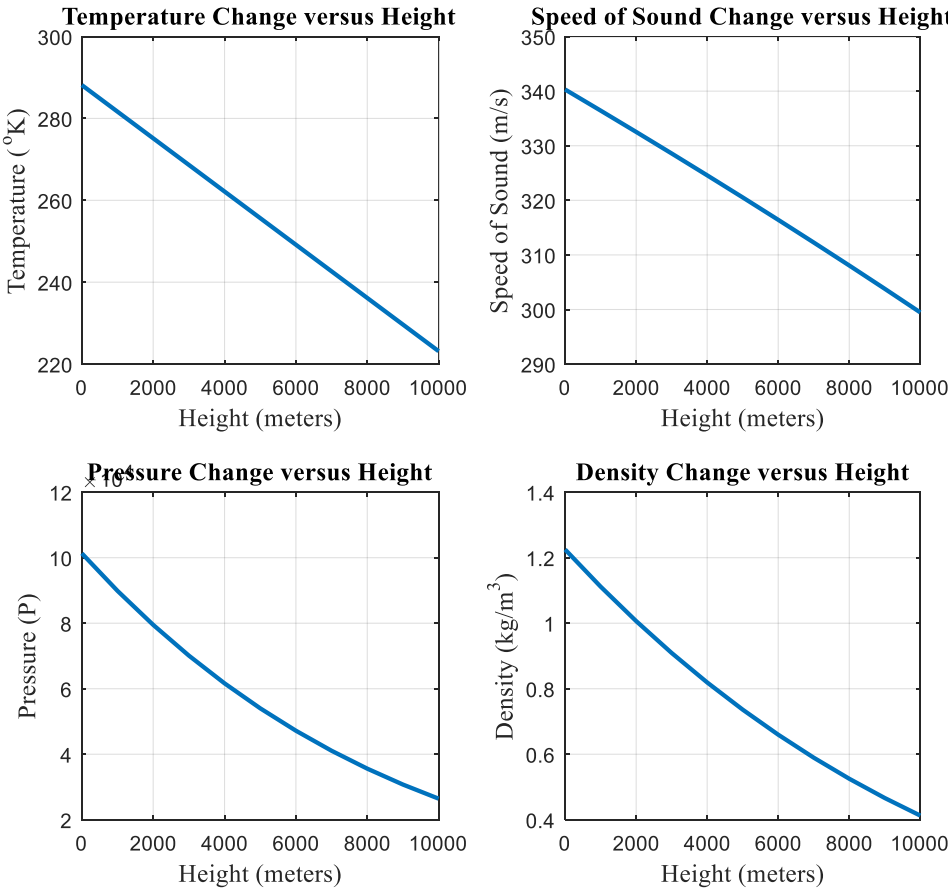

Figure 45 Change of temperature, speed of sound, pressure and density with height

As shown in Figure 45, whereas the height increases, the other parameters decrease because of the physical fact that when the air rises, the pressure gets lower because of the gravity and in the same way, the density goes down. With the low density, the sound is transmitted slowly.

The equation (6.1) is used to calculate thrust force with the coefficients of BADA inputs and the height of the aircraft.

$$T_{maxclimb} = C_{Tc,1}\left(1 - \frac{h}{C_{Tc,2}} + C_{Tc,3}\, h^2\right) \tag{6.1}$$

By using the same aircraft coefficients, the change of trust force with respect to height is drawn in Figure 46.
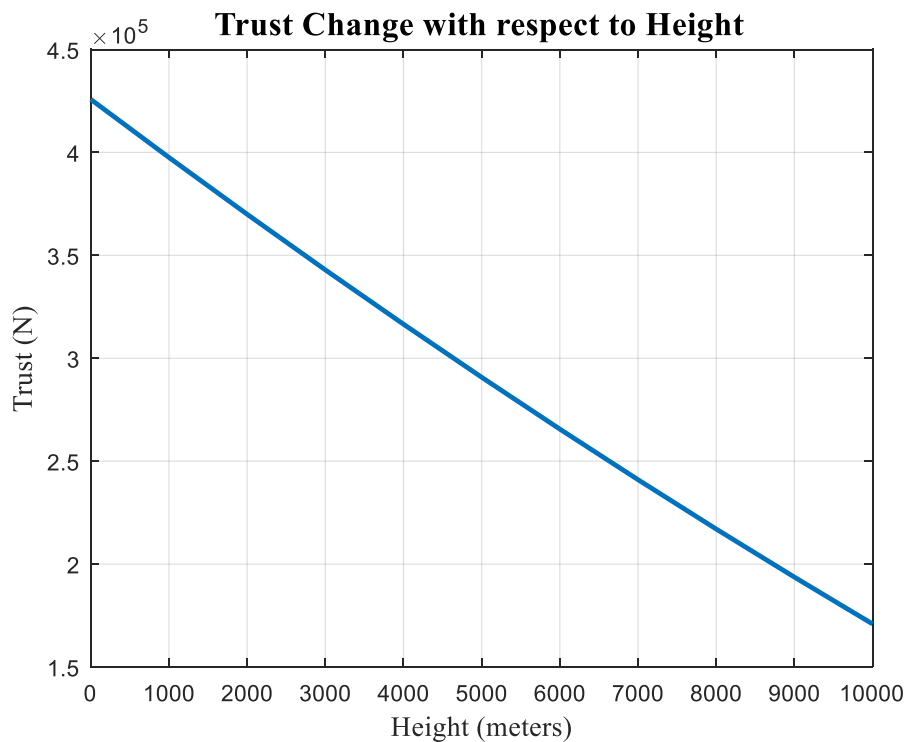

Figure 46 Trust change with respect to height

To create thrust force, aircrafts use their engines to take the air into them and then release the air into the engines with higher pressure to have a force reverse to the air. When the air density decreases, this means the air into the engine to create high pressure also decreases.

Drag force is also affected by density change. Drag is generated while moving in the air because of friction which is called parasitic drag and lift generating which is induced drag. The equations below show the coefficients and parameters which contribute the drag force.

$$D = \left(\frac{1}{2} C_{D0} \, \rho V^2 S + \frac{1}{2} C_{D2} C_L^{\,2} \rho V^2 S \right) \qquad (6.2)$$

$$C_L = 2 \frac{L}{\rho V^2 S} \qquad (6.3)$$

As shown in the equations, the surface area, lift force, density and velocity have effects on the drag force generation.
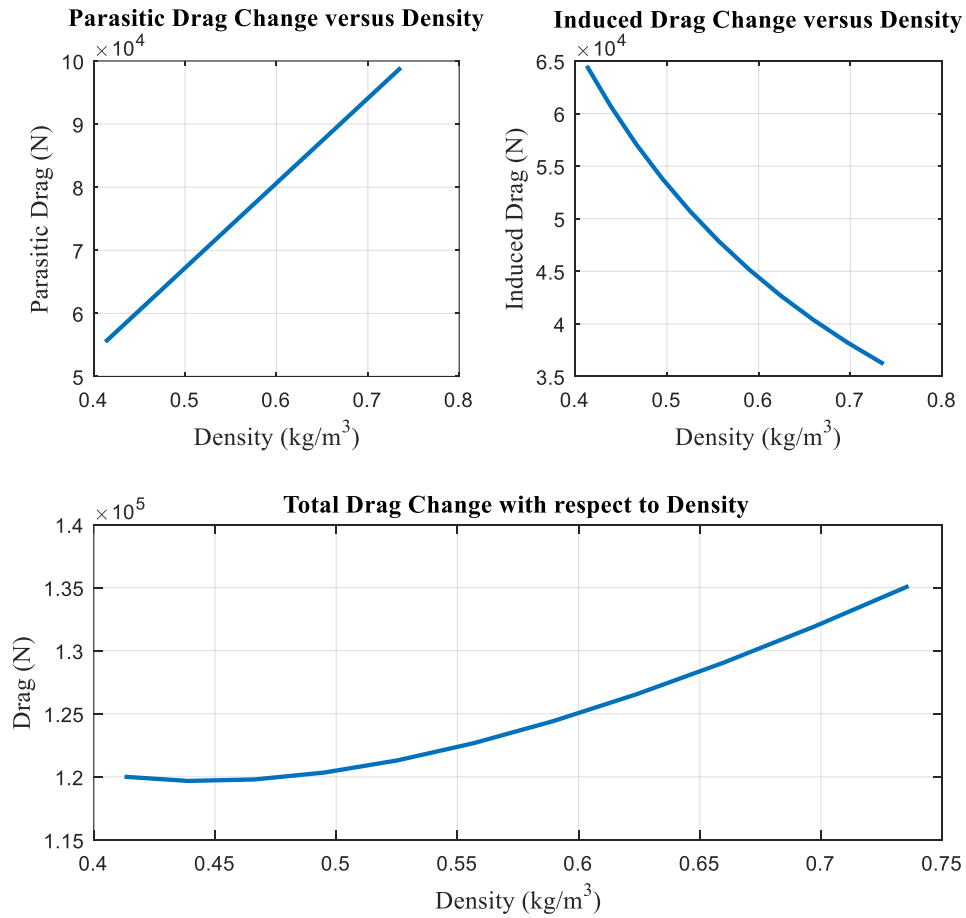
Figure 47 Drag force change with respect to density

Figure 47 shows the drag force change with respect to density change from 0.4127 to 0.7361 kg/m^3 (the height change from 10000 m to 5000m) where velocity is 200 m/s, mass is 237600 kg, the wings surfaces area is 428.0400 m^2 and parasitic drag coefficient for cruise flight is 0.0157. The density increment means that the force generated by friction gets higher whereas the induced drag has inverse correlation with this increment. The total drag is the summation of induced and parasitic drag so totally, the drag force increases with the rise of density.
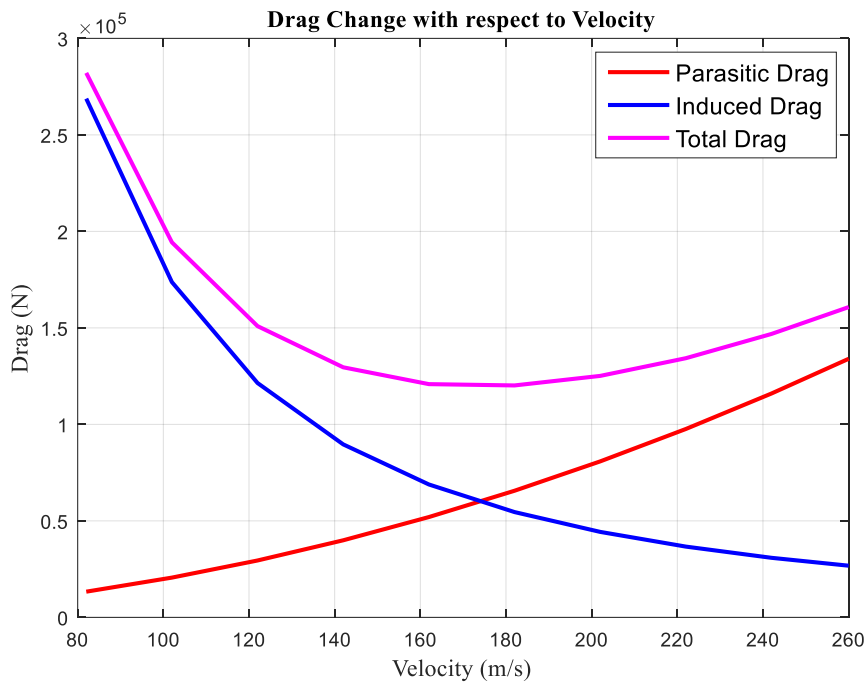
Figure 48 Drag change with respect to velocity

To extend parameter effects on the algorithm, the other example of the drag force change with respect to velocity is shown in Figure 48. The velocity in the figure changes from the stall speed 82.31 m/s to maximum speed 262.5 m/s and the other parameters are kept stable. In the beginning, induced drag decrease is very sharp that total force is lowered. Then the velocity increment enhances the friction so that the total drag force gets higher.

6.2   Lateral Trajectory Tracking Algorithm Design

The flow chart of the lateral trajectory tracking algorithm is shown in Figure 49.

Figure 49 The flow chart of the algorithm

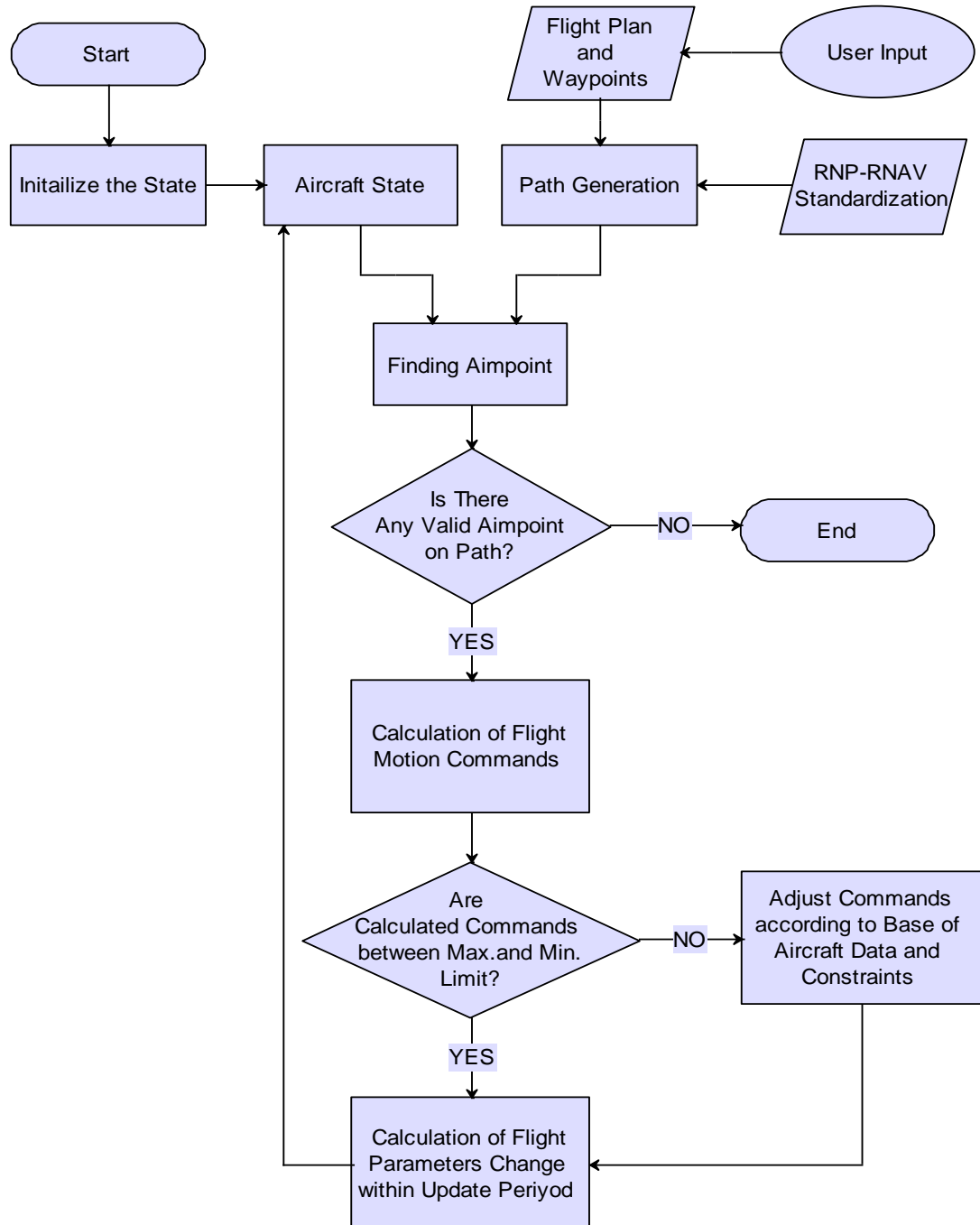The algorithm can be divided into four functional blocks which are path generation, aimpoint determination, modelling and controlling the aircraft and performance evaluation as shown in Figure 50.
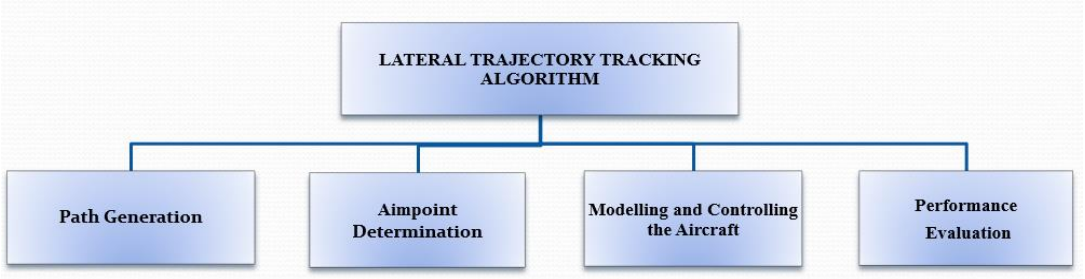

Figure 50 The functional blocks of the algorithm

Waypoint transition methods and special pattern creation with respect to standardization are aimed to create in path generation block. The flight plan is the input of the block and the standardizations are used for calculations and limitations. Aimpoint determination block is one of the most important parts of the lateral trajectory algorithm. The aircraft state and the generated path are the inputs of this block. After calculating the aimpoint, the aircraft needs to generate its commands for the guidance to the point, so the algorithm calculates the flight motion commands by using flight motion dynamics. The calculated commands are checked to determine whether they are in the constraints of Base of Aircraft Data. If any commands are out of the constraints, the commands are adjusted according to the maximum or minimum limits in BADA. The changes of the flight parameters which are velocity, lateral heading, flight path angle, height, distance and weight   are calculated within update period. Then the algorithm updates the aircraft state. The performance block includes all algorithm design because the path is created within the standardization's requirements and the aircraft commands are calculated and updated by using the real aircraft restrictions and coefficients. The blocks of the algorithm on the flow chart can be seen in Figure 51.

Figure 51 The functional blocks on the flow chart

6.3   Path Algorithm

Even though the algorithms which are available in lateral trajectory tracking provide very good performance while following straight lines, the same performance cannot be mentioned for curved patterns and narrow area tracking. Finding new aim points during the lateral desired path tracking can offer a better approach for the more complicated patterns.

Figure 52 illustrates the main concept of the path tracking approach with radius 'R', velocity 'V' and lateral acceleration command '$a_{s_{cmd}}$'.
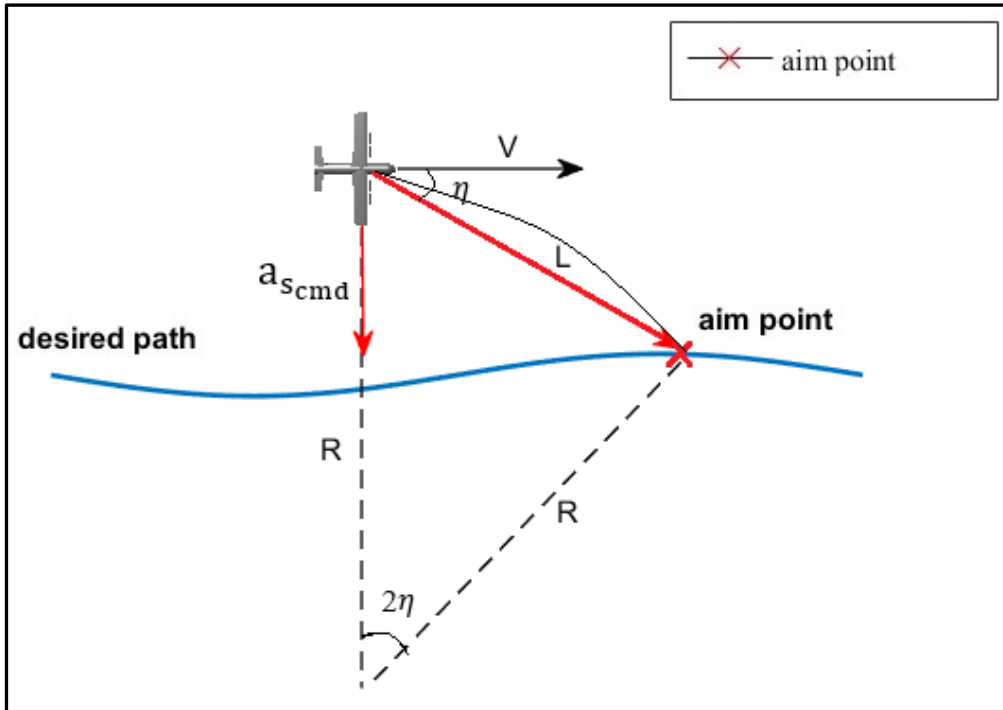
Figure 52 The path tracking approach with radius R

Lateral acceleration command, also named as centripetal acceleration, is calculated in the algorithm depending on chosen aim point with the equation (6.4).

$$a_{s_{cmd}} = \frac{V^2}{R} \qquad (6.4)$$

$$L = 2R \sin \eta \qquad (6.5)$$

From equation (6.4) and (6.5), the formula gets independent from the variable of R as shown in equation (6.6).

$$a_{s_{cmd}} = \frac{2V^2}{L} \sin \eta \qquad (6.6)$$

After eliminating the radius (R) of the circle which is shown in Figure 52, the path tracking formula becomes just dependent on the parameter of L. The simplified formula gives a chance to design a new approach for finding the path in lateral axis. L parameter is a distance from the aircraft, so it can be considered that the aircraft is a center of a circle with radius of L. In this way, when the circle intersects with the path, it means the point is far from the plane with distance of L. However, there can be more than one intersection with the desired path. In this condition, the algorithm is programmed following the point ahead of the aircraft. To understand whether the aircraft is on the path or not, the projected point is used. The projected point is the projection of aircraft on the desired path. If the circle has a junction with desired path ahead of the aircraft, it is called aimpoint. The aircraft tries to reach the aimpoint by changing its commands like velocity, pitch angle and bank angle until it gets to the next aimpoint. This process continues until the path ends.

There are some conditions which aircraft can be in while doing trajectory tracking. The four main conditions can be mentioned to design the aimpoint algorithm. The first condition is shown in Figure 53. In this condition, the projected point exists which means the aircraft has a projection on the path and the circle intersect the path to create an aimpoint for the aircraft. Thus, the aircraft needs to give directions to reach the aimpoint.
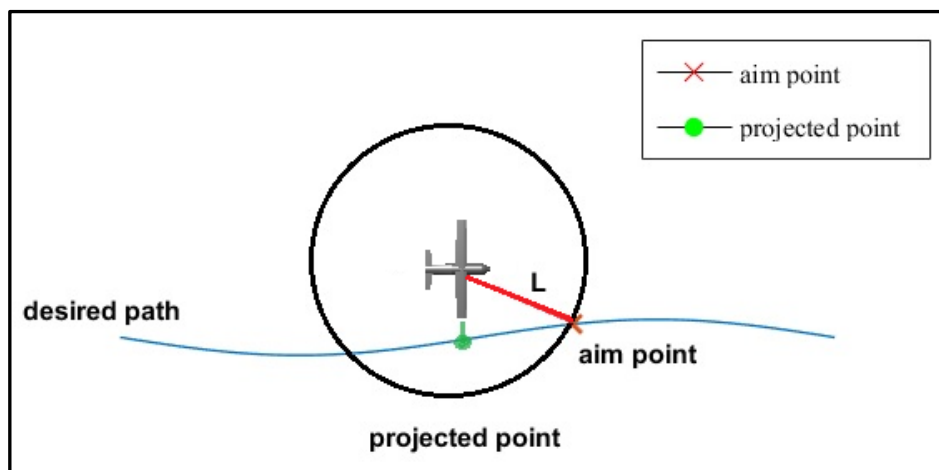

Figure 53 Existence of aim-point and projected-point

The second condition is illustrated in Figure 54. In this condition, the projection of the aircraft is present, but the circle is so far from the path that there is no junction between the path and the circle. To supply an aimpoint to the aircraft to get closer to the path, a point is chosen as aimpoint which is L distance far from the projected point. Projected point is the minimum distance between the aircraft and the desired path. Until the circle doesn't have a junction and has a projected point, this condition continues to find aimpoints.
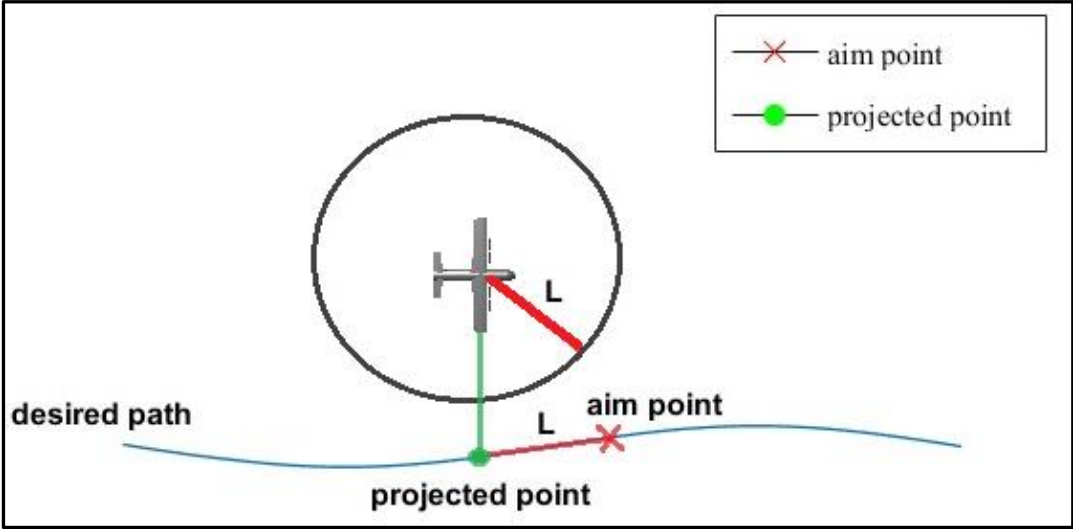

Figure 54 Existence of projected-point

The next condition is for the absence of both points which is given in Figure 55. In this condition, there is no projection on the desired path which means the aircraft is yet to be somewhere on the line. Furthermore, the circle doesn't have a mutual point with the path. As a result of the conditions, the aircraft should get close to the path at first, so the first point of the path is taken as the aimpoint of the aircraft. Until finding any projected point or aimpoint, the aircraft tries to reach the beginning of the desired path.
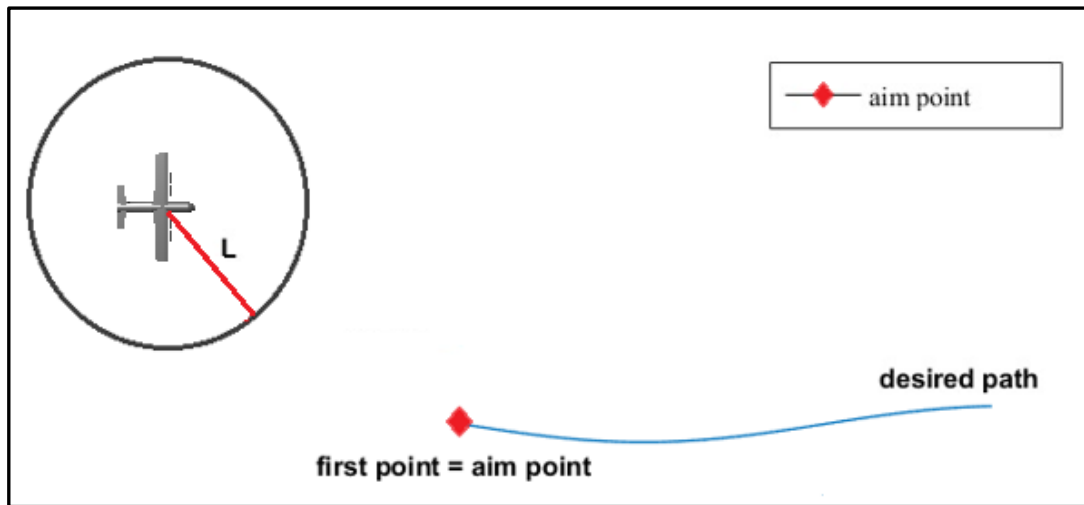
Figure 55 Absence of aim-point and projected-point

After fitting the desired path, the aircraft is supposed to follow the path till the end. Even though following the path till the end after fitting is very easy for the straight trajectories, it is not easy for the curved or direction changed paths. The paths are needed to be tracked in case of any change in the path. The last condition is to cover this situation and make sure the aircraft keeps tracking the path until the end. Finding the aimpoint has the same logic with the first condition. If L is on the same direction with where the aircraft goes, the aircraft stay with the same command. Otherwise, the aircraft must give new commands to catch the new aimpoint. The last condition is given as follows.
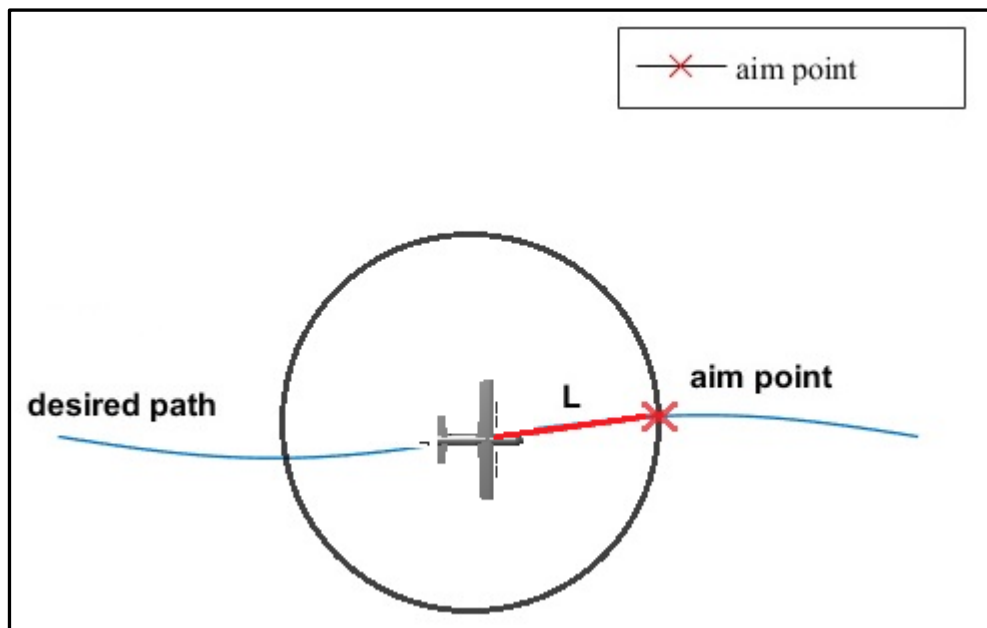
Figure 56 Aircraft on the path

Choosing optimal 'L' distance is a very important matter to achieve high performance trajectory tracking. Choosing a very small L distance means a small circle and very near aimpoint to the aircraft's current position. To go toward the aimpoint, the aircraft must make very sharp movements like increasing the velocity enormously, giving a very big bank angle or pitch angle. Even though the algorithm uses the safety limitations which prevent the aircraft to get dangerous commands by the pilots or autopilot to minimize these dramatic changes, small aimpoint choice still has impact on the trajectory tracking algorithm. The aircraft frequently gets dramatic command changes when the aimpoints are near to each other and the aircraft's location so it causes oscillations while tracking the path. Figure 57 shows that the result of the lateral path tracking when L equals to 0.01 NM. The magenta color is the path that the aircraft followed during the trajectory tracking. The aircraft has never fitted to the path after finding aimpoints on the path. Furthermore, the oscillation gets bigger while following the path.
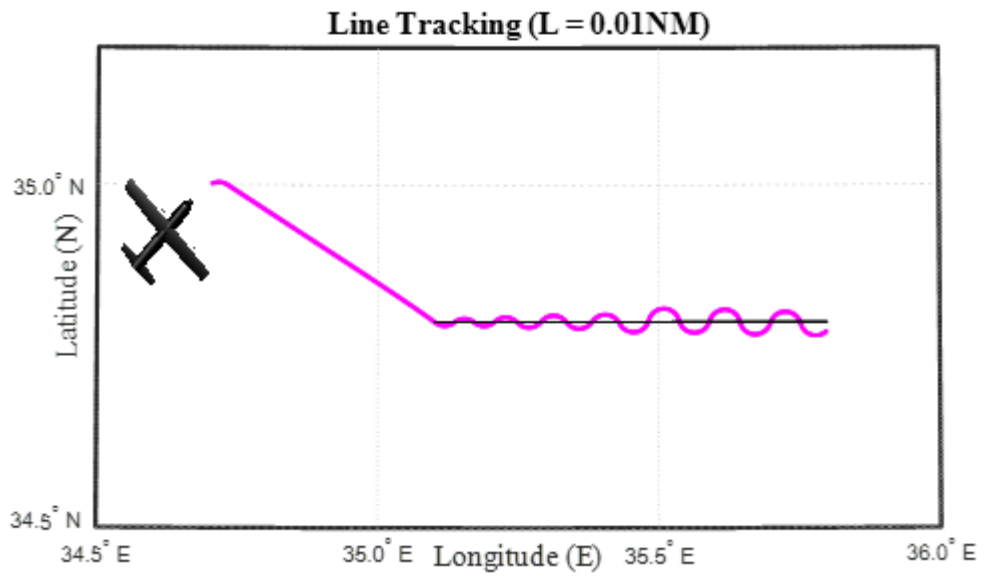
Figure 57 Line tracking when L= 0.01 NM

Figure 58 presents the comparison between small L values. The result shows that the more L increases for the small values, the less oscillation it creates. None of the values given in the figure below fit the pattern during the trajectory.
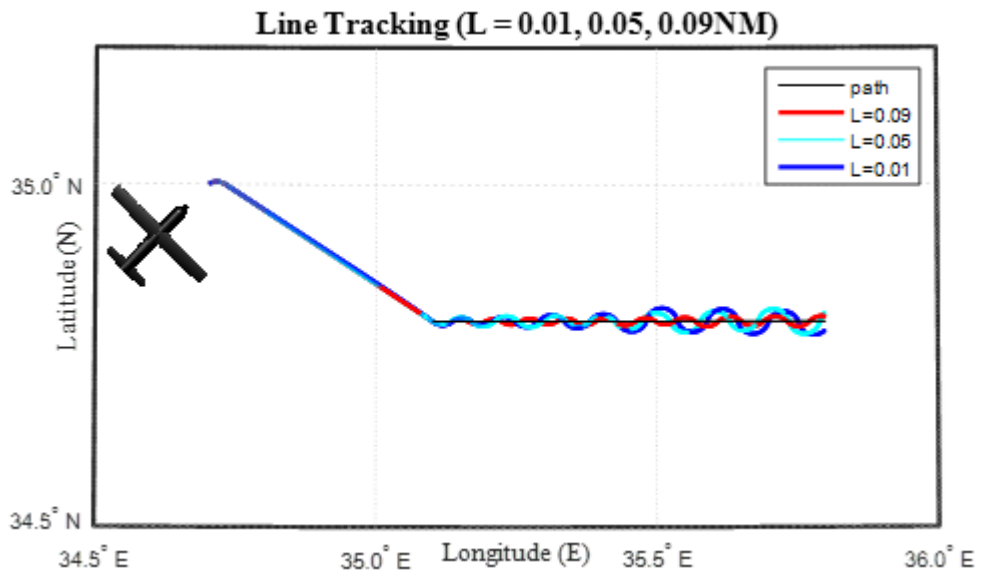

Figure 58 Line tracking when L= 0.01 NM, L= 0.05 NM and L= 0.09 NM

Choosing a viable 'L' distance can solve this oscillation problem with an optimal aimpoint distance because the aircraft gets normal commands which the aircraft do without making sharp movements. Line tracking when L is chosen as 0.5 NM is shown in Figure 59. The magenta color is the line the aircraft followed, and it is perfectly fit on the trajectory.
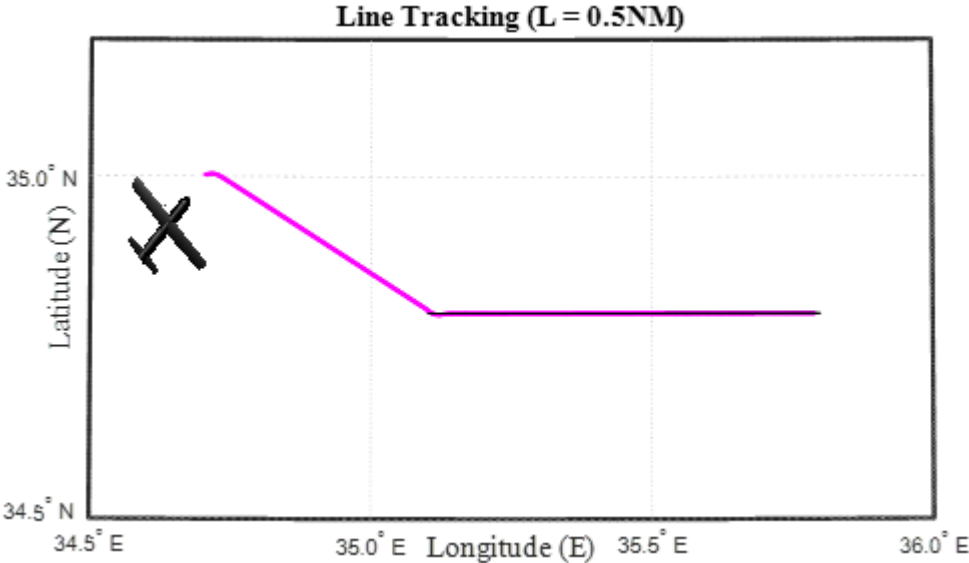

Figure 59 Line tracking when L= 0.5 NM

As much as giving a small distance is not suitable for path tracking, very large distance also causes problems in the algorithm. The result with a large distance is shown in Figure 60. After finding aimpoint on the path, the aircraft gets very small command which are almost ignorable, and after some time, even before finishing the path the next aimpoint gets too far from the trajectory. If the path had infinite length, the aircraft would never fit the desired path. It would fly parallel to the path but not on it at infinity because of the distance of the aim point.
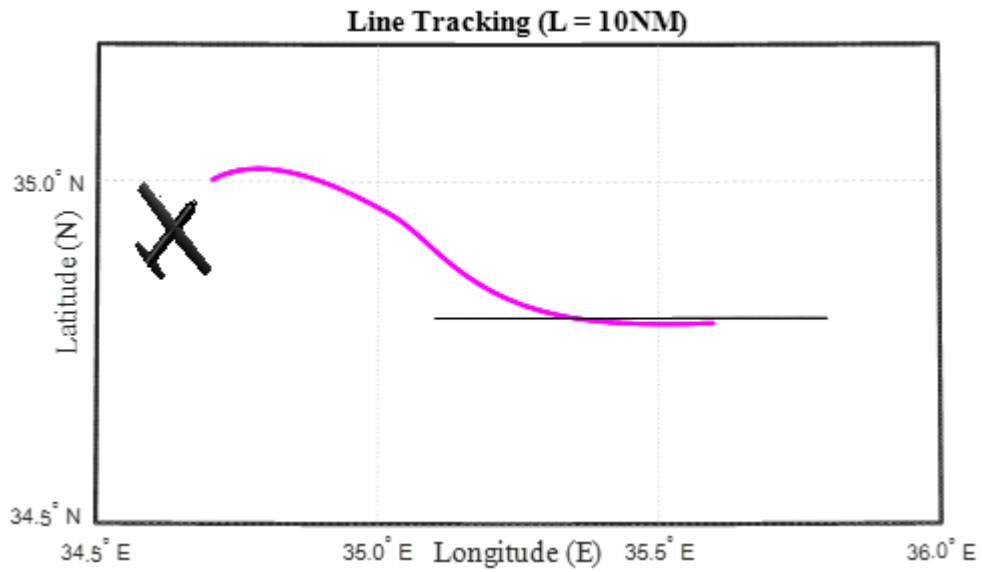
Figure 60 Line tracking when L= 10 NM

The discrete representation of the lateral path tracking result is shown in Figure 61. The result illustrates four different aimpoints finding steps. When the aircraft is not closed to the desired path, the line between the aircraft and the aimpoint with the length of L has a large angle. On the contrary, the closer the aircraft gets, the smaller the line direction gets.

As shown in the figure, the algorithm tries to lead the aircraft's heading and velocity vector slightly towards the path. When the angle gets smaller near to the desired path, it helps to fix the aircraft on the path with a smooth way to prevent the oscillation.
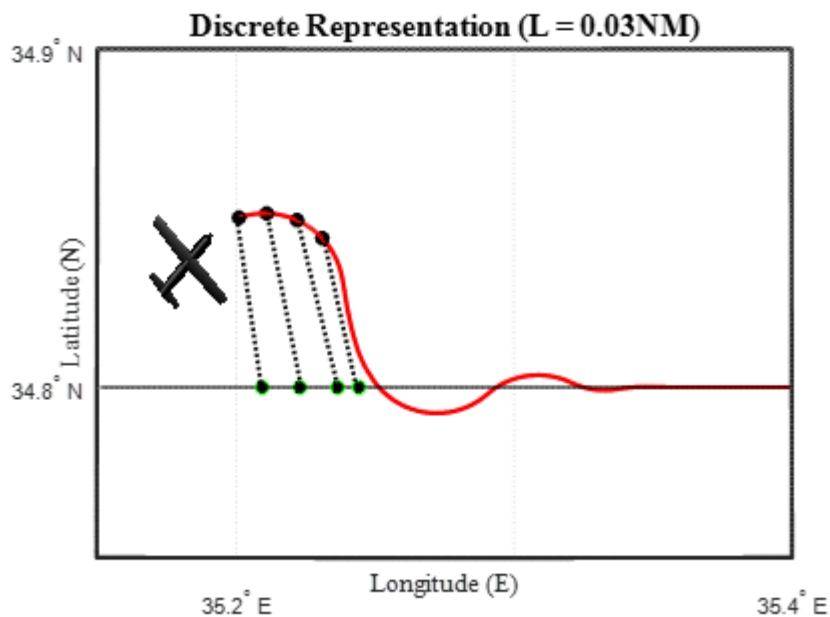
Figure 61 Discrete representation

6.4 Circle Path Design and Path Tracking

Circle pattern is a path type for aircrafts to track especially while holding. Generally, when air traffic is very busy, ATC guides the aircraft to hold in a specific area. It is a special pattern which means aircraft position with reference to pattern-fix point and turning direction matters how to fly on the pattern. There are three main sectors an airplane can enter from which are Sector 1- Direct entry, Sector 2- Teardrop entry, Sector 3- Parallel entry. Also, turning direction can be categorized as clockwise and counter clockwise. Figure 62 and Figure 63 show the pattern-fix, turning direction and sectors.
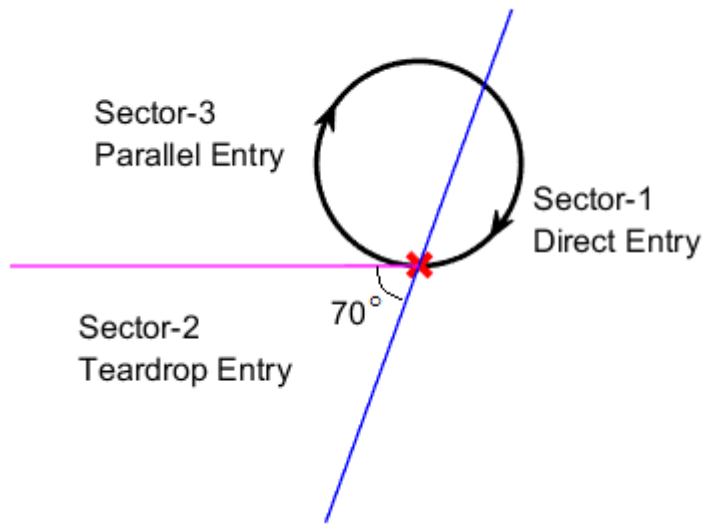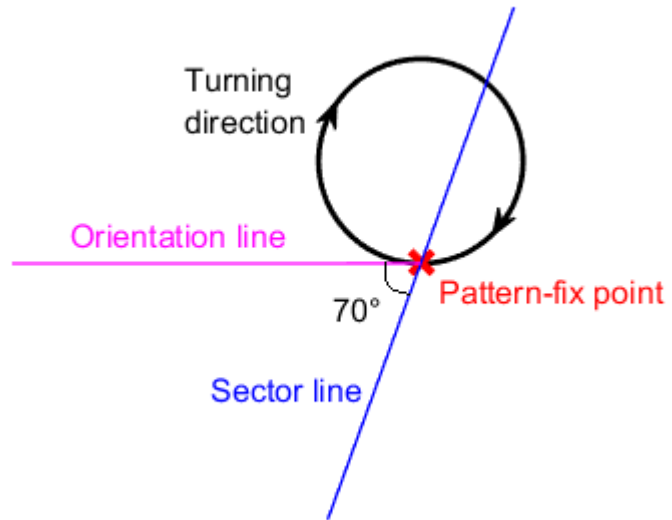
Figure 62 Circle pattern

Figure 63 Elements of circle pattern

The circle pattern is drawn depending on four parameters which are pattern-fix points, the width of the circle, turning direction and the orientations. Figure 64 illustrates the sector change depending on pattern-fix orientations. Orientation is the angle between true north and the orientation line. As shown in the figure, depending on the orientation the entrance of the aircraft to the sector changes.
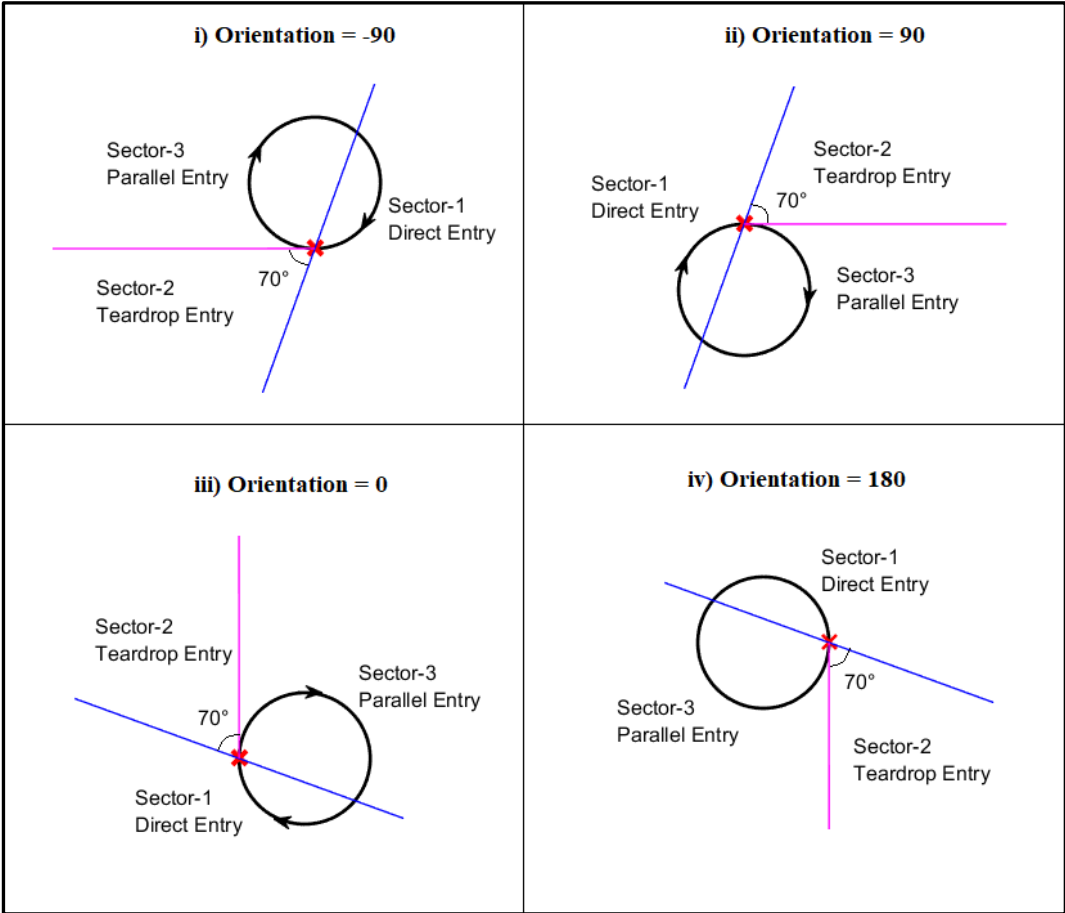
Figure 64 Sector change depending on pattern-fix orientation

To enter the pattern, the aircraft heading must be pointed out pattern-fix point wherever the aircraft is regardless of the sector. However, aircraft cannot follow and fit the path from every entrance while the heading is pointing out pattern-fix. To solve this problem depending on the entrance sector, aerodynamically and geometrically viable routes are needed to be drawn by the algorithm.

Sector-1 is the easiest sector to fit the pattern. For this sector, the aircraft is only needed to be guided to pattern-fix. The road design and the aircraft's pattern following results are shown below.

Figure 65 Sector-1 Result

The Figure 65 gives the result which L equals to 0,4 NM, pattern-fix is located at 40.4557 °N and 32.5165 °E, aircraft position is at 40.4033 °N and 32.6029 °E, and the heading points out the pattern-fix which means 308.5576° heading angle. The magenta color represents the road the aircraft tracked. As shown in the figure, the aircraft could completely follow the pattern without any deviation.
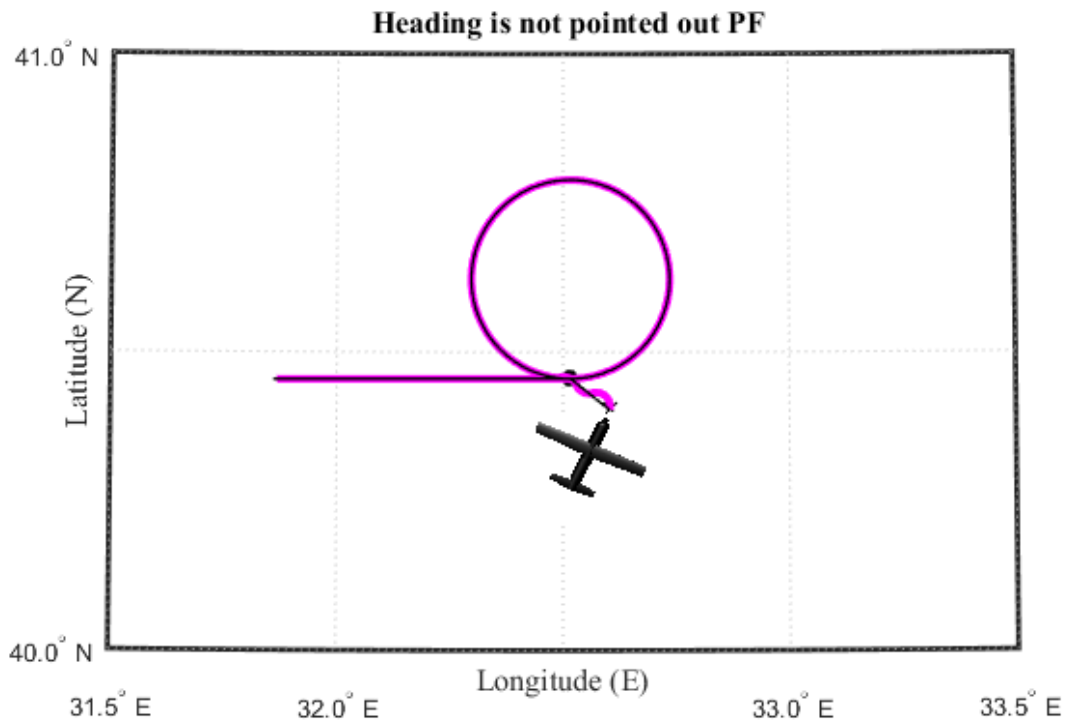
Figure 66 Heading is not pointed out pattern-fix in Sector-1

Figure 66 illustrates the result when the aircraft's heading doesn't point out the pattern fix in the beginning. In this scenario, the heading is 243.55° which means there is 65° difference between the aircraft heading and the heading which the aircraft is supposed to show while going to the pattern-fix. The algorithm tries to bring the heading in the correct position within aircraft limitations. Until correcting the heading, the aircraft makes a sinusoidal movement to fit the pattern.

Entrance to Sector-2 is more complicated than Sector-1 while the heading points out the pattern-fix. The aircraft should fly on a different pattern outside of the original path to be able to follow the pattern easily. The sector-2 pattern design is shown below.
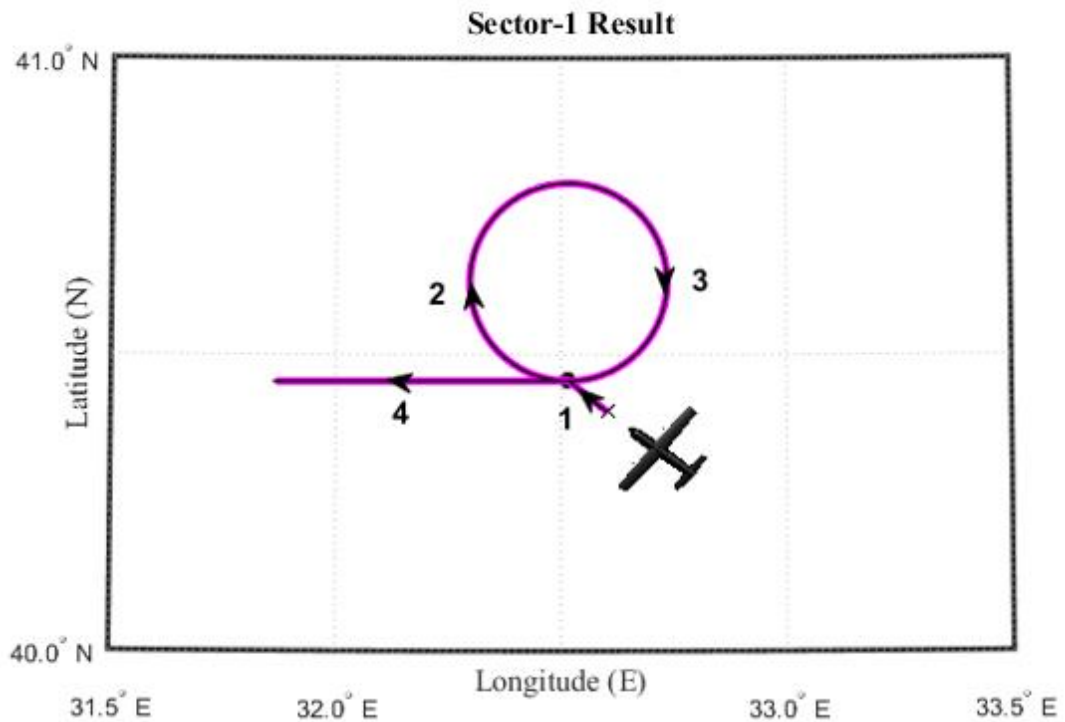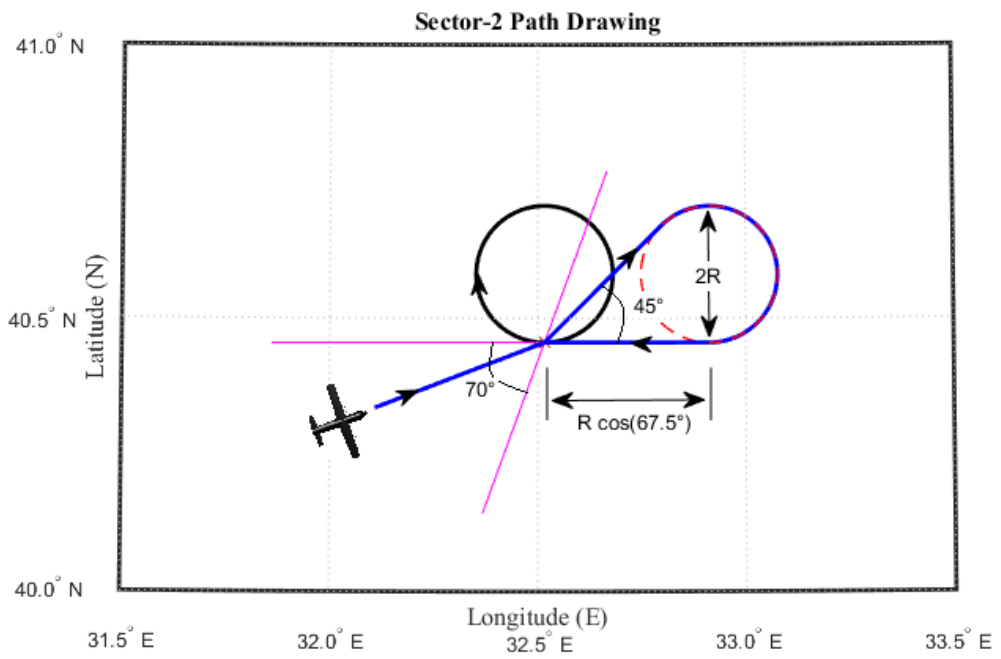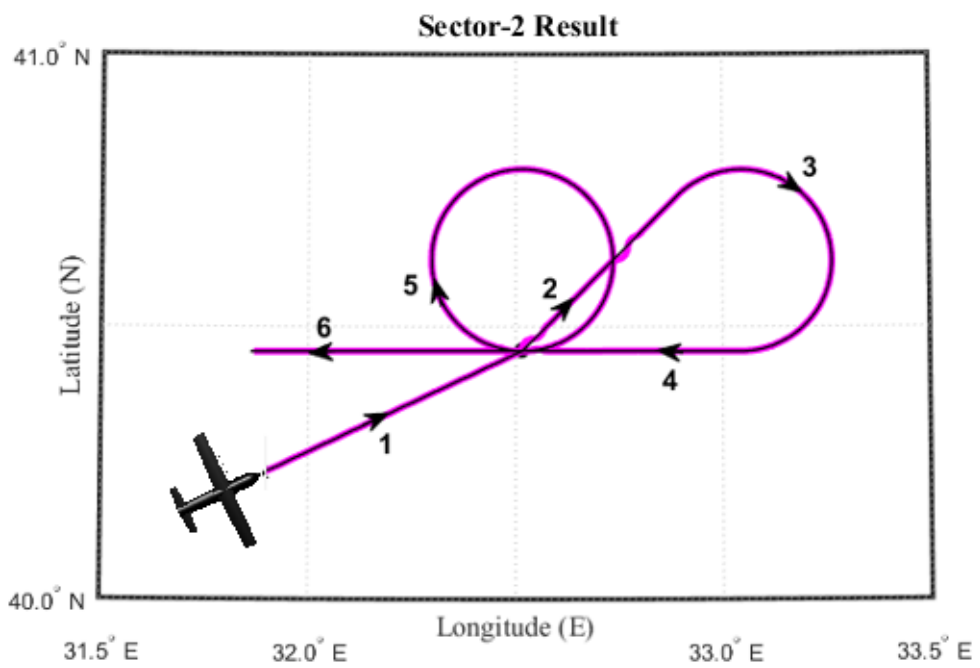
Figure 67 Sector-2 path drawing

Figure 68 Sector-2 result

The Figure 68 presents the result which L equals to 0,4 NM, pattern-fix is located at 40.4557 °N and 32.5165 °E, aircraft position is at 40.23 °N and 31.889 °E, and the heading points out the pattern-fix which means 64.534° heading angle. The magenta color represents the road the aircraft tracked. As shown in the figure, the aircraft almost followed the pattern without any deviation except the junction parts. In the junction parts, the algorithm can intersect several aimpoints, so it creates some smooth sinusoidal movement in very narrow junction parts.
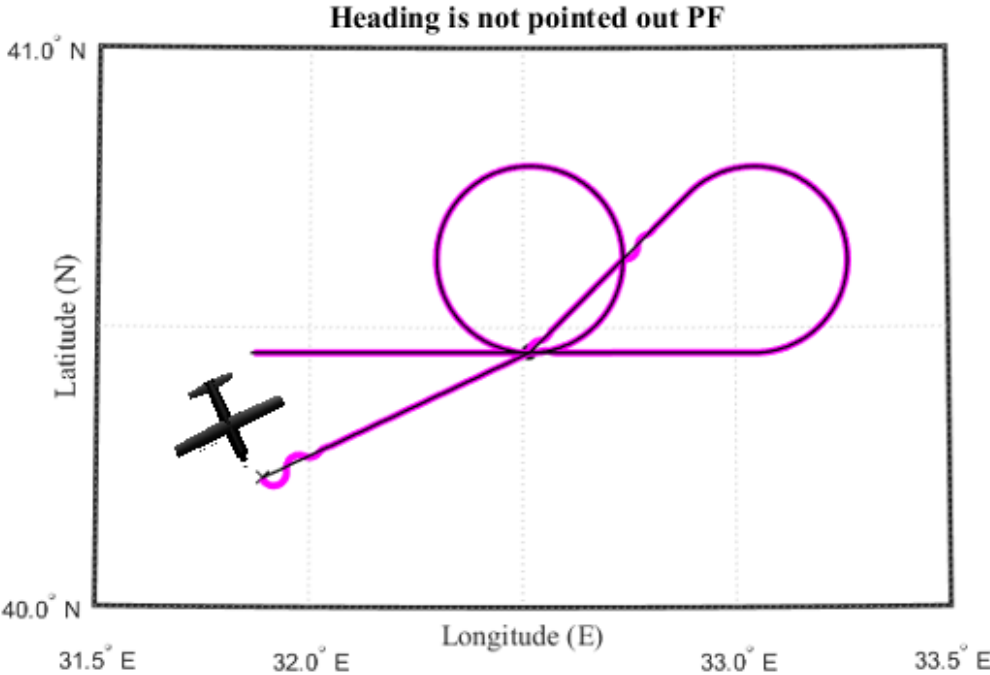
Figure 69 Heading is not pointed out pattern-fix in Sector-2

In Figure 69, the result is given when the aircraft's heading doesn't point out the pattern fix in the beginning. In this scenario, the heading is 154.534°. The algorithm tries to bring the heading in the correct position within the aircraft limitations. The aircraft makes a sinusoidal movement to fit the pattern while correcting the heading. After that on the pattern, the same junction issue can be seen when the pattern lines cross.

Figure 70 illustrates what radius of the circle pattern changes on the pattern. When the radius gets bigger, at the same time the outside circle which is needed to be turn on gets bigger.
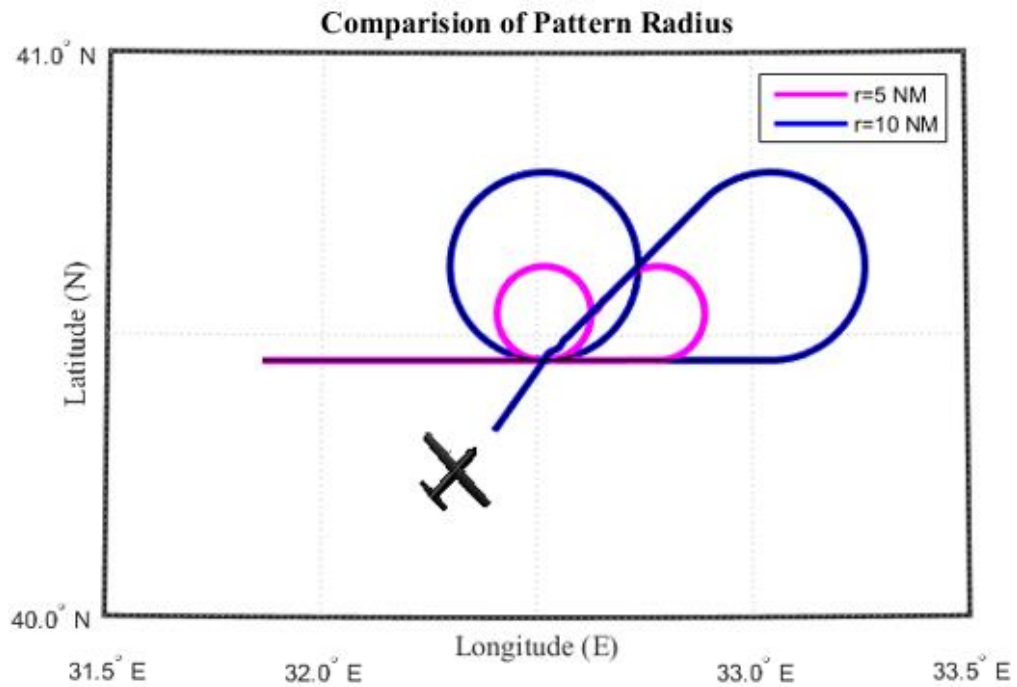
Figure 70 Comparison of pattern radius

In the figure above, magenta represent the pattern followed by the aircraft when the circle has 5 NM radius while the blue route is for the radius of 10 NM. Furthermore, in this result L is taken as 0.2 NM which decreases the junction part problem as shown in the figure. This result makes the thesis lead the conclusion that taking small L values enough, but not so small that can cause oscillation, to find aimpoint gives more accurate results in junction parts.

Sector-3 is similar to Sector-2 path shape in general. However, because of the entrance area to the path, it is needed to make another circular movement before the circle outside. The path design is given in Figure 71.
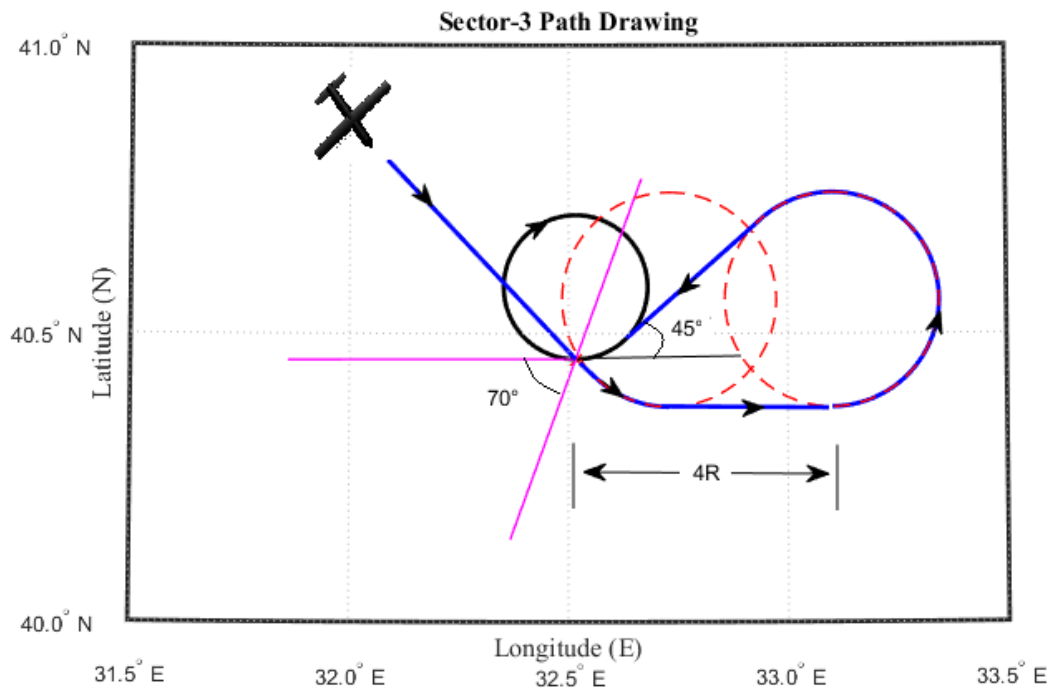
Figure 71 Sector-3 path drawing

6.5   Waypoint Transition and Path Algorithm Performance

As explained in CHAPTER 5, fly-by or fly-over transition is needed while planning to fly on three or more waypoints. The algorithm provides an opportunity to the pilots and autopilots to track the pattern. The algorithm gives the limitations to let the pilot and autopilot know when the earliest time is to start the transition and when is the last time the aircraft can start the transition which are applicable in the avionic standardizations. And also, the algorithm supplies the optimum transition time for turning and creates the path. Furthermore, the aircraft can start the transition within these low and high limits. Figure 72 illustrates the results of fly-by transition with low limit, high limit and current turn.
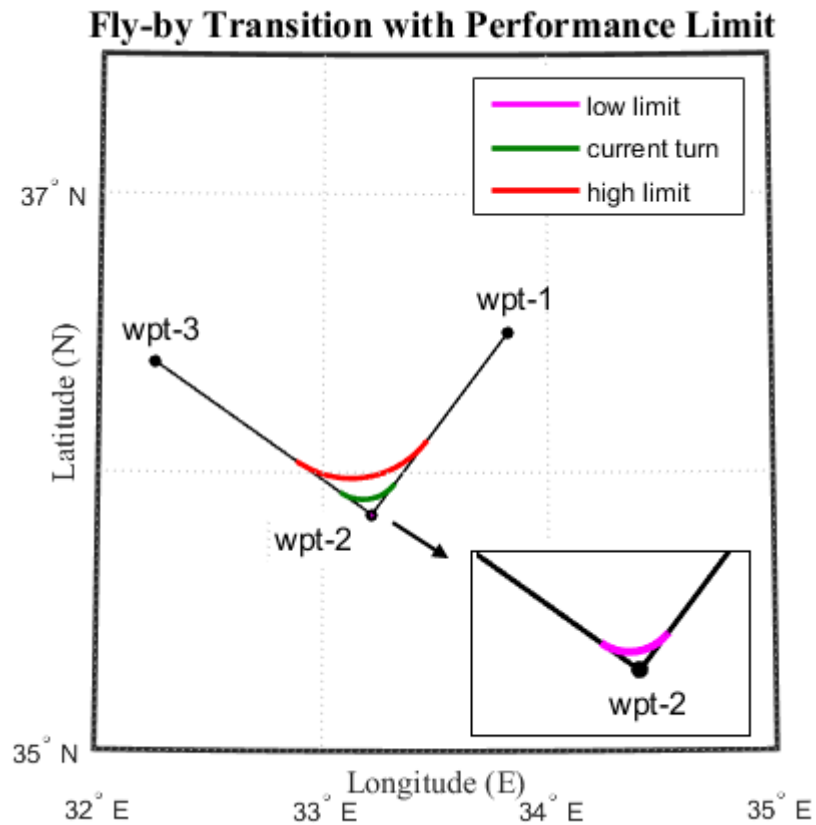
Figure 72 Fly-by transition with performance limit

The transition turn is like an arc shape and is calculated like drawing a circle with a radius outside. So entering the transition too early means drawing a circle center too far from the real location so the arc can't be drawn properly for the transition. Moreover, entering the transition so early might mean a circle which has center at infinity. Low limit's circle center represents the smallest circle can be drawn for the transition. After that point, the arc can be drawn with a circle center which becomes impossible for the path. It means after the low limit, the aircraft miss the chance to make a fly-by transition for the waypoint and to fit the path following.
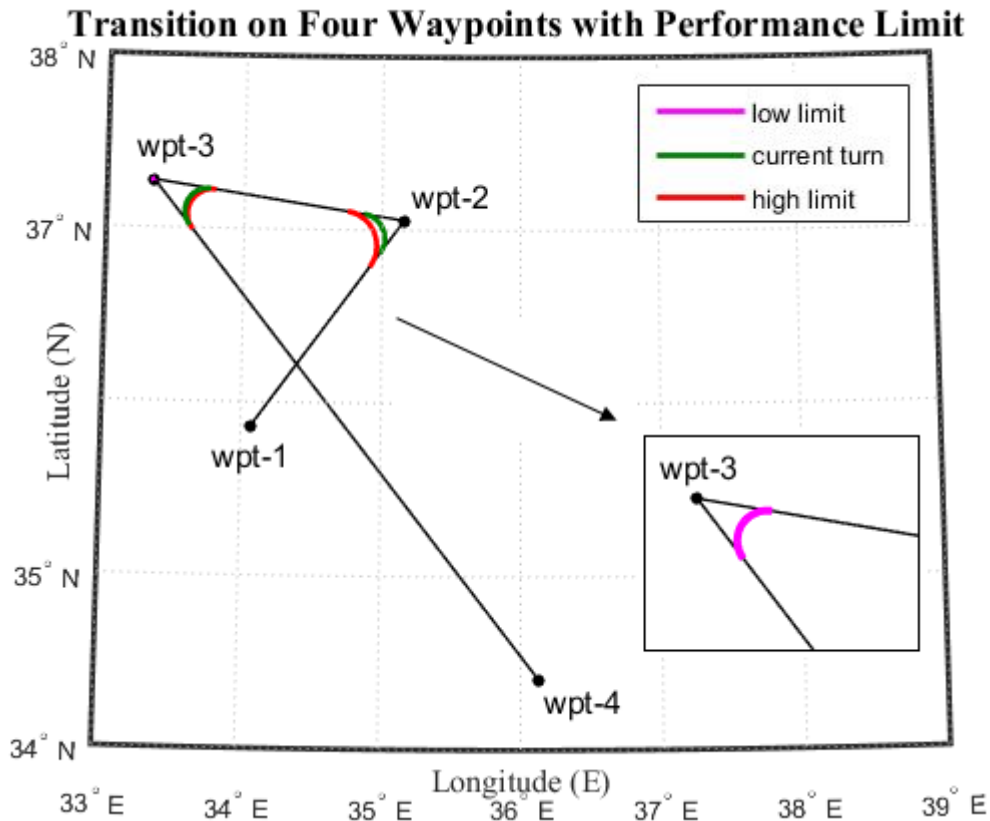
Figure 73 Transition on four waypoints with performance limits

Transition between four waypoints are shown in Figure 73. The waypoint numbers are given respectively which show the route the aircraft is following. As illustrated in the figure, there are two fly-by transitions. In the first transition between wpt-1, wpt-2 and wpt-3, the angle is larger than the transition between wpt-2, wpt-3 and wpt-4. The result presents that when the angle get smaller between waypoints while transition, the limitations get smaller and closer to each other because creating an arc which is geometrically possible becomes impossible in the narrow angle transitions. As shown in the second fly-by transition, the optimal turn is very near to high limit band.

6.6   Required Navigation Performance Evaluation in The Path Algorithm

The performance evaluation depends on the phase of the flight as explained in 5.4.
RNP-RNAV Types. The aircraft must stay in the limitations 95% of the flight time to
meet the performance requirements. The performance computations of the algorithm
are presented here. Figure 74 presents the performance result of enroute phase of the
flight in lateral axis.
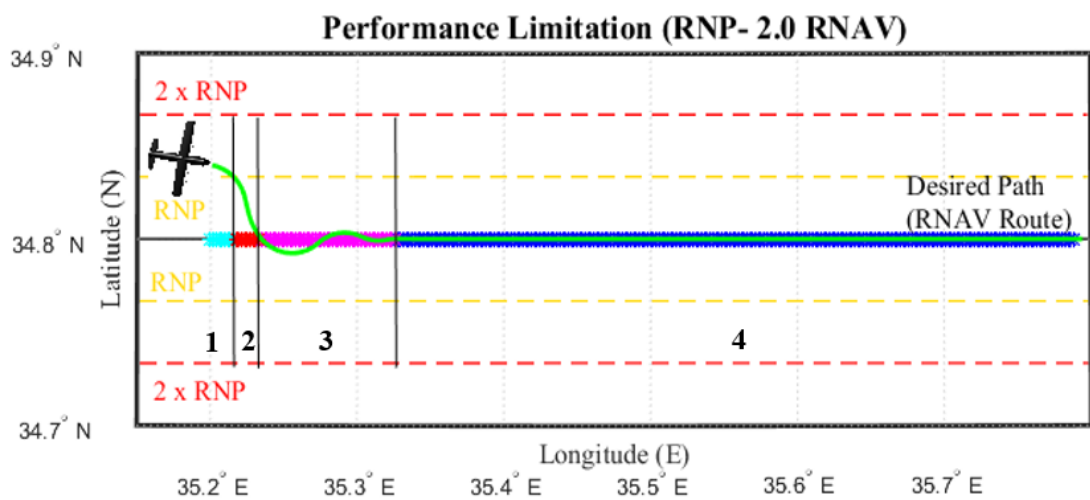
Figure 74 Performance limitation (RNP- 2.0 RNAV)

The result is given where the first aircraft position is at 34.84 °N and 35.2 °E, the
heading is at 70° and the altitude is at 7000m. The yellow lines represent the 2.0 NM
RNAV limitation and the red lines show the cross-track containment error limit lines.
The initial distance between the first position of the aircraft and the desired path is
2.3896 NM. Stars (*) on the desired path shows the aimpoints which have been
calculated during the flight. The first aimpoint is located at 34.8002 °N and 35.1998
°E. The result is divided to four regions to be able to calculate the performance of the
flight. The first region represents the area the aircraft is out of RNP- 2.0 RNAV line.
The second region shows the flight the aircraft touches the desired path for the first

time. The third region is for the oscillation part until fitting the path completely. The last region illustrates the perfect tracking part on the path.
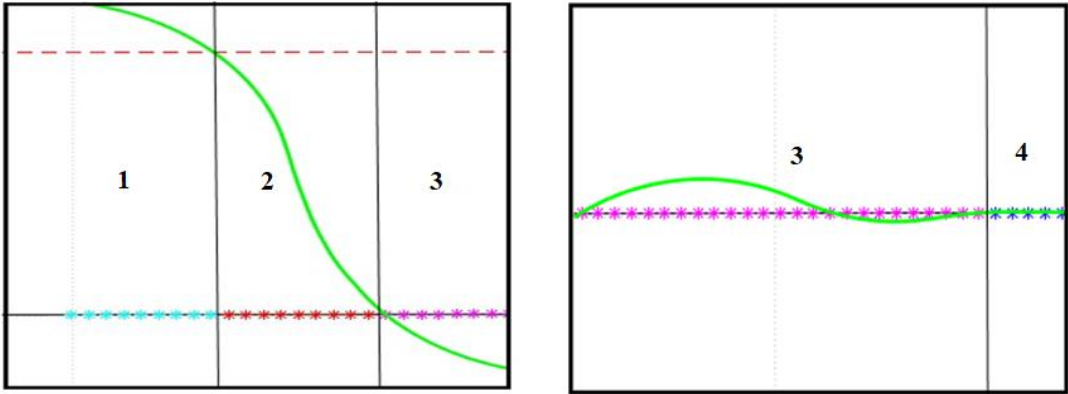
Figure 75 Aimpoint distribution on the blocks

To calculate the performance the points out of the limits and the total point numbers in Figure 75 are needed. Table 8 illustrates the number of the points in every region. Equations (6.7) and (6.8) are used for performance calculation. The flight is achieved 96.04 % performance during the flight time.

Table 8 Number of the points with respect to the regions

	Region-1	Region-2	Region-3	Region-4	Total
Number of the Points	19	42	87	332	480

Performance (%)= (Total Point-Region_1) / (Total Point) x 100　　　(6.7)

Performance (%)= (480-19)/480 x 100=96.04　　　(6.8)
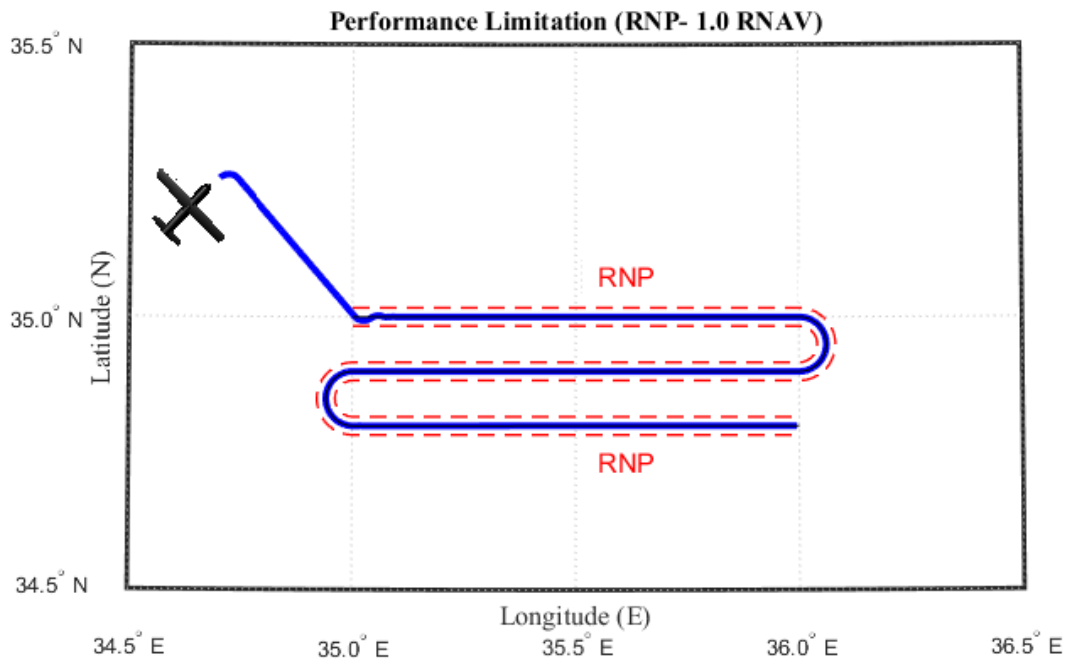
Figure 76 Performance limitation (RNP- 1.0 RNAV)

Figure 76 provides the results of terminal phases of the flight where the first aircraft position is at 35.25 °N and 34.7 °E, the heading is at 45° and the altitude is at 2000m. The red lines represent the 1.0 NM RNAV limitation. The algorithm shows a great performance while curved turn and narrow areas too on the path which is designed with respect to the standardization in the turn limitations.

CHAPTER 7

CONCLUSION

The thesis discussed some methods to improve lateral trajectory tracking and flight safety. With this purpose, an algorithm which aimed to achieve several functions was designed. FMS is a very complicated system which includes navigation, flight planning, trajectory tracking, performance evaluation and guidance. To process this complicated system, step by step improvement was provided for each block. Fundamentals of aircraft flight mechanism, aircraft coordinate systems and their transformations were supplied as base information for the algorithm to be developed on. Flight motion dynamic equations and base of aircraft data were used to represent real aircraft motions and limitations. In this way, the algorithm had a chance to represent the real aircraft commands and to get these commands as inputs to create more accurate results. The effects of the parameters and coefficients in the motion equations and base of aircraft data were observed and the impact of this observation were presented in the thesis. Path design was the other main aim which was achieved in this study. Minimum, maximum and optimal transitions between waypoints were calculated to generate trajectories to the path algorithm with respect to avionic standardizations. The transition limitations showed that the angle between waypoint changes the possible transition's beginning and the distance between limitation bands. Some specific patterns like circle pattern and curved patterns were designed depending on geometric and avionic limitations. The main path tracking algorithm targeted to minimize the variables while finding aim point in lateral axis. A new approach was presented by giving all possible conditions between path and aircraft position. A circle

method whose center point was defined as the aircraft was used to find aim points. The choice of the distance which means the radius of the circle was observed to put forth the impact on the path tracking. Very small distance choice created an oscillation problem while tracking the path whereas very big distance caused not to fix the path till the end. Thus, the optimum distance determination became more of an issue in the algorithm design. The results were compared and discussed to find better optimal distance range to get maximum accurate tracking. The distance choice also applied on the path which had several junctions that cause problems while finding aim point. To minimize this discrepancy, the distance (L) was needed to be chosen as the possible minimum value from the inside of the optimum values. Discrete representation of the lateral path tracking was analyzed to evaluate the angle change while approaching to the path. The angle was observed that it got smaller when it was close to the desired path. Furthermore, geometrically independent aimpoint determination was achieved by calculating a new aimpoint for each cycle. The last part of the thesis was about evaluating performance with RNP-RNAV standardization. The results showed that the algorithm had the required performance by staying in the limitations. While designing the algorithm in every phase, the limitations were implemented to the create more accurate outputs such as while modelling the aircraft and designing the path. The flight commands were calculated and updated with the real aircraft restrictions and coefficients in BADA file. The possible sensor errors were also taken into consideration to estimate whether or not the performance requirement was successful. In view of all these results, the thesis was able to achieve its goal in every component that was planned in the beginning which were path generation, controlling the motion, modelling the aircraft, trajectory tracking and performance computation.

REFERENCES

[1] Sandraey, M. H., *Aircraft Design: A Systems Engineering Approach,* First Edition, **2013**

[2] Fedaral Aviation Adminstration (FAA), *Pilot's Handbook of Aeronautical Knowledge,* **2016**

[3]   J., *Force and Motion,* The Johns Hopkins University Press, **2009**

[4] Panaras, A. G., *Aerodynamic Principles of Flight Vehicles*, American Institute of Aeronautics and Astronautics, **2012**

[5] CAE Oxford Aviation Academy, *Principles of Flight ATPL Ground Trainig Series*, **2014**

[6] Axes control surfaces, https://www.nasa.gov, last visited on:19/2/2018.

[7] Cook, M. V., *Flight Dynamics Principles: A Linear Systems Approach to Aircraft Stability and Control*, Elsevier Aerospace Engineering Series, Second Edition, **2007**

[8] Fedaral Aviation Adminstration (FAA), *Airplane Flying Handbook,* **2016**

[9] Zipfel, P. H., *Modeling and Simulation of Aerospace Vehicle Dynamics,* University of Florida, Second Edition, **2007**

[10] Wozniak, J. G., *Nonlinear Six Degree of Freedom Simulation of a Twin Jet Engine Transport Aircraft*, M.Sc. Thesis, Ohio University, **1997**

[11] Nelson, R.C., *Flight Stability and Automatic Control*, Aerospace and Mechanical Engineering Department University of Notre Dame, McGraw Hill, **1989**

[12] Aviation Adminstration (FAA), *Advanced Avionics Handbook,* **2009**

[13] McCormick, B. W., *Aerodynamics, Aeronautics and Flight Mechanics*, Wiley, Second Edition, **1995**

[14] Beard, R. W., McLain, T. W., *Small Unmanned Aircraft Theory and Practice,* Princeton University Press, **2012**

[15] Johnson, E. N., Stevens, B. L., Lewis, F. L., *Aircraft Control and Simulation*, **2015**

[16] Pamadi, B. N., Performance, *Stability, Dynamics and Control of Airplanes*, AIAA, **1998**

[17] Schmidt, L. V., *Introduction to Aircraft Flight Dynamics*, AIAA, **1997**

[18] EUROCONTROL, *RNAV Application in Terminal Airspace*, European Air Traffic Management Programme, **2009**

[19] International Civil Aviation Organization (ICAO), *Air Traffic Services*, 11th Edition, **1997**

[20] Park, S., Deyst, J., How, J. P., *A New Nonlinear Guidance Logic for Trajectory Tracking*, Massachusetts Institute of Technology, Cambridge, **2004**

[21] DO-283A, *Minimum Operational Performance Standards for Required Navigation Performance for Area Navigation*, RTCA Inc, **2003**

[22] EUROCONTROL, *Base of Aircraft Data (BADA) Product Management Document,* **2009**

[23] Altınöz, B., *Identification of Inertial Sensor Error Parameters*, M.Sc. Thesis, METU, **2015**

[24] Gunhan, Y., *Detection and Compensation of Inertial Measurement Unit Error*, Hacettepe University, **2014**

[25] Gao, C. Zhang, P., *An Introduction to a New Proportional Navigation Method and Its Application,* Chinese Control and Decision Conference, **2008**

[26] Park, S., Vaddi, S., Kwan, J., *Next Generation Flight Management System Simulator*, American Institute of Aeronautics and Astronautics, **2016**

[27] Cho, N., Kim, Y., *Lyapunov-Based Three-Dimensional Nonlinear Path-Following Guidance Law,* American Institute of Aeronautics and Astronautics, **2015**

[28] Lorenz, S., Dauer, J., *Evaluation of Time-Shifted Feedforward Control for Unmanned Helicopter Path Tracking,* American Institute of Aeronautics and Astronautics, **2012**

[29] Hayoun, S., Gronat, A., Shima, T., *Path Following Using Trajectory Shaping Guidance,* Journal of Guidance, Control and Dynamics, **2015**

[30] Gates, D., *Nonlinear Path Following Method,* Journal of Guidance, Control and Dynamics, **2010**